A CONTINUOUS FLUORESCENCE ASSAY FOR POLYMERASE ACTIVITY

by

Jesse L. Montgomery

A dissertation submitted to the faculty of
The University of Utah
in partial fulfillment of the requirements for the degree of

Doctor of Philosophy

Department of Bioengineering

The University of Utah

December 2013

The University of Utah Graduate School

STATEMENT OF DISSERTATION APPROVAL

The dissertation of **Jesse L. Montgomery**

has been approved by the following supervisory committee members:

Carl T. Wittwer	, Chair	**10/28/2013** Date Approved
Vladimir Hlady	, Member	**10/28/2013** Date Approved
David W. Grainger	, Member	**10/28/2013** Date Approved
Robert A. Palais	, Member	**10/28/2013** Date Approved
James N. Herron	, Member	**10/28/2013** Date Approved

and by **Patrick A. Tresco** , Chair/Dean of

the Department/College/School of **Bioengineering**

and by David B. Kieda, Dean of The Graduate School.

ABSTRACT

Little is known about the kinetic limitations of the polymerase chain reaction (PCR). Advancements in chemistry and instrumentation have increased its speed and specificity. Further improvements will be facilitated by a more complete understanding of the rates of the individual reactions that comprise PCR. A continuous fluorescent assay is developed to study DNA polymerase extension. Nucleotide incorporation is monitored with noncovalent DNA dyes using a defined hairpin template. The extension rate is measured in nucleotides incorporated per second per molecule of polymerase and has greater relevance to PCR than traditional activity methods. This assay was developed and validated on a stopped-flow instrument and subsequently adapted for real-time PCR instruments to extend its utility to any laboratory setting. The influences of a variety of buffer components were determined and optimal conditions for fast polymerase extension are recommended. The incorporation rates of each nucleotide were determined and extension was found to depend on template sequence. When DMSO was included in the reaction to reduce inhibition from secondary structure, extension rates of random sequences were closely approximated by their base composition. Extension rates as a function of temperature were determined and were applied to a kinetic model. This model accounts for extension during temperature transitions and more accurately portrays fast PCR with rapid thermal cycling. A complete model of PCR based on differential equations derived from mass action equations is provided. This can be used to incorporate experimentally derived parameters obtained for the other reactions of PCR. Knowledge of the temperature and chemistry dependence of reaction rates will enable improved thermal cycling and solution conditions for more rapid and efficient PCR.

CONTENTS

LIST OF FIGURES

LIST OF TABLES

ACKNOWLEDGMENTS

This work was made possible by the kind support of many individuals. I extend my gratitude to my fellow lab mates who have provided a positive atmosphere for me to conduct my studies. They each have offered many words of encouragement and a fresh and optimistic perspective on my challenges. I consider them my dear friends. A special thanks is due to Luming Zhou who has taught me many principles of mental discipline and perseverance required of great scientists. Words are inadequate to describe my great debt to my advisor and mentor. He has been an outstanding example of patience and generosity, one that I strive to emulate. I am grateful for the assistance of my family who have eagerly relieved me of many burdens to allow me to continue my work. Most of all, I thank my wife who has sustained me through every difficulty and whose faith in my abilities has given me strength beyond my own.

CHAPTER 1

INTRODUCTION

1.1 Advancements in the Speed of PCR

The introduction of the polymerase chain reaction (PCR) revolutionized molecular biology. First developed in the mid-1980s [1], this technique allowed analysis of DNA in a fraction of the time and with orders of magnitude greater sensitivity than other methods available at the time such as cloning and Southern blotting [2]. PCR continues to benefit from technological advancements, increasing its speed and sensitivity. Initially, thermal cycling was accomplished by manually transferring reaction tubes between water baths set at different temperatures [3]. Because a heat-labile polymerase was used (commonly the Klenow fragment of DNA polymerase from *Escherichia coli*), additional polymerase was required after each cycle. PCR typically required more than 4.5 h for 35 cycles.

Time requirements for PCR were greatly reduced with the use of a thermostable DNA polymerase from *Thermus aquaticus* [4]. Because the polymerase did not need to be replenished, PCR could be automated with block thermal cycling machines. This allowed PCR to be accomplished in less than half the time, with 35 cycles typically completed in 1.5 to 2 h. Further advancements were accomplished with instrumentation. Rather than thermal cycling microcentrifuge tubes with metal blocks, reactions have been placed in thin glass capillaries and heated and cooled with forced air [5], [6]. This enabled PCR in less than 15 min. Not only did rapid thermal cycling reduce time requirements, it also improved PCR by amplifying DNA with greater yield and specificity [7].

Additional instrumentation configurations have been developed. These include microfluidic and continuous flow designs [8]–[14], shuttle PCR [15]–[17], magnetic flow systems with ferrofluid [18], micro-electro-mechanical systems (MEMS) [19], [20], and droplet and emulsion PCR [21]–[23] including amplification on beads for second generation sequencing [24], [25]. Thermal cycling has been accomplished with thin-film resistors [26], [27], infrared lamps [28]–[31], electrically conductive buffers [32], and liquid gallium [33]. These designs address a number of factors including throughput, cost, and miniaturization. However, the

common objective of most instrumentation modifications is to reduce time requirements. Advancements in PCR speed have been accomplished with several systems, demonstrating DNA amplification in under 5 min [13], [16], [18], [27], [29], [33]. PCR will continue to improve through advancements in both chemistry and instrumentation.

1.2 The Need for Speed

Fast PCR is not just a luxury, but an essential asset in medical diagnostics. This is especially true for infectious disease. Hospital acquired infections have become a great burden on the healthcare system. These occur in about 1 in 20 hospitalizations [34] with one-third of those resulting in readmission [35]. The annual cost of these infections in the United States is estimated at between 5 and 10 billion dollars [36]. This has led many hospitals to implement screening procedures for a variety of problematic infections. Screening is only feasible with rapid and cost-effective molecular assays. High sensitivity, low cost, and speed of PCR-based methods make them especially suited for this purpose. These have been used for screening of vancomycin-resistant *Enterococcus* [37], [38], *Clostridium difficile* [39], methicillin-resistant *Staphylococcus aureus* [40]–[43], *Klebsiella pneumoniae* [44], [45], and *Mycobacterium tuberculosis* [46], [47].

Rapid diagnostics are also essential for surveillance and management of influenza outbreaks. Clinics and laboratories are already heavily burdened with seasonal influenza. Improved diagnostic tools are needed to cope with potential endemic and pandemic outbreaks. PCR-based methods are viable solutions as they require little expertise to perform and are quickly adaptable to rapidly evolving pathogens. Since the pandemic outbreak of 2009 influenza A H1N1, PCR-based methods have become the primary techniques for tracking and diagnosing influenza [48]. Increasing the speed of PCR will bring screening solutions closer to the point of care, improving management of infectious disease and decreasing healthcare costs. This will be facilitated by a thorough understanding of PCR kinetics.

1.3 A More Accurate Model of PCR Kinetics

Understanding the kinetics of PCR is essential to realizing its full potential. PCR consists of three main reactions—denaturation of template DNA, annealing of DNA primers to the template, and extension of primed template by DNA polymerase. Amplification of DNA is accomplished by thermal cycling between the optimal temperatures for these reactions. Traditionally, PCR is viewed from an equilibrium paradigm (Figure 1.1). The three reactions are thought to occur independently at defined temperatures. Only hold times at set temperatures are considered while transitions between temperatures are neglected.

However, PCR is more accurately considered from a kinetic paradigm, especially in the case of rapid thermocycling. More time is spent in transition between temperatures than at any individual temperature. The three reactions of PCR overlap with rates that vary as a function of temperature.

A more complete understanding of PCR can be obtained by measuring the kinetics of each reaction in isolation. The rates of reactions can be determined in a variety of buffer conditions over a range of temperatures relevant to PCR. This would allow identification of rate limiting processes and optimal conditions. Improved buffer chemistries and instrumentation with optimal thermal cycling parameters can be developed to achieve PCR with maximum speed and specificity. The work presented here isolates DNA polymerase extension and measures the rates of this reaction under a variety of conditions. This is accomplished with the development of a new assay for polymerase activity. This assay represents a significant improvement over the standard method used to measure polymerase activity.

1.4 The Standard Polymerase Activity Assay

The most common assay for polymerase activity was first used in the discovery of DNA polymerase [49]. Enzyme fractions were combined with radiolabelled dNTPs and calf thymus DNA as the extension template. Polymerization of the radiolabelled dNTPs formed an acid-insoluble product. After incubating the reaction for 30 min, the reaction was quenched. The DNA product was precipitated with acid, rinsed, and assayed for radioactivity. Radioactivity measurements were correlated to polymerase activity. This method is in frequent use today and has remained almost unchanged. It has been used to characterize the activity of a wide variety of polymerases [50]–[54], and is currently the only assay used to measure the activity of polymerases used for PCR.

Early in the development of this assay, activated DNA was established as the extension template [55]. Activated DNA is prepared by enzymatic digestion or mechanical shearing of genomic DNA, usually from salmon sperm or calf thymus. The result is a random and heterogenous mixture of single-stranded and double-stranded DNA. The template for extension cannot be standardized. This is quite different from PCR in which polymerase extends a template of defined length and sequence. Some studies have altered the radioactive assay by using a defined template with primers [56]–[58]. One study compared activity measured with activated DNA and a defined template for two polymerases [56]. Both polymerases exhibited changes in activity with temperature optimums differing by as much as 10°C between the two templates. Activity measurements using a defined template will

more accurately reflect the kinetics of PCR.

The standard radioactive assay provides end-point measurements. It is incapable of providing initial rates of nucleotide incorporation that exist during PCR. In addition, the units of activity are not intuitive. Activity is described as the amount of radiolabelled nucleotides converted into acid-precipitable material in a given length of time. With such an obscure definition, it is difficult to know how a polymerase will perform in amplification of a defined template during PCR.

1.5 Alternative Polymerase Activity Assays

While the standard radioactive assay is commonly used to characterize the activity of polymerases, it is not commonly used in detailed kinetic studies. This is likely due to the drawbacks of a heterogenous template and end-point measurements. Several additional assays have been developed.

1.5.1 Quench-Flow

Quench-flow is capable of monitoring fast reactions. Reactants are rapidly mixed and quenched with ethylenediaminetetraacetic acid (EDTA) at specified time points. Either radiolabeled dNTPs or primers are used. Products are collected on filter paper or resolved on polyacrylamide gels and the radioactivity assessed. Radioactivity as a function of time is plotted and fit to kinetic models to obtain nucleotide incorporation rates. This technique has been used to measure extension rates of DNA polymerases [59], [60], RNA polymerases [61]–[63], and reverse transcriptase enzymes [64], [65]. Detailed kinetic mechanisms have been elucidated with this method. However, it is laborious and time-consuming and unlikely to be adopted as a general activity assay.

1.5.2 Stopped-Flow

Continuous monitoring of product formation makes stopped-flow methods a more convenient alternative to quench-flow. There is no need for radiolabeled reagents or analysis of products on gels. Several methods have been used to monitor polymerase extension. The fluorescent base analog 2-aminopurine has been placed within the extension region of the template [61], [66]–[68]. The fluorescence of the base is quenched upon incorporation of the complementary nucleotide and can be monitored during extension. Rates can only be measured for bases complementary to 2-aminopurine.

Incorporation of nucleotides is accompanied by the release of pyrophosphate. One study took advantage of this to follow polymerase extension indirectly [63]. An enzyme-coupled

reaction converted pyrophosphate to a product that could be measured by absorbance. Another study used fluorescence polarization [69]. The extension template was labeled with fluorescein. As the template was elongated, the end of the strand became more restricted and anisotropy increased. These assays are capable of measuring fast reactions, but require modified template or additional reagents not used in PCR.

1.5.3 Microtiter Plate Format

Activity assays adapted for microtiter plates greatly increase throughput. The stopped-flow fluorescence polarization assay discussed previously was initially developed on a fluorescence microplate reader [70]. Because the speed of polymerization was faster than the time required for temperature equilibration, this assay was only capable of end-point measurements. Misincorporation of noncomplementary bases could be monitored in real-time. A radioactive assay was developed for a microtiter plate format [71]. This measures the incorporation of radiolabelled dNTPs into extension templates that are immobilized on well surfaces. The reaction is quenched with EDTA at different time points and the radioactivity measured. This is not a continuous assay and multiple experiments must be performed to obtain kinetic data.

1.5.4 Benchtop Fluorometer and Spectrophotometer

The accessibility, convenience, and cost of assays are improved with the use of common laboratory instrumentation. Polymerase activity assays have been developed for fluorometers and spectrophotometers available to most laboratories. One assay relied on the intrinsic fluorescence of single-stranded binding protein [72]. Saturating amounts of the protein were added to the extension template. As the template is extended, single-stranded binding protein is displaced and the intrinsic fluorescence of the protein increases. An enzyme-coupled reaction was developed for a spectrophotometer [73]. Like the stopped-flow assay discussed earlier, pyrophosphate was converted to a product that could be monitored by absorbance. Activated calf thymus DNA was used as the template. Both of these are continuous assays capable of providing initial rates but are complicated by the need for additional reagents.

Fluorescent probes were used to screen the activity of T7 RNA polymerase variants [74]. Molecular beacons were designed complementary to transcripts formed by RNA polymerase from a synthetic DNA template. Molecular beacons hybridize to the transcripts as they are produced, resulting in an increase in fluorescence. Activity is expressed as the number of molecular beacons recognizing a transcript per min per mg of polymerase. Absolute

extension rates are not obtained. Activity measurements obtained with this assay may be influenced by hybridization kinetics of the molecular beacon.

Another spectrophotometer assay was based on light scattering [75]. As the template is extended, the scattering of the reaction solution increases by 10%. Despite being a continuous assay, no kinetic constants were calculated. This may have been due to difficulties in calibration because of high light scattering background.

1.5.5 Microscopy

The activity of RNA polymerase was measured with light microscopy [76]. Polymerase molecules were attached to glass coverslips by nonspecific adsorption and extension templates were attached to gold particles. Extension was monitored by acquiring images averaged over 2 s intervals. The length of extension was correlated to the range of Brownian motion of the particles. Lengths of extension as a function of time provided extension rates. The effect of nonspecific adsorption on activity of the polymerase is unknown.

The activity of the Klenow Fragment polymerase was measured with fluorescence microscopy [77]. Template was immobilized on glass coverslips. The template contained a hairpin structure downstream from the primer. The hairpin kept a fluorophore and a quencher in close proximity. As the polymerase extended the template, the hairpin was opened and fluorescence increased. Gradual opening of the hairpin during extension allowed real-time monitoring of nucleotide incorporation.

An optical trap assay was used to measure the extension rate and mechanical force associated with extension of T7 polymerase [78]. Both ends of the template were attached to beads. One end was immobilized with a glass pipette and the other was held with an optical trap. Extension was monitored by imaging the distance between the beads as a function of time. These distances were compared to the distance of beads with double or single stranded DNA to obtain extension rates. All of these methods obtain extension rates at a single-molecule level but are technically difficult to perform.

1.5.6 Quartz Crystal Microbalance

Quartz crystal microbalance uses thin quartz wafers to measure changes in mass. The quartz oscillates with an applied alternating current. The frequency of oscillation decreases as mass is accumulated. This technique was used to monitor extension of immobilized template [79]. Klenow Fragment was first equilibrated to achieve a baseline. Then dNTPs were added and the change in frequency observed. Calibration provides correlation of changes in frequency to increases in mass. This allowed calculation of nucleotide incorporation rates

from the initial slopes of frequency decreases during polymerase extension. In this study, the extension of the majority of templates could not be monitored. This may be due to reduced sensitivity as the signal from addition of nucleotides was small compared to the signal from the binding of polymerase.

1.5.7 Atomic Force Microscopy

Atomic force microscopy was used to measure transcription of a template by an RNA polymerase [80]. Polymerases were attached to mica surfaces by nonspecific adsorption. Surfaces were scanned in a flow-through system following addition of dNTP. Templates of known length were observed at different time points as they were extended by the polymerase. This technique suffers from low time resolution and the concentration of dNTP was intentionally kept low to reduce extension rates. Adsorption of the polymerases in the presence of high concentrations of zinc may have an impact on polymerase activity.

1.6 A Continuous Fluorescence Assay Using Noncovalent Dyes

All of the polymerase activity assays described here use reagents that are foreign to PCR. In contrast, the assay introduced here is a continuous fluorescent assay that monitors nucleotide incorporation with noncovalent fluorescent dyes used ubiquitously in real-time PCR. The template has a defined length and sequence. This allows simple calibration of data and provides activity in units of nucleotides per second per molecule of polymerase and are intuitive within the context of PCR. The template is a hairpin with a high melting temperature of 92°C, enabling measurement of polymerase extension rates at high temperatures. As a self-priming template, contributions from primer annealing are eliminated and the extension reaction is isolated. Using this assay, the extension rates of a variety of polymerases are compared. The effects of several common buffer components are determined and recommendations for optimal conditions for fast extension are provided. In addition, the influence of temperature and template sequence including base composition and secondary structure are also studied. Finally, temperature-dependent extension rates are applied to a kinetic model of polymerase extension and compared to an equilibrium model.

1.7 References

[1] K. Mullis, F. Faloona, S. Scharf, R. Saiki, G. Horn, and H. Erlich, "Specific enzymatic amplification of DNA in vitro: the polymerase chain reaction," *Cold Spring Harbor Symp. Quant. Biol.*, vol. 51 Pt 1, pp. 263–73, 1986.

[2] R. K. Saiki, S. Scharf, F. Faloona, K. B. Mullis, G. T. Horn, H. A. Erlich, and N. Arnheim, "Enzymatic amplification of beta-globin genomic sequences and restriction site analysis for diagnosis of sickle cell anemia," *Science*, vol. 230, no. 4732, pp. 1350–4, 1985.

[3] K. B. Mullis and F. A. Faloona, "Specific synthesis of DNA in vitro via a polymerase-catalyzed chain reaction," *Methods Enzymol.*, vol. 155, pp. 335–50, 1987.

[4] R. K. Saiki, D. H. Gelfand, S. Stoffel, S. J. Scharf, R. Higuchi, G. T. Horn, K. B. Mullis, and H. A. Erlich, "Primer-directed enzymatic amplification of DNA with a thermostable DNA polymerase," *Science*, vol. 239, no. 4839, pp. 487–91, 1988.

[5] C. T. Wittwer, G. C. Fillmore, and D. J. Garling, "Minimizing the time required for DNA amplification by efficient heat transfer to small samples," *Anal. Biochem.*, vol. 186, no. 2, pp. 328–31, 1990.

[6] C. T. Wittwer, G. C. Fillmore, and D. R. Hillyard, "Automated polymerase chain reaction in capillary tubes with hot air," *Nucleic Acids Res.*, vol. 17, no. 11, pp. 4353–7, 1989.

[7] C. T. Wittwer and D. J. Garling, "Rapid cycle DNA amplification: time and temperature optimization," *Biotechniques*, vol. 10, no. 1, pp. 76–83, 1991.

[8] S. K. Njoroge, H.-W. Chen, M. A. Witek, and S. A. Soper, "Integrated microfluidic systems for DNA analysis," *Top. Curr. Chem.*, vol. 304, pp. 203–60, 2011.

[9] S. Park, Y. Zhang, S. Lin, T.-H. Wang, and S. Yang, "Advances in microfluidic PCR for point-of-care infectious disease diagnostics," *Biotechnol. Adv.*, vol. 29, no. 6, pp. 830–9, 2011.

[10] C. Zhang, J. Xu, W. Ma, and W. Zheng, "PCR microfluidic devices for DNA amplification," *Biotechnol. Adv.*, vol. 24, no. 3, pp. 243–84, 2006.

[11] Y. Zhang and P. Ozdemir, "Microfluidic DNA amplification–a review," *Anal. Chim. Acta*, vol. 638, no. 2, pp. 115–25, 2009.

[12] H. Ogawa, T. Yamaguchi, and H. Fukushi, "Duplex shuttle PCR for differential diagnosis of budgerigar fledgling disease and psittacine beak and feather disease," *Microbiol. Immunol.*, vol. 49, no. 3, pp. 227–37, 2005.

[13] Y. Fuchiwaki, H. Nagai, M. Saito, and E. Tamiya, "Ultra-rapid flow-through polymerase chain reaction microfluidics using vapor pressure," *Biosens. Bioelectron.*, vol. 27, no. 1, pp. 88–94, 2011.

[14] N. Crews, C. Wittwer, and B. Gale, "Continuous-flow thermal gradient PCR," *Biomed. Microdevices*, vol. 10, no. 2, pp. 187–95, 2008.

[15] J. T. Chiou, P. T. Matsudaira, and D. J. Ehrlich, "Thirty-cycle temperature optimization of a closed-cycle capillary PCR machine," *Biotechniques*, vol. 33, no. 3, pp. 557–8, 560, 562 passim, 2002.

[16] O. Frey, S. Bonneick, A. Hierlemann, and J. Lichtenberg, "Autonomous microfluidic multi-channel chip for real-time PCR with integrated liquid handling," *Biomed. Microdevices*, vol. 9, no. 5, pp. 711–8, 2007.

[17] J. Chen, M. Wabuyele, H. Chen, D. Patterson, M. Hupert, H. Shadpour, D. Nikitopoulos, and S. A. Soper, "Electrokinetically synchronized polymerase chain reaction microchip fabricated in polycarbonate," *Anal. Chem.*, vol. 77, no. 2, pp. 658–66, 2005.

[18] Y. Sun, Y. C. Kwok, and N. T. Nguyen, "A circular ferrofluid driven microchip for rapid polymerase chain reaction," *Lab Chip*, vol. 7, no. 8, pp. 1012–7, 2007.

[19] D. Lee, P.-J. Chen, and G.-B. Lee, "The evolution of real-time PCR machines to real-time PCR chips," *Biosens Bioelectron*, vol. 25, no. 7, pp. 1820–4, 2010.

[20] C. Potrich, L. Lunelli, S. Forti, D. Vozzi, L. Pasquardini, L. Vanzetti, C. Panciatichi, M. Anderle, and C. Pederzolli, "Effect of materials for micro-electro-mechanical systems on PCR yield," *Eur. Biophys. J.*, vol. 39, no. 6, pp. 979–86, 2010.

[21] Z. Zhu, G. Jenkins, W. Zhang, M. Zhang, Z. Guan, and C. J. Yang, "Single-molecule emulsion PCR in microfluidic droplets," *Anal BioAnal. Chem.*, vol. 403, no. 8, pp. 2127–43, 2012.

[22] X. Leng and C. J. Yang, "Agarose droplet microfluidics for highly parallel and efficient single molecule emulsion PCR," *Methods Mol. Biol.*, vol. 949, pp. 413–22, 2013.

[23] F. Wang and M. A. Burns, "Performance of nanoliter-sized droplet-based microfluidic PCR," *Biomed. Microdevices*, vol. 11, no. 5, pp. 1071–80, 2009.

[24] M. Margulies, M. Egholm, W. E. Altman, S. Attiya, J. S. Bader, L. A. Bemben, J. Berka, M. S. Braverman, Y.-J. Chen, Z. Chen, S. B. Dewell, L. Du, J. M. Fierro, X. V. Gomes, B. C. Godwin, W. He, S. Helgesen, C. H. Ho, C. H. Ho, G. P. Irzyk, S. C. Jando, M. L. I. Alenquer, T. P. Jarvie, K. B. Jirage, J.-B. Kim, J. R. Knight, J. R. Lanza, J. H. Leamon, S. M. Lefkowitz, M. Lei, J. Li, K. L. Lohman, H. Lu, V. B. Makhijani, K. E. McDade, M. P. McKenna, E. W. Myers, E. Nickerson, J. R. Nobile, R. Plant, B. P. Puc, M. T. Ronan, G. T. Roth, G. J. Sarkis, J. F. Simons, J. W. Simpson, M. Srinivasan, K. R. Tartaro, A. Tomasz, K. A. Vogt, G. A. Volkmer, S. H. Wang, Y. Wang, M. P. Weiner, P. Yu, R. F. Begley, and J. M. Rothberg, "Genome sequencing in microfabricated high-density picolitre reactors," *Nature*, vol. 437, no. 7057, pp. 376–80, 2005.

[25] J. Shendure, G. J. Porreca, N. B. Reppas, X. Lin, J. P. McCutcheon, A. M. Rosenbaum, M. D. Wang, K. Zhang, R. D. Mitra, and G. M. Church, "Accurate multiplex polony sequencing of an evolved bacterial genome," *Science*, vol. 309, no. 5741, pp. 1728–32, 2005.

[26] P. Belgrader, W. Benett, D. Hadley, G. Long, R. Mariella, Jr, F. Milanovich, S. Nasarabadi, W. Nelson, J. Richards, and P. Stratton, "Rapid pathogen detection using a microchip PCR array instrument," *Clin. Chem.*, vol. 44, no. 10, pp. 2191–4, 1998.

[27] P. Neuzil, C. Zhang, J. Pipper, S. Oh, and L. Zhuo, "Ultra fast miniaturized real-time PCR: 40 cycles in less than six minutes," *Nucleic Acids Res.*, vol. 34, no. 11, p. e77, 2006.

[28] A. F. Hühmer and J. P. Landers, "Noncontact infrared-mediated thermocycling for effective polymerase chain reaction amplification of DNA in nanoliter volumes," *Anal. Chem.*, vol. 72, no. 21, pp. 5507–12, 2000.

[29] B. C. Giordano, J. Ferrance, S. Swedberg, A. F. Huhmer, and J. P. Landers, "Polymerase chain reaction in polymeric microchips: DNA amplification in less than 240 seconds," *Anal. Biochem.*, vol. 291, no. 1, pp. 124–32, 2001.

[30] R. P. Oda, M. A. Strausbauch, A. F. Huhmer, N. Borson, S. R. Jurrens, J. Craighead, P. J. Wettstein, B. Eckloff, B. Kline, and J. P. Landers, "Infrared-mediated thermocycling for ultrafast polymerase chain reaction amplification of DNA," *Anal. Chem.*, vol. 70, no. 20, pp. 4361–8, 1998.

[31] M. G. Roper, C. J. Easley, L. A. Legendre, J. A. C. Humphrey, and J. P. Landers, "Infrared temperature control system for a completely noncontact polymerase chain reaction in microfluidic chips," *Anal. Chem.*, vol. 79, no. 4, pp. 1294–300, 2007.

[32] D. M. Heap, M. G. Herrmann, and C. T. Wittwer, "PCR amplification using electrolytic resistance for heating and temperature monitoring," *Biotechniques*, vol. 29, no. 5, pp. 1006–12, 2000.

[33] G. Maltezos, M. Johnston, K. Taganov, C. Srichantaratsamee, J. Gorman, D. Baltimore, W. Chantratita, and A. Scherer, "Exploring the limits of ultrafast polymerase chain reaction using liquid for thermal heat exchange: a proof of principle," *Appl. Phys. Lett.*, vol. 97, no. 26, p. 264101, 2010.

[34] R. M. Klevens, J. R. Edwards, C. L. Richards, Jr, T. C. Horan, R. P. Gaynes, D. A. Pollock, and D. M. Cardo, "Estimating health care-associated infections and deaths in U.S. hospitals, 2002," *Public Health Rep.*, vol. 122, no. 2, pp. 160–6, 2007.

[35] C. B. Emerson, L. M. Eyzaguirre, J. S. Albrecht, A. C. Comer, A. D. Harris, and J. P. Furuno, "Healthcare-associated infection and hospital readmission," *Infect. Control Hosp. Epidemiol.*, vol. 33, no. 6, pp. 539–44, 2012.

[36] P. W. Stone, E. C. Hedblom, D. M. Murphy, and S. B. Miller, "The economic impact of infection control: making the business case for increased infection control resources," *Am. J. Infect. Control*, vol. 33, no. 9, pp. 542–7, 2005.

[37] J. W. Pearman, P. L. Perry, F. P. Kosaras, C. R. Douglas, R. C. Lee, A. M. Peterson, C. T. Orrell, C. H. Khinsoe, C. H. Heath, and K. J. Christiansen, "Screening and electronic labelling of ward contacts of vancomycin-resistant Enterococcus faecium vanB carriers during a single-strain hospital outbreak and after discharge from hospital," *Commun. Dis. Intell. Q. Rep.*, vol. 27 Suppl, pp. S97–102, 2003.

[38] A. Kurup, M. P. Chlebicki, M. L. Ling, T. H. Koh, K. Y. Tan, L. C. Lee, and K. B. M. Howe, "Control of a hospital-wide vancomycin-resistant Enterococci outbreak," *Am. J. Infect. Control*, vol. 36, no. 3, pp. 206–11, 2008.

[39] J. W. Marsh, M. M. O'Leary, K. A. Shutt, A. W. Pasculle, S. Johnson, D. N. Gerding, C. A. Muto, and L. H. Harrison, "Multilocus variable-number tandem-repeat analysis for investigation of Clostridium difficile transmission in hospitals," *J. Clin. Mircrobiol.*, vol. 44, no. 7, pp. 2558–66, 2006.

[40] H. Fang and G. Hedin, "Rapid screening and identification of methicillin-resistant Staphylococcus aureus from clinical samples by selective-broth and real-time PCR assay," *J. Clin. Mircrobiol.*, vol. 41, no. 7, pp. 2894–9, 2003.

[41] S. Harbarth, C. Fankhauser, J. Schrenzel, J. Christenson, P. Gervaz, C. Bandiera-Clerc, G. Renzi, N. Vernaz, H. Sax, and D. Pittet, "Universal screening for methicillin-resistant Staphylococcus aureus at hospital admission and nosocomial infection in surgical patients," *JAMA*, vol. 299, no. 10, pp. 1149–57, 2008.

[42] T. G. Fraser, C. Fatica, M. Scarpelli, A. C. Arroliga, J. Guzman, N. K. Shrestha, E. Hixson, M. Rosenblatt, S. M. Gordon, and G. W. Procop, "Decrease in Staphylococcus aureus colonization and hospital-acquired infection in a medical intensive care unit after institution of an active surveillance and decolonization program," *Infect. Control Hosp. Epidemiol.*, vol. 31, no. 8, pp. 779–83, 2010.

[43] M. H. Wernitz, S. Swidsinski, K. Weist, D. Sohr, W. Witte, K.-P. Franke, D. Roloff, H. Rüden, and S. K. Veit, "Effectiveness of a hospital-wide selective screening programme for methicillin-resistant Staphylococcus aureus (MRSA) carriers at hospital admission to prevent hospital-acquired MRSA infections," *Clin. Microbiol. Infect.*, vol. 11, no. 6, pp. 457–65, 2005.

[44] D. Ben-David, Y. Maor, N. Keller, G. Regev-Yochay, I. Tal, D. Shachar, A. Zlotkin, G. Smollan, and G. Rahav, "Potential role of active surveillance in the control of a hospital-wide outbreak of carbapenem-resistant Klebsiella pneumoniae infection," *Infect. Control Hosp. Epidemiol.*, vol. 31, no. 6, pp. 620–6, 2010.

[45] M. V. Villegas, A. Correa, F. Perez, M. C. Miranda, T. Zuluaga, J. P. Quinn, and Colombian Nosocomial Resistance Study Group, "Prevalence and characterization of extended-spectrum beta-lactamases in Klebsiella pneumoniae and Escherichia coli isolates from Colombian hospitals," *Diagn. Microbiol. Infect. Dis.*, vol. 49, no. 3, pp. 217–22, 2004.

[46] H. Nguyen Binh, K. Pham Huyen, C. Hennig, H. Chu Thi, C. Le Xuan, V. Le Thuong, and K. Lönnroth, "A descriptive study of TB cases finding practices in the three largest public general hospitals in Vietnam," *BMC Public Health*, vol. 12, p. 808, 2012.

[47] E. P. A. Bensi, P. C. Panunto, and M. d. C. Ramos, "Incidence of tuberculous and non-tuberculous mycobacteria, differentiated by multiplex PCR, in clinical specimens of a large general hospital," *Clinics (Sao Paulo)*, vol. 68, no. 2, pp. 179–84, 2013.

[48] R. Wang and J. K. Taubenberger, "Methods for molecular surveillance of influenza," *Expert Rev. Anti. Infect. Ther.*, vol. 8, no. 5, pp. 517–27, 2010.

[49] I. R. Lehman, M. J. Bessman, E. S. Simms, and A. Kornberg, "Enzymatic synthesis of deoxyribonucleic acid. I. Preparation of substrates and partial purification of an enzyme from Escherichia coli," *J. Biol. Chem.*, vol. 233, no. 1, pp. 163–70, 1958.

[50] A. Chien, D. B. Edgar, and J. M. Trela, "Deoxyribonucleic acid polymerase from the extreme thermophile Thermus aquaticus," *J. Bacteriol.*, vol. 127, no. 3, pp. 1550–7, 1976.

[51] H. Kong, R. B. Kucera, and W. E. Jack, "Characterization of a DNA polymerase from the hyperthermophile archaea Thermococcus litoralis. Vent DNA polymerase, steady state kinetics, thermal stability, processivity, strand displacement, and exonuclease activities," *J. Biol. Chem.*, vol. 268, no. 3, pp. 1965–75, 1993.

[52] S. S. Cho, K. P. Kim, K. K. Lee, M.-H. Youn, and S.-T. Kwon, "Characterization and PCR application of a new high-fidelity DNA polymerase from Thermococcus waiotapuensis," *Enzyme Microb. Technol.*, vol. 51, no. 6-7, pp. 334–41, 2012.

[53] M. Takagi, M. Nishioka, H. Kakihara, M. Kitabayashi, H. Inoue, B. Kawakami, M. Oka, and T. Imanaka, "Characterization of DNA polymerase from Pyrococcus sp. strain KOD1 and its application to PCR," *Appl. Environ. Microbiol.*, vol. 63, no. 11, pp. 4504–10, 1997.

[54] J. J. Choi and S.-T. Kwon, "Cloning, expression, and characterization of DNA polymerase from hyperthermophilic bacterium Aquifex pyrophilus," *J. Microbiol. Biotechnol.*, vol. 14, no. 5, pp. 1022–1030, 2004.

[55] H. V. Aposhian and A. Kornberg, "Enzymatic synthesis of deoxyribonucleic acid. IX. The polymerase formed after T2 bacteriophage infection of Escherichia coli: a new enzyme," *J. Biol. Chem.*, vol. 237, pp. 519–25, 1962.

[56] F. C. Lawyer, S. Stoffel, R. K. Saiki, S. Y. Chang, P. A. Landre, R. D. Abramson, and D. H. Gelfand, "High-level expression, purification, and enzymatic characterization of full-length Thermus aquaticus DNA polymerase and a truncated form deficient in 5' to 3' exonuclease activity," *PCR Methods Appl.*, vol. 2, no. 4, pp. 275–87, 1993.

[57] F. R. Bryant, K. A. Johnson, and S. J. Benkovic, "Elementary steps in the DNA polymerase I reaction pathway," *Biochemistry*, vol. 22, no. 15, pp. 3537–46, 1983.

[58] A. H. Polesky, T. A. Steitz, N. D. Grindley, and C. M. Joyce, "Identification of residues critical for the polymerase activity of the Klenow fragment of DNA polymerase I from Escherichia coli," *J. Biol. Chem.*, vol. 265, no. 24, pp. 14 579–91, 1990.

[59] R. D. Kuchta, V. Mizrahi, P. A. Benkovic, K. A. Johnson, and S. J. Benkovic, "Kinetic mechanism of DNA polymerase I (Klenow)," *Biochemistry*, vol. 26, no. 25, pp. 8410–7, 1987.

[60] S. S. Patel, I. Wong, and K. A. Johnson, "Pre-steady-state kinetic analysis of processive DNA replication including complete characterization of an exonuclease-deficient mutant," *Biochemistry*, vol. 30, no. 2, pp. 511–25, 1991.

[61] G. Q. Tang, V. S. Anand, and S. S. Patel, "Fluorescence-based assay to measure the real-time kinetics of nucleotide incorporation during transcription elongation," *J. Mol. Biol.*, vol. 405, no. 3, pp. 666–78, 2011.

[62] J. J. Arnold and C. E. Cameron, "Poliovirus RNA-dependent RNA polymerase (3Dpol): pre-steady-state kinetic analysis of ribonucleotide incorporation in the presence of Mg2+," *Biochemistry*, vol. 43, no. 18, pp. 5126–37, 2004.

[63] R. S. Johnson, M. Strausbauch, R. Cooper, and J. K. Register, "Rapid kinetic analysis of transcription elongation by Escherichia coli RNA polymerase," *J. Mol. Biol.*, vol. 381, no. 5, pp. 1106–13, 2008.

[64] W. M. Kati, K. A. Johnson, L. F. Jerva, and K. S. Anderson, "Mechanism and fidelity of HIV reverse transcriptase," *J. Biol. Chem.*, vol. 267, no. 36, pp. 25 988–97, 1992.

[65] J. E. Reardon, "Human immunodeficiency virus reverse transcriptase: steady-state and pre-steady-state kinetics of nucleotide incorporation," *Biochemistry*, vol. 31, no. 18, pp. 4473–9, 1992.

[66] J. Ahn, V. S. Kraynov, X. Zhong, B. G. Werneburg, and M. D. Tsai, "DNA polymerase beta: effects of gapped DNA substrates on dNTP specificity, fidelity, processivity and conformational changes," *Biochem. J.*, vol. 331 (Pt 1), pp. 79–87, 1998.

[67] J. W. Arndt, W. Gong, X. Zhong, A. K. Showalter, J. Liu, C. A. Dunlap, Z. Lin, C. Paxson, M. D. Tsai, and M. K. Chan, "Insight into the catalytic mechanism of DNA polymerase beta: structures of intermediate complexes," *Biochemistry*, vol. 40, no. 18, pp. 5368–75, 2001.

[68] V. Purohit, N. D. F. Grindley, and C. M. Joyce, "Use of 2-aminopurine fluorescence to examine conformational changes during nucleotide incorporation by DNA polymerase I (Klenow fragment)," *Biochemistry*, vol. 42, no. 34, pp. 10 200–11, 2003.

[69] P. Gong, G. Campagnola, and O. B. Peersen, "A quantitative stopped-flow fluorescence assay for measuring polymerase elongation rates," *Anal. Biochem.*, vol. 391, no. 1, pp. 45–55, 2009.

[70] S. P. Mestas, A. J. Sholders, and O. B. Peersen, "A fluorescence polarization-based screening assay for nucleic acid polymerase elongation activity," *Anal. Biochem.*, vol. 365, no. 2, pp. 194–200, 2007.

[71] D. L. Earnshaw and A. J. Pope, "Flashplate scintillation proximity assays for characterization and screening of DNA polymerase, primase, and helicase activities," *J. Biomol. Screening*, vol. 6, no. 1, pp. 39–46, 2001.

[72] M. A. Griep, "Fluorescence recovery assay: a continuous assay for processive DNA polymerases applied specifically to DNA polymerase III holoenzyme," *Anal. Biochem.*, vol. 232, no. 2, pp. 180–9, 1995.

[73] A. S. Suarez, A. Stefan, S. Lemma, E. Conte, and A. Hochkoeppler, "Continuous enzyme-coupled assay of phosphate- or pyrophosphate-releasing enzymes," *Biotechniques*, vol. 53, no. 2, pp. 99–103, 2012.

[74] J.-C. Boulain, J. Dassa, L. Mesta, A. Savatier, N. Costa, B. H. Muller, G. L'hostis, E. A. Stura, A. Troesch, and F. Ducancel, "Mutants with higher stability and specific activity from a single thermosensitive variant of T7 RNA polymerase," *Protein Eng. Des. Sel.*, 2013.

[75] K. A. Johnson, F. R. Bryant, and S. J. Benkovic, "Continuous assay for DNA polymerization by light scattering," *Anal. Biochem.*, vol. 136, no. 1, pp. 192–4, 1984.

[76] D. A. Schafer, J. Gelles, M. P. Sheetz, and R. Landick, "Transcription by single molecules of RNA polymerase observed by light microscopy," *Nature*, vol. 352, no. 6334, pp. 444–8, 1991.

[77] J. J. Schwartz and S. R. Quake, "Single molecule measurement of the "speed limit" of DNA polymerase," *Proc. Natl. Acad. Sci. U.S.A.*, vol. 106, no. 48, pp. 20 294–9, 2009.

[78] G. J. Wuite, S. B. Smith, M. Young, D. Keller, and C. Bustamante, "Single-molecule studies of the effect of template tension on T7 DNA polymerase activity," *Nature*, vol. 404, no. 6773, pp. 103–6, 2000.

[79] H. Matsuno, K. Niikura, and Y. Okahata, "Direct monitoring kinetic studies of DNA polymerase reactions on a DNA-immobilized quartz-crystal microbalance," *Chemistry*, vol. 7, no. 15, pp. 3305–12, 2001.

[80] S. Kasas, N. H. Thomson, B. L. Smith, H. G. Hansma, X. Zhu, M. Guthold, C. Bustamante, E. T. Kool, M. Kashlev, and P. K. Hansma, "Escherichia coli RNA polymerase activity observed using atomic force microscopy," *Biochemistry*, vol. 36, no. 3, pp. 461–8, 1997.

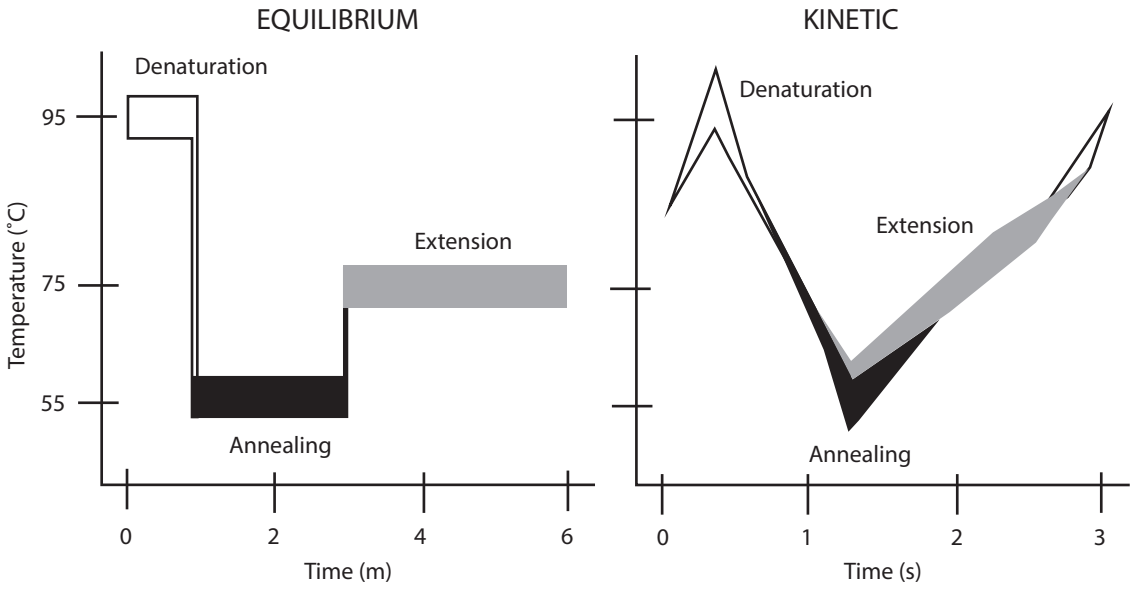

Figure 1.1. Comparison of equilibrium and kinetic models of PCR. In the equilibrium model of PCR, denaturation, annealing, and extension are treated as independent reactions. Reactions occur at defined temperatures and rates are constant. Temperature changes are assumed instantaneous. The kinetic model of PCR accounts for continuously changing temperatures with temperature-dependent rate constants and more adequately describes rapid PCR.

CHAPTER 2

STOPPED-FLOW DNA POLYMERASE ASSAY BY CONTINUOUS MONITORING OF DNTP INCORPORATION BY FLUORESCENCE

Reprinted from Analytical Biochemistry, vol. 441, no. 2, J. L. Montgomery, N. Rejali, and C. T. Wittwer, "Stopped-flow DNA polymerase assay by continuous monitoring of dNTP incorporation by fluorescence," pp. 133-139, 2013, with permission of Elsevier.

Contents lists available at ScienceDirect

Analytical Biochemistry

journal homepage: www.elsevier.com/locate/yabio

Stopped-flow DNA polymerase assay by continuous monitoring of dNTP incorporation by fluorescence

Jesse L. Montgomery, Nick Rejali, Carl T. Wittwer *

Department of Pathology, University of Utah, Salt Lake City, UT 84132, USA

ARTICLE INFO

Article history:
Received 17 April 2013
Received in revised form 3 July 2013
Accepted 6 July 2013
Available online 16 July 2013

Keywords:
Activity assay
Polymerase
Stopped-flow
Intercalating dye

ABSTRACT

DNA polymerase activity was measured by a stopped-flow assay that monitors polymerase extension using an intercalating dye. Double-stranded DNA formation during extension of a hairpin substrate was monitored at 75 °C for 2 min. Rates were determined in nucleotides per second per molecule of polymerase (nt/s) and were linear with time and polymerase concentration from 1 to 50 nM. The concentrations of 15 available polymerases were quantified and their extension rates determined in 50 mM Tris, pH 8.3, 0.5 mg/ml BSA, 2 mM $MgCl_2$, and 200 μM each dNTP as well as their commercially recommended buffers. Native Taq polymerases had similar extension rates of 10–45 nt/s. Three alternative polymerases showed faster speeds, including KOD (76 nt/s), Klentaq I (101 nt/s), and KAPA2G (155 nt/s). Fusion polymerases including Herculase II and Phusion were relatively slow (3–13 nt/s). The pH optimum for Klentaq extension was between 8.5 and 8.7 with no effect of Tris concentration. Activity was directly correlated to the $MgCl_2$ concentration and inversely correlated to the KCl concentration. This continuous assay is relevant to PCR and provides accurate measurement of polymerase activity using a defined template without the need of radiolabeled substrates.

The extension rates of DNA polymerases under PCR conditions have not been characterized. A wide variety of polymerases are available and many are designed for increased fidelity and speed. The conventional way to measure the activity of DNA polymerase is in terms of units, most commonly defined as the number of nanomoles of radiolabeled dNTPs incorporated into activated calf thymus or salmon sperm DNA at 72 to 75 °C for 30 min. This is a time-consuming endpoint assay and does not provide information about the initial extension rates of polymerases. In addition, assay conditions are not standardized and often differ from those used during PCR.

A number of alternative assays have been introduced for DNA and RNA polymerases. These include methods based on atomic force microscopy [1], light microscopy [2], single-molecule optical trapping [3], quartz crystal microbalance [4], and radiometric assays [5]. Others use enzyme-coupled reactions to monitor pyrophosphate release [6,7]. Fluorescence-based methods have monitored the displacement of single-stranded DNA-binding protein [8] or polarization of labeled extension templates [9,10]. Quench–flow [6] has been used and allows kinetic analysis of rapid reactions. However, this method requires stopping the reaction at several time points, followed by analyzing the products on gels or by chromatography methods. Stopped-flow [6,9,11] assays have been developed and enable continuous reaction monitoring, but these use covalent fluorescent labels or nucleotide analogs. Some of these methods are capable of providing extension rates in terms of individual nucleotide incorporation [1–3,8,9,11]. However, they all require template modifications (fluorescent or radioactive) or immobilization of either template or polymerase onto a substrate.

We introduce a fluorescent stopped-flow assay for monitoring polymerase extension that requires no modification of the template or polymerase. This method relies on the increase in fluorescence of double-stranded DNA dyes during nucleotide incorporation. These dyes are frequently used in real-time PCR, eliminating the need to change reaction chemistry. Measured extension rates are directly applicable to PCR. We use this assay to compare the speed of 15 polymerases at equimolar concentrations. Because their activity was strongly dependent on the reaction buffer, we then measured the effects of common buffer conditions, including pH and KCl, $MgCl_2$, and Tris concentration.

Materials and methods

Oligonucleotides

The sequence tagcgaaggatgtgaacctaatcccTGCTCCCGCGGCCG atctgcCGGC-CGCGGGAGCA was used as the extension template and a baseline fluorescence standard (capital letters denote self-complementary sequences). The oligonucleotide forms a hairpin with a 14-bp stem that has a free 3′ end and a 25-base overhang

* Corresponding author. Fax: +1 801 581 6001.
E-mail address: carl.wittwer@path.utah.edu (C.T. Wittwer).

0003-2697/$ - see front matter © 2013 Elsevier Inc. All rights reserved.
http://dx.doi.org/10.1016/j.ab.2013.07.008

for extension. The fully extended template was also synthesized as a fluorescence standard: TAGCGAAGGATGTGAACCTAATCCCTGCTC CCGC-GGCCGatctgcCGGCCGCGGGAGCAGGGATTAGGTTCACATCCT TCGCTA. Oligonucleotides were ordered from Integrated DNA Technologies with the extension substrate purified by high-pressure liquid chromatography and the fully extended standard purified by polyacrylamide gel electrophoresis. Each was quantified by absorbance at 260 nm following digestion by purified phosphodiesterase [12] for accurate quantification.

DNA polymerases

Fifteen polymerases were included in this study: Amplitaq (Invitrogen), KOD (EMD Millipore), Taq (New England Biolabs), Platinum Taq (Invitrogen), GoTaq (Promega), Titanium Taq (Clontech), Paq5000 (Agilent), Herculase II (Agilent), Phusion (New England Biolabs), KAPA2G (Kapa Biosystems), MyTaq (Bioline), Ex Taq (Clontech), Taq (Roche), SpeedSTAR (Clontech), and Klentaq I (purchased from either AB Peptides or Washington University in St. Louis, MO, USA).

Polymerases were quantified on sodium dodecylsulfate (SDS) polyacrylamide gels stained with Sypro orange (Invitrogen). Gel images were obtained using a Gel Doc XR+ with XcitaBlue (Bio-Rad) conversion screen accessory and analyzed with Image Lab (Bio-Rad) software. Prior to being loaded on the gels, samples were reduced in 30 mM Tris, pH 6.8, 12.5% glycerol, 1% SDS, and 360 mM β-mercaptoethanol at 96 °C for 5 min. Klentaq I (purchased from Washington University in St. Louis) was used as the quantification standard. The standard was quantified by absorbance at 280 nm using an extinction coefficient of $6.91 \times 10^4\ M^{-1}\ cm^{-1}$ calculated from the amino acid content of the published sequence [13]. The purity of this standard was determined by fluorescence integration from polyacrylamide gels and the concentration adjusted proportionately. Two replicates of each quantity standard (50, 100, 200, and 300 ng) and four replicates of each polymerase were included on each gel. Major bands at expected molecular masses were considered to be the polymerase of interest. The integrated fluorescence intensity of these bands was used to calculate the concentration and purity of the polymerases. Molecular masses used in concentration calculations were measured from the gels or taken from the literature [14,15], including vendor product information. Klentaq I was measured by mass spectrometry (Mass Spectrometry and Proteomics core facility at the University of Utah) after dialyzing for 48 h at room temperature in PBS buffer (150 mM NaCl, 2.5 mM KCl, 10 mM disodium phosphate, 1.5 mM dipotassium phosphate, pH 7.4). A molecular mass of 62,596 Da was determined compared to 62,097 Da predicted from the amino acid sequence [13].

The specific activity in units per milligram of polymerase (U/mg) was calculated from the unit concentration provided by the manufacturer and the concentration of polymerase measured on the gels. Most manufacturers define 1 U of polymerase as the amount required to incorporate 10 nmol of dNTPs in 30 min. However, the manufacturers of Klentaq I (ABPeptides) and Taq (NEB) define a unit as the incorporation of 60 and 15 nmol dNTP, respectively. The specific activities of these polymerases were scaled to allow comparison to other polymerases (i.e., the specific activity calculated for Klentaq I was multiplied by 6 and that of Taq (NEB) was multiplied by 1.5). The specific activities for Herculase II and Titanium were not calculated because the manufacturers do not provide the polymerase activities.

Polymerase extension assay

Polymerase extension studies were performed with a stopped-flow instrument (SFM-300, Bio-Logic SAS). Excitation was set at 495 nm with a monochromator and fluorescence collected with a photomultiplier tube and a 530 ± 15 nm discriminating filter. Thermoelectric heaters separately maintained the temperature of the mixing lines and the reaction cuvette. Each line was held at 75 °C. Reactants were added to two separate mixing lines and mixed in a 1:1 ratio at a flow rate of 9 ml/s. The estimated dead time for mixing was 6.6 ms. Extension reactions were carried out in 1× EvaGreen (Biotium) and either the buffer supplied by the manufacturer of each polymerase or a common buffer (50 mM Tris, 0.5 mg/ml bovine serum albumin (BSA), and 2 mM $MgCl_2$, pH 8.3). When $MgCl_2$ was not included in the vendor buffer (KOD and Platinum Taq), a final concentration of 2 mM was used. Preliminary experiments determined maximal extension rates for Klentaq I with 200 μM each dNTP with a K_m of 39 μM. Polymerase extension was initiated by mixing 400 μM each dNTP with 10 nM polymerase and 200 nM oligonucleotide (final concentrations were 200 μM each dNTP, 5 nM polymerase, and 100 nM oligonucleotide). To prevent template degradation, extension experiments for polymerases exhibiting 3′ to 5′ exonuclease activity (Herculase II, KOD, and Phusion) were initiated by mixing the polymerase with dNTP and oligonucleotide. MyTaq includes dNTPs in the vendor buffer at a final concentration of 250 μM each. For this polymerase, extension reactions were initiated by mixing the polymerase with the oligonucleotide.

Polymerase extension curves were calibrated either by allowing the reaction to go to completion or by using fluorescence standards. Except where indicated, calibration was performed with fluorescence standards. Polymerase was omitted from reactions containing fluorescence standards and calibration was repeated for each experiment to account for influences of buffer conditions on absolute fluorescence. Seven to ten stopped-flow shots were repeated for each experiment and the means and standard deviations reported. Data were acquired for 2 min every 50 ms.

Buffer component study

The effects of pH and the concentrations of Tris, KCl, and $MgCl_2$ on extension rate were observed. One parameter was varied while the other three were kept constant. Final conditions were Tris concentrations at 10, 20, 30, 40, and 50 mM, KCl at 0, 12.5, 25, 37.5, 50, and 62.5 mM, and $MgCl_2$ at 1, 1.5, 2, 2.5, 3, 4, 5, and 6 mM, and pH was at 7, 7.5, 8, 8.3, 8.5, 8.7, and 9. Unless varied, Tris concentration was held at 50 mM, KCl at 0 mM, and $MgCl_2$ at 2 mM and the pH at 8.0. Studies were done with Klentaq I at 5 nM, 200 μM each dNTP, 100 nM template, 1× EvaGreen, and 0.5 mg/ml BSA final concentrations. Reaction completion was used to calibrate the data in this study except when the extension was so slow that saturation could not be observedwithin 2 min. This occurred only when KCl concentration was 62.5 mM, the pH was 7, and $MgCl_2$ concentration was 1 mM.

Results

Polymerase quantification

A typical quantification gel and standard curve are shown in Fig. 1. Antibody hot-start polymerases (Platinum, Titanium, MyTaq, ExTaq, and SpeedSTAR) showed characteristic heavy- and light-chain bands at around 50 and 25 kDa. Paq5000 showed a prominent band of unknown identity at 62.5 kDa. Phusion had a diffuse band centered around 150 kDa and a prominent band at 64.5 kDa. Neglecting bands known to be other components, the purity of all polymerases was calculated at greater than 90%, with the exception of KOD (70%), Phusion (50%), and KAPA2G (65%). Measured concentrations for all polymerases are shown in Table 1. Most

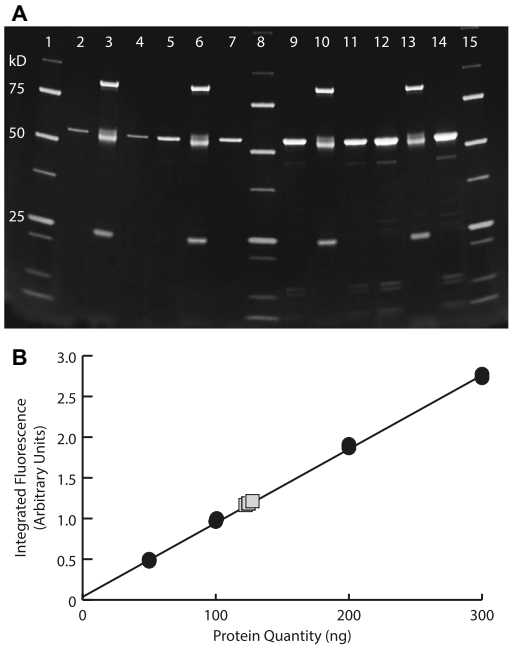

Fig.1. Quantification of polymerases. The purity and size of polymerases were determined on reducing polyacrylamide gels after staining with Sypro orange. (A) Quantification of SpeedStar. Four replicates of the SpeedStar (lanes 3, 6, 10, and 13) were compared to Klentaq I standards at 50 ng (lanes 2 and 4), 100 ng (lanes 5 and 7), 200 ng (lanes 9 and 11), and 300 ng (lanes 12 and 14). Molecular mass markers (Precision Plus Protein, Bio-Rad) are shown in lanes 1, 8, and 15. SpeedStar is an antibody hot-start polymerase and bands corresponding to heavy and light chains are shown near 25 and 50 kDa. The top band near 90 kDa is the polymerase. (B) Quantification of polymerases from a standard curve. The integrated fluorescence intensity of the unknown polymerase (squares) is projected on a regression line through the Klentaq I quantification standards (circles). The R^2 of the regression line is 0.999.

Table 1
Polymerase concentrations of stock solutions purchased from the manufacturers and their recommended concentrations in PCR.

Polymerase	Source	Stock concentration (μM)	Recommended PCR concentration (nM)
Taq (NEB)	Native Taq	1.06 ± 0.01	5.3 ± 0.1
Taq (Roche)	Native Taq	0.26 ± 0.01	5.2 ± 0.1
Amplitaq	Native Taq	0.52 ± 0.02	2.6 ± 0.1
GoTaq	Native Taq	0.98 ± 0.08	4.9 ± 0.4
MyTaq	Native Taq	1.31 ± 0.04	26.1 ± 0.8
ExTaq	Native Taq	1.28 ± 0.08	10.2 ± 0.7
Platinum	Native Taq	0.65 ± 0.02	2.6 ± 0.1
Herculase II	*Pfu* fusion variants	1.9 ± 0.1	19.4 ± 1.3
Phusion	*Pfu* fusion variants	1.01 ± 0.05	10.1 ± 0.5
Klentaq I [13] (ABPeptides)	Deletion variant	39.4 ± 1.5	63 ± 2.5
Titanium [13]	Deletion variant	9.9 ± 0.2	197 ± 3.6
KAPA2G	Engineered Taq	1.11 ± 0.09	4.4 ± 0.4
Paq5000 [16]	*Pfu*	0.85 ± 0.02	8.5 ± 0.2
KOD [15,17]	*Thermococcus kodakaraensis*	4.7 ± 0.2	95 ± 4.1
SpeedStar	Proprietary	1.08 ± 0.06	5.4 ± 0.3

vendors supply polymerases at a concentration around 1 μM. Additionally, the concentration of polymerase in PCR is typically in the range of 5 to 20 nM. Exceptions are KOD (94.5 nM), Klentaq I (63 nM), and Titanium (197 nM), which are supplied and used at considerably higher concentrations.

Assay validation and calibration

Extension rates were derived from the initial slope of the extension curves. Fig. 2 shows that the initial slope is proportional to polymerase concentration from at least 1 to 50 nM. To obtain rates in absolute units, extension curves were calibrated in one of two ways.

Substrate exhaustion

Polymerase extension reactions are allowed to proceed to saturation with complete extension of the template. The maximum and minimum data points of individual extension curves are normalized between 0 and the total number of nucleotides that each polymerase molecule can extend. This is calculated as:

$$[\text{Template}] \times L/[\text{Poly}], \quad (1)$$

where [Template] is the concentration of template, L is the length of extension in base pairs, and [Poly] is the concentration of the polymerase. Normalized this way, the initial slope of extension curves directly yields extension rate in nucleotides per second per molecule of polymerase (nt/s).

Calibration with standards

Extension curves can be normalized using oligonucleotide standards (Fig. 3). The baseline fluorescence is measured from the extension template without polymerase present. A synthetic analog of the fully extended template is used as a maximum fluorescence standard. The average fluorescence of the baseline standard is taken as 0 and the average fluorescence of the maximum standards is scaled to the value calculated by Eq. (1). The same offset and scaling factor are also applied to each experimental curve.

Both analyses were compared using Klentaq I at 75 °C. Ten experiments of 8 to 10 shots each were acquired. Substrate exhaustion yielded an extension rate of 102 ± 4.2 nt/s, whereas calibration with oligonucleotide standards gave 99 ± 8.4 nt/s. The standard deviations of individual shots within an experiment were similar for both methods at 3.8 and 3.4%, respectively. Both

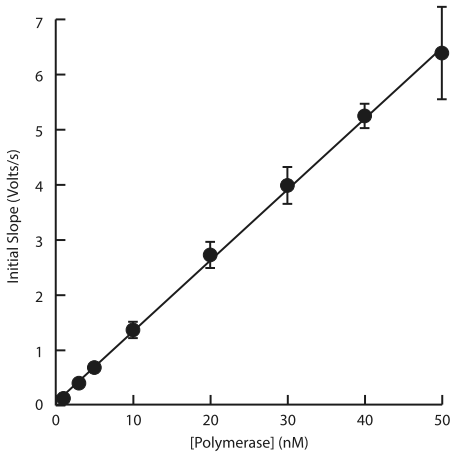

Fig.2. Linearity of extension rates with polymerase concentration. The initial slope of polymerase extension curves is linear with polymerase concentration. A linear regression yields $R^2 = 0.999$. Experiments were performed with Klentaq I.

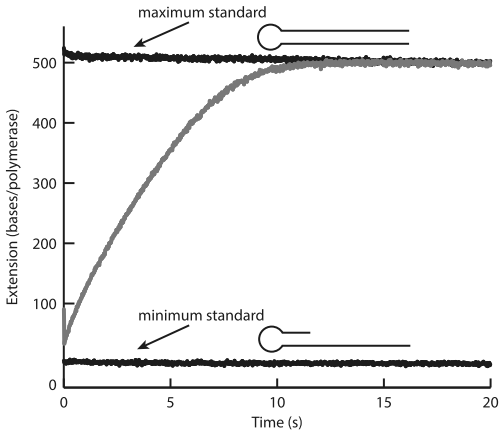

Fig.3. Quantitative analysis of polymerase extension curves. Extension curves are analyzed in one of two ways: (1) by measuring the fluorescence of oligonucleotide standards without polymerase (the minimum standard is the extension template and the maximum standard is a synthetic oligonucleotide identical to the sequence of the fully extended template) or (2) by substrate exhaustion, using time 0 as the fluorescence minimum. In both cases, the maxima and minima are scaled between 0 and the total number of bases extended by each polymerase calculated using Eq. (1). The initial slope is then the extension rate in nucleotides per second per molecule of polymerase (nt/s). Both approaches yield extension rates concordant within 3%.

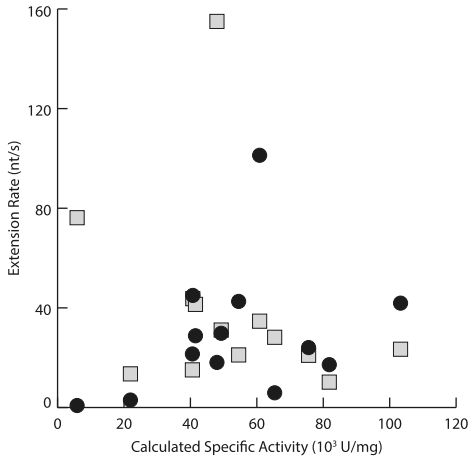

Fig.5. Measured extension rates (nt/s) versus calculated specific activity (U/mg). The specific activity of each polymerase was calculated from the unit concentration supplied by the manufacturer and the mass of polymerase measured from polyacrylamide gels. There is little relationship between the two measurements of specific activity. The correlation is positive in the common buffer (circles), with a Pearson's r coefficient of 0.32, and negative in the vendor buffers (squares), with a Pearson's r coefficient of −0.30.

analysis methods were concordant to within 3%. The advantage of using standards is that reactions need not proceed to exhaustion, greatly reducing acquisition time when the activity is low. However, increased precision makes substrate exhaustion preferable when the activity is high.

Polymerase comparison

The extension rates of various polymerases were measured in their corresponding vendor buffers as well as in a common buffer composed of 50 mM Tris, pH 8.3, 0.5 mg/ml BSA, 2 mM $MgCl_2$, and 200 μM each dNTP (Fig. 4). Most native Taq polymerases varied in extension rate within a factor of 4. MyTaq showed the fastest performance in either buffer, whereas Platinum Taq was the slowest. Overall, rates for the native polymerases were faster in the common buffer with an average of 31.3 nt/s compared to 25.8 nt/s for the vendor buffers. The fusion variants had the slowest extension rates. These are *Pyroccocus furiosis* (*Pfu*) polymerases fused to a double-stranded DNA binding domain intended to improve fidelity. Comparing these rates to that of PAQ5000, an unmodified *Pfu* polymerase [16], the fused domains hinder extension. The deletion

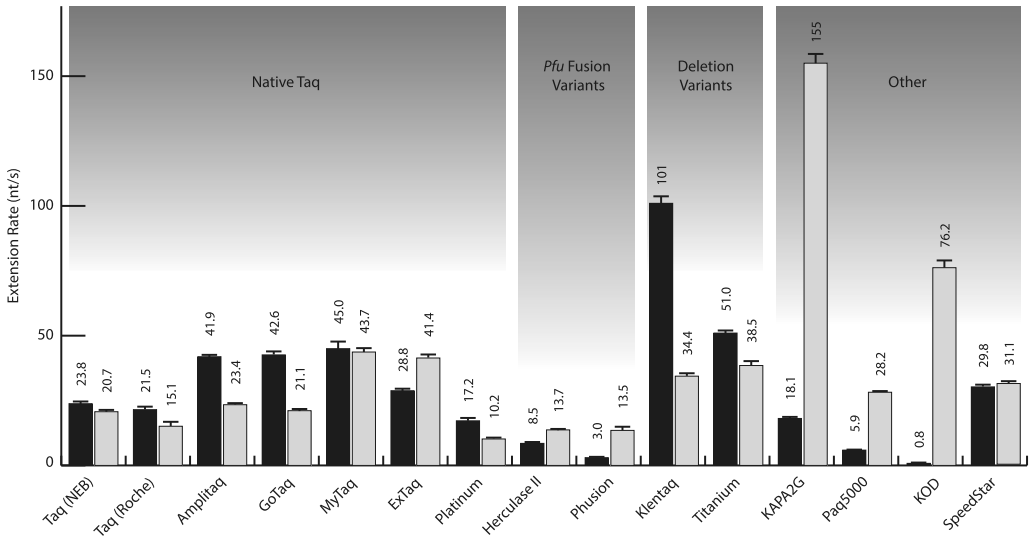

Fig.4. Extension rates of polymerases in the common (black bars) and vendor (gray bars) buffers. Extension rates were strongly influenced by buffer conditions. KOD, Klentaq I, and KAPA2G were the fastest polymerases.

variants are mutants of Taq with a deletion of the 5′ exonuclease domain [13]. These showed faster extension, especially in the common buffer. KAPA2G, an engineered variant of Taq, showed the fastest extension rates. KOD is a polymerase from the *Thermococcus kodakaraensis* KOD1 archae [15,17]. In the vendor buffer, it was the third fastest polymerase. SpeedStar is a polymerase from an organism undisclosed by the manufacturer, but extension rates are similar to those observed for the native Taq polymerases.

The specific activity was calculated from unit concentrations provided by the vendor and the mass of polymerase measured from gels. For most polymerases the specific activity was between 40,000 and 65,000 U/mg. Specific activities were higher for Amplitaq (103,300 U/mg), Platinum Taq (81,800 U/mg), and Taq (NEB) (75,600 U/mg). The specific activities for Phusion (21,900 U/mg) and KOD (5900 U/mg) were lower.

Fig. 5 contrasts the measured extension rates to calculated specific activities. These are analogous measurements of polymerase speed. Both are nucleotide incorporation rates normalized to the amount of polymerase used in the assay. In this study, extension rate is a measurement of the initial rate of nucleotide incorporation using a defined template and is expressed per molecule of polymerase. Specific activity is the rate of nucleotide incorporation into activated DNA and is expressed per milligram of the polymerase. Pearson correlation coefficients were calculated to assess the linear relationship between these two measurements. The relationship is weakly positive when measured in the common buffer and weakly negative when measured in the vendor buffers.

Buffer components

The difference between extension rates in the common versus the vendor buffers for many polymerases is striking. Nearly a 3-fold increase with the common buffer was observed for Klentaq I. The enhancement of KOD and KAPA2G in the vendor buffer approached 100-fold. It is apparent that buffer components strongly influence extension rates.

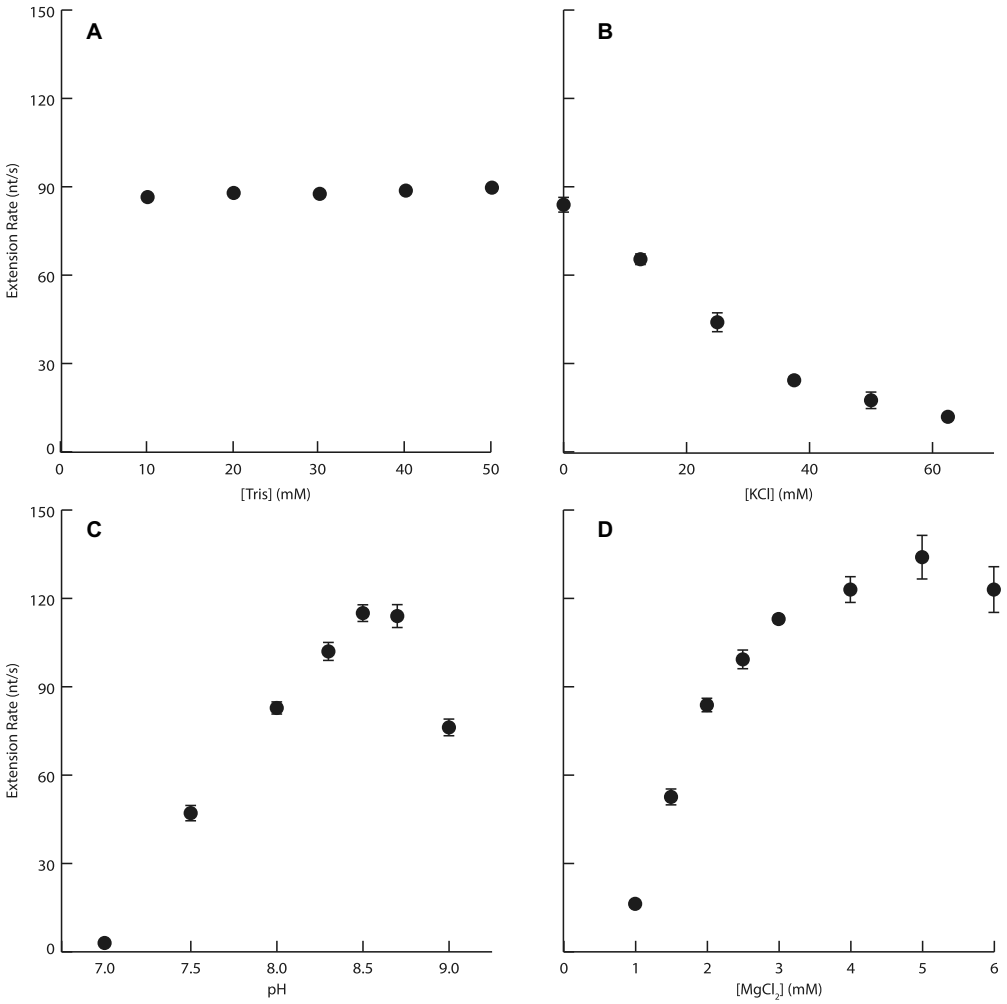

Fig.6. Effects of buffer components on KlenTaq extension rates. (A) Tris has little effect. (B) KCl strongly inhibits extension. (C) Optimal pH for extension is between 8.5 and 8.7, with rapid decreases outside these values. (D) Magnesium increases extension rates with saturation near 5 mM.

The effects of four common components of PCR buffers on extension rates were studied for Klentaq I (Fig. 6). The concentration of Tris has very little influence on extension rates (Fig. 6A). KCl concentration inhibits polymerase activity (Fig. 6B). Extension rates decline linearly between 0 and 37.5 mM with over a 70% decrease. Only 21% of total activity was measured at 50 mM. Optimal pH is between 8.5 and 8.7, with rapid decreases outside of this value (Fig. 6C). Extension is almost entirely inhibited at pH 7. Rates quickly increase with total $MgCl_2$ concentration (Fig. 6D), saturating at 5 mM. At 1.5 mM $MgCl_2$, extension rates were 43% of the maximum at 5 mM.

Discussion

The homogeneous stopped-flow assay presented here provides a simple and precise measurement of polymerase activity. The use of double-stranded DNA dyes allows continuous monitoring of extension. These dyes are commonly used in real-time PCR and eliminate the need for template modifications including covalent labels, radioactivity, or nucleotide analogs that are used in other assays. Template and buffer conditions reflect those found in PCR. Performance of polymerases can easily be tested under a variety of conditions and can aid in screening polymerases and buffer conditions for various applications.

EvaGreen was used in these studies and inhibits PCR with increasing concentration [18]. The same effect has been observed for SYBR Green I [19] and Syto 9 [20]. Comparative studies have shown that the degree of inhibition varies across dyes [18,20,21]. The effect of DNA dyes on polymerase activity has not yet been studied.

In these experiments, template was in 20-fold excess of the polymerase and each polymerase molecule bound and extended multiple templates just as in PCR. It has been shown that template binding is not a limiting step in polymerase extension [22] and is not expected to contribute to the rates measured here. Extension rates are measured in nt/s and have greater relevance to PCR than the standard unit definition. PCR amplifies templates of defined length and knowledge of the extension rates in nt/s provides better insight into the speeds obtainable during PCR. For example, this could guide optimization of thermal cycling protocols for faster and more efficient PCR.

As shown in Fig. 5, vendor-claimed specific activities correlate poorly with measured extension rate per molecule. These are both normalized measurements of the rate of nucleotide incorporation into a template and should be directly comparable. Extension rate is expressed per molecule of polymerase and specific activity is expressed per milligram of polymerase. However, these normalization approaches are similar because the molecular masses of all the polymerases in this study other than Klentaq and Titanium are within about 4%. Poor correlation between the two measurements of activity can be attributed to differences in buffer conditions and extension templates. Buffers used in traditional radiometric assays for polymerase activity vary widely and differences in pH, denaturants, and $MgCl_2$, KCl, template, and dNTP concentration may contribute to disagreement in specific activities reported for polymerases. The average specific activity calculated for the native Taq polymerases in this study is nearly fivefold lower than in a study that measured the specific activity of Taq polymerase at 292,000 U/mg [23] under different conditions. Wide variance in assay conditions complicates comparison of specific activities across studies.

Different templates also introduce variability. Radiometric assays use activated DNA, which is prepared with a variety of techniques including enzymatic digestion and mechanical shearing. This results in a heterogeneous template that does not reflect PCR conditions. PCR amplifies defined templates and is processive rather than random. One study compared the activity of polymerase with activated salmon sperm DNA and a defined template using single-stranded M13 with a primer [23]. The activity differed between the templates by about 60% at 70 °C with Taq polymerase. Activity measurements of DNA polymerases will have greater relevance to their intended use if assay conditions are similar.

Manufacturers claim superior speed for 7 of the 15 polymerases that were studied. Of the native Taq polymerases, fast extension rates are claimed only for MyTaq. This polymerase was the fastest in the category of native Taq polymerases and the fifth fastest polymerase overall (Fig. 4). Fast extension rates are claimed for both the fusion polymerases, Herculase II and Phusion, though they were among the slowest polymerases studied. Phusion claims to be 10-fold faster than unmodified *Pfu* polymerase; however, Phusion was 13.5 nt/s while 28.2 nt/s was observed for Paq5000, a native *Pfu* polymerase. Speed claims are also made for Paq5000, though this polymerase exhibited only moderate activity. KAPA2G and KOD both have fast extension rates as indicated by the manufacturer, but this is dependent on the buffer used. SpeedStar did not demonstrate superior speed as claimed, with a maximum extension rate (31.1 nt/s) only marginally faster than the average extension rate of all native Taq polymerases (28.3 nt/s). The second fastest extension rate was observed with Klentaq I, though this is not generally considered a fast polymerase.

Although the native Taq polymerases should be molecularly similar, their extension rates vary by nearly a factor of 3 in the common buffer. These differences indicate there is some variability in the activity of the same polymerase prepared under different conditions. Also, polymerase extension rates are strongly dependent on buffer conditions and the vendor buffer is not always optimal (Fig. 4). Faster speeds were observed in the common buffer (with 95% confidence) for both of the Taq polymerase deletion variants and five of the seven native Taq polymerases—Taq (NEB), Taq (Roche), Amplitaq, GoTaq, and Platinum Taq. In contrast, faster extension rates were observed in vendor buffers for KAPA2G and KOD.

KCL and $MgCl_2$ concentration and pH greatly influence extension rates. The range of optimal pH is narrow (Fig. 6C). Below the optimum of pH 8.5 to 8.7, extension rates declined about 60% with each pH unit. Above the optimum, the decline was nearly twice as rapid. Another study using a radiometric assay found that optimal pH was dependent on the buffer system [24]. Optimums for Tris, glycine, and potassium phosphate buffers ranged between pH 7.0 and 8.0. For each buffer system, rapid decreases in activity were also observed outside the optimal pH. The highest activity for the Tris buffer was at pH 7.8 and was lower than the pH optimum in our study. This buffer contained components not included in the Tris buffer we used, including 2-mercaptoethanol, KCl, and fivefold higher $MgCl_2$ concentration. This suggests that other components in addition to the buffer system may also influence the optimal pH for extension.

Extension rates continued to increase with $MgCl_2$ concentration until saturating at 5 mM (Fig. 6D). This is a higher concentration than is typically used in PCR, often because of concerns with nonspecific amplification. Greater specificity is achieved with faster thermal cycling [25–27] and higher $MgCl_2$ concentration may be most appropriate in rapid PCR.

KCl strongly inhibits extension (Fig. 6B). A number of methods have been used to study the effect of KCl concentration on polymerase activity, including sequencing [28] and measuring the rate of incorporation of radiolabeled dNTPs [23,24]. The outcome of these studies varied with optimal activity at 0 mM [28], 60 mM [24], or either 10 or 55 mM KCl depending on the template [23]. Two studies used a defined template with primers as opposed to activated DNA [23,28]. These also showed KCl inhibition with

activity greatest in the absence of KCl or at the lowest concentration studied.

The manufacturers of Taq (NEB), Taq (Roche), and Amplitaq disclose the contents of their PCR buffers. Each has 10 mM Tris, 50 mM KCl, and 1.5 mM $MgCl_2$ at pH 8.3. Speeds were similar in the vendor buffer, with extension rates between 15.1 and 23.4 nt/s. These polymerases were faster in the common buffer, presumably because of lower KCl concentration (0 mM) and higher $MgCl_2$ concentration (2 mM). In the common buffer, Klentaq is nearly twofold faster than Titanium but has slightly lower activity in the vendor buffers. This behavior is not adequately explained by the influence of the components studied. Both vendor buffers have identical $MgCl_2$ concentration. The pH of the Klentaq buffer is 9.1 and that of the Titanium buffer is 8.0. Our results in Fig. 6Cindicate that the pH's of both buffers are suboptimal. In addition, the Titanium buffer contains KCl at 16 mM, whereas the Klentaq buffer does not. Also included in the Klentaq buffer is ammonium sulfate at 16 mM, which was not studied here. Further studies of this component as well as other PCR additives will allow more complete elucidation of optimal buffer components.

Buffer conditions affect the fidelity of nucleotide incorporation. For example, the rate of base substitution error increases fivefold for Taq polymerase when increasing $MgCl_2$ concentrationfrom 1 to 5 mM [29]. In contrast, the error decreases threefold for *Pfu* polymerase over the same concentration range [30]. The pH of buffers has also been shown to positively and negatively affect fidelity [29–31]. For applications sensitive to nucleotide misincorporation, additional methods should be used to verify adequate fidelity.

Accurate measurement of polymerase activity under PCR conditions has strong implications in achieving rapid PCR. Advancements in instrumentation continue to decrease thermal cycling times, allowing amplification within a few minutes [32–34]. Realizing the full potential of PCR will require optimization of both instrumentation and chemistry. Conditions that are sufficient for standard PCR may not be well suited to very fast PCR. As cycling times are reduced, even small differences in activity may have an impact on the success of amplification. Measurements of activity are more relevant when defined in terms of nucleotides per second per molecule of polymerase rather than units per milligram. Accurate quantification of polymerase activity under optimal reaction conditions will facilitate PCR with maximum speed and efficiency.

Acknowledgment

This work was supported by a Grant from BioFire Diagnostics.

References

[1] S. Kasas, N.H. Thomson, B.L. Smith, H.G. Hansma, X. Zhu, M. Guthold, C. Bustamante, E.T. Kool, M. Kashlev, P.K. Hansma, Escherichia coli RNA polymerase activity observed using atomic force microscopy, Biochemistry 36 (1997) 461–468.
[2] D.A. Schafer, J. Gelles, M.P. Sheetz, R. Landick, Transcription by single molecules of RNA polymerase observed by light microscopy, Nature 352 (1991) 444–448.
[3] G.J. Wuite, S.B. Smith, M. Young, D. Keller, C. Bustamante, Single-molecule studies of the effect of template tension on T7 DNA polymerase activity, Nature 404 (2000) 103–106.
[4] H. Matsuno, K. Niikura, Y. Okahata, Direct monitoring kinetic studies of DNA polymerase reactions on a DNA-immobilized quartz-crystal microbalance, Chemistry 7 (2001) 3305–3312.
[5] D.L. Earnshaw, A.J. Pope, FlashPlate scintillation proximity assays for characterization and screening of DNA polymerase, primase, and helicase activities, J. Biomol. Screen. 6 (2001) 39–46.
[6] R.S. Johnson, M. Strausbauch, R. Cooper, J.K. Register, Rapid kinetic analysis of transcription elongation by *Escherichia coli* RNA polymerase, J. Mol. Biol. 381 (2008) 1106–1113.
[7] A.S. Suarez, A. Stefan, S. Lemma, E. Conte, A. Hochkoeppler, Continuous enzyme-coupled assay of phosphate- or pyrophosphate-releasing enzymes, Biotechniques 53 (2012) 99–103.
[8] M.A. Griep, Fluorescence recovery assay: a continuous assay for processive DNA polymerases applied specifically to DNA polymerase III holoenzyme, Anal. Biochem. 232 (1995) 180–189.
[9] P. Gong, G. Campagnola, O.B. Peersen, A quantitative stopped-flow fluorescence assay for measuring polymerase elongation rates, Anal. Biochem. 391 (2009) 45–55.
[10] S.P. Mestas, A.J. Sholders, O.B. Peersen, A fluorescence polarization-based screening assay for nucleic acid polymerase elongation activity, Anal. Biochem. 365 (2007) 194–200.
[11] G.Q. Tang, V.S. Anand, S.S. Patel, Fluorescence-based assay to measure the real-time kinetics of nucleotide incorporation during transcription elongation, J. Mol. Biol. 405 (2011) 666–678.
[12] G. Kallansrud, B. Ward, A comparison of measured and calculated single- and double-stranded oligodeoxynucleotide extinction coefficients, Anal. Biochem. 236 (1996) 134–138.
[13] W.M. Barnes, Thermostable DNA polymerase with enhanced thermostability and enhanced length and efficiency of primer extension. Official Gazette of the United States Patent and Trademark Office Patents 1176 (1995) 2601–2601.
[14] F.C. Lawyer, S. Stoffel, R.K. Saiki, K. Myambo, R. Drummond, D.H. Gelfand, Isolation, characterization, and expression in *Escherichia coli* of the DNA polymerase gene from Thermus aquaticus, J. Biol. Chem. 264 (1989) 6427–6437.
[15] M. Takagi, M. Nishioka, H. Kakihara, M. Kitabayashi, H. Inoue, B. Kawakami, M. Oka, T. Imanaka, Characterization of DNA polymerase from *Pyrococcus* sp. strain KOD1 and its application to PCR, Appl. Environ. Microbiol. 63 (1997) 4504–4510.
[16] K.S. Lundberg, D.D. Shoemaker, M.W. Adams, J.M. Short, J.A. Sorge, E.J. Mathur, High-fidelity amplification using a thermostable DNA polymerase isolated from *Pyrococcus furiosus*, Gene 108 (1991) 1–6.
[17] M. Nishioka, H. Mizuguchi, S. Fujiwara, S. Komatsubara, M. Kitabayashi, H. Uemura, M. Takagi, T. Imanaka, Long and accurate PCR with a mixture of KOD DNA polymerase and its exonuclease deficient mutant enzyme, J. Biotechnol. 88 (2001) 141–149.
[18] F. Mao, W.Y. Leung, X. Xin, Characterization of EvaGreen and the implication of its physicochemical properties for qPCR applications, BMC Biotechnol. 7 (2007) 76.
[19] C.T. Wittwer, M.G. Herrmann, A.A. Moss, R.P. Rasmussen, Continuous fluorescence monitoring of rapid cycle DNA amplification, Biotechniques 22 (1997) 130–131. 134–138.
[20] P.T. Monis, S. Giglio, C.P. Saint, Comparison of SYTO9 and SYBR Green I for real-time polymerase chain reaction and investigation of the effect of dye concentration on amplification and DNA melting curve analysis, Anal. Biochem. 340 (2005) 24–34.
[21] H. Gudnason, M. Dufva, D.D. Bang, A. Wolff, Comparison of multiple DNA dyes for real-time PCR: effects of dye concentration and sequence composition on DNA amplification and melting temperature, Nucleic Acids Res. 35 (2007) e127.
[22] R.D. Kuchta, V. Mizrahi, P.A. Benkovic, K.A. Johnson, S.J. Benkovic, Kinetic mechanism of DNA polymerase I (Klenow), Biochemistry 26 (1987) 8410–8417.
[23] F.C. Lawyer, S. Stoffel, R.K. Saiki, S.Y. Chang, P.A. Landre, R.D. Abramson, D.H. Gelfand, High-level expression, purification, and enzymatic characterization of full-length *Thermus aquaticus* DNA polymerase and a truncated form deficient in 5′ to 3′ exonuclease activity, PCR Methods Appl. 2 (1993) 275–287.
[24] A. Chien, D.B. Edgar, J.M. Trela, Deoxyribonucleic acid polymerase from the extreme thermophile *Thermus aquaticus*, J. Bacteriol. 127 (1976) 1550–1557.
[25] T.G. Mamedov, E. Pienaar, S.E. Whitney, J.R. TerMaat, G. Carvill, R. Goliath, A. Subramanian, H.J. Viljoen, A fundamental study of the PCR amplification of GC-rich DNA templates, Comput. Biol. Chem. 32 (2008) 452–457.
[26] C.T. Wittwer, D.J. Garling, Rapid cycle DNA amplification: time and temperature optimization, Biotechniques 10 (1991) 76–83.
[27] C.T. Wittwer, B.C. Marshall, G.H. Reed, J.L. Cherry, Rapid cycle allele-specific amplification: studies with the cystic fibrosis delta F508 locus, Clin. Chem. 39 (1993) 804–809.
[28] M.A. Innis, K.B. Myambo, D.H. Gelfand, M.A. Brow, DNA sequencing with *Thermus aquaticus* DNA polymerase and direct sequencing of polymerase chain reaction-amplified DNA, Proc. Natl. Acad. Sci. U.S.A. 85 (1988) 9436–9440.
[29] K.A. Eckert, T.A. Kunkel, High fidelity DNA synthesis by the *Thermus aquaticus* DNA polymerase, Nucleic Acids Res. 18 (1990) 3739–3744.
[30] J. Cline, J.C. Braman, H.H. Hogrefe, PCR fidelity of pfu DNA polymerase and other thermostable DNA polymerases, Nucleic Acids Res. 24 (1996) 3546–3551.
[31] K.A. Eckert, T.A. Kunkel, Effect of reaction pH on the fidelity and processivity of exonuclease-deficient Klenow polymerase, J. Biol. Chem. 268 (1993) 13462–13471.
[32] M. Hashimoto, P.C. Chen, M.W. Mitchell, D.E. Nikitopoulos, S.A. Soper, M.C. Murphy, Rapid PCR in a continuous flow device, Lab Chip 4 (2004) 638–645.
[33] E.K. Wheeler, C.A. Hara, J. Frank, J. Deotte, S.B. Hall, W. Benett, C. Spadaccini, N.R. Beer, Under-three minute PCR: probing the limits of fast amplification, Analyst 136 (2011) 3707–3712.
[34] C.T. Wittwer, R.P. Rasmussen, K.M. Ririe, Rapid polymerase chain reaction and melting analysis, in: S.A. Bustin (Ed.), The PCR Revolution: Basic Technologies and Applications, Cambridge Univ. Press, New York, 2010, pp. 48–69.

CHAPTER 3

THE INFLUENCE OF PCR REAGENTS ON DNA POLYMERASE EXTENSION RATES MEASURED ON REAL-TIME PCR INSTRUMENTS

Reprinted from Clinical Chemistry, clinchem.2013.212829 Published-Ahead-of-Print, September 30, 2013, Jesse L. Montgomery and Carl T. Wittwer, "Influence of PCR Reagents on DNA Polymerase Extension Rates Measured on Real-Time PCR Instruments," with permission of the American Association for Clinical Chemistry.

Influence of PCR Reagents on DNA Polymerase Extension Rates Measured on Real-Time PCR Instruments

Jesse L. Montgomery,[1] and Carl T. Wittwer[1*]

BACKGROUND: Radioactive DNA polymerase activity methods are cumbersome and do not provide initial extension rates. A simple extension rate assay would enable study of basic assumptions about PCR and define the limits of rapid PCR.

METHODS: A continuous assay that monitors DNA polymerase extension using noncovalent DNA dyes on common real-time PCR instruments was developed. Extension rates were measured in nucleotides per second per molecule of polymerase. To initiate the reaction, a nucleotide analog was heat activated at 95 °C for 5 min, the temperature decreased to 75 °C, and fluorescence monitored until substrate exhaustion in 30–90 min.

RESULTS: The assay was linear with time for over 40% of the reactions and for polymerase concentrations over a 100-fold range (1–100 pmol/L). Extension rates decreased continuously with increasing monovalent cation concentrations (lithium, sodium, potassium, cesium, and ammonium). Melting-temperature depressors had variable effects. DMSO increased rates up to 33%, whereas glycerol had little effect. Betaine, formamide, and 1,2-propanediol decreased rates with increasing concentrations. Four common noncovalent DNA dyes inhibited polymerase extension. Heat-activated nucleotide analogs were 92% activated after 5 min, and hot start DNA polymerases were 73%–90% activated after 20 min.

CONCLUSIONS: Simple DNA extension rate assays can be performed on real-time PCR instruments. Activity is decreased by monovalent cations, DNA dyes, and most melting temperature depressors. Rational inclusion of PCR components on the basis of their effects on polymerase extension is likely to be useful in PCR, particularly rapid-cycle or fast PCR.

Several methods have been developed to measure the activity of DNA polymerases, but complexity, time requirements, and specialized instrumentation have prevented their widespread use. Polymerase activity is most often characterized with radiometric assays. These assays measure the incorporation of radiolabelled deoxyribonucleotide triphosphates (dNTPs)[2] into mechanically sheared or enzymatically digested complex genomic DNA. Activity is measured in terms of units that are generally defined as the amount of enzyme required to incorporate 10 nmol of dNTP in 30 min. However, assay conditions and unit definitions are not standardized, making comparison between measurements difficult. In addition, end-point methods do not provide initial rates and application to PCR kinetics is limited.

Other methods have been used to measure polymerase kinetics, including atomic force microscopy *(1)*, light microscopy *(2)*, single molecule optical trapping *(3)*, quench flow *(4)*, stopped flow *(4–7)*, and quartz crystal microbalance *(8)*. Each of these requires instrumentation not found in most laboratories and has relatively low throughput. Other assays have been adapted for more common instruments, including benchtop fluorometers and microplate readers *(9–11)*. However, these require covalent fluorescent labels, enzyme-coupled reactions, or saturating amounts of single-stranded DNA binding protein.

Previously we reported a continuous polymerase activity assay that uses a stopped-flow instrument *(7)*. Nucleotide incorporation was monitored with DNA dyes typically used in real-time PCR, eliminating the need to alter reaction chemistry. In the investigation we report here, the assay was modified for use on common real-time PCR instruments. The effects of monovalent cations, melting temperature (Tm) depressors, and DNA dyes on polymerase extension rates were measured.

Materials and Methods

DNA POLYMERASES

Klentaq I (purchased from Wayne M. Barnes at Washington University in St. Louis), FastStart™ (Roche),

[1] Department of Pathology, University of Utah Health Sciences Center, Salt Lake City, UT.
* Address correspondence to this author at: Department of Pathology, University of Utah Medical School, 50 N. Medical Drive, Salt Lake City, Utah 84132. Fax 801-581-6001; e-mail carl.wittwer@path.utah.edu.

Received July 9, 2013; accepted August 27, 2013.
Previously published online at DOI: 10.1373/clinchem.2013.212829

Platinum® (Invitrogen), Amplitaq® (Invitrogen), *Taq* (New England Biolabs), GoTaq® (Promega), Titanium® *Taq* (Clontech), KAPA2G (Kapa Biosystems), MyTaq™ (Bioline), Ex *Taq*® (Clontech), *Taq* (Roche), SpeedSTAR™ (Clontech), KOD (EMD Millipore), Paq5000 (Agilent), Herculase II (Agilent), Phusion® (New England Biolabs), and Amplitaq® Gold (Invitrogen) were quantified as described previously *(7)* on SDS gels stained with Sypro® Orange (Invitrogen).

POLYMERASE EXTENSION TEMPLATE

A self-complementary oligonucleotide with the sequence tagcgaaggatgtgaacctaatcccTGCTCCCGCGGC CGatctgcCGGCCGCGGGAGCA was used as the extension template (capital letters denote self-complementary sequences). This forms a hairpin with a 14-bp stem that has a free 3′ end and a 25-base overhang for extension. The oligonucleotide was ordered from Integrated DNA Technologies and purified by high-pressure liquid chromatography. Concentrations were determined by absorbance at 260 nm following digestion with purified phosphodiesterase *(12)*.

POLYMERASE EXTENSION ASSAY

Extension reactions were performed with a LightCycler® 480 (Roche). Except where otherwise indicated, final concentrations were 50 mmol/L Tris (pH 8.3), 3 mmol/L $MgCl_2$, 1× LCGreen Plus, 50 pmol/L Klentaq I, 100 nmol/L oligonucleotide template, and 200 μmol/L of each nucleotide. CleanAmp™ dGTP (TriLink BioTechnologies) was mixed with unmodified dATP, dCTP (deoxycytidine triphosphate), and dTTP (deoxythymidine triphosphate) (Bioline) to limit extension of the template before temperature equilibration. Preliminary studies showed that the use of a single heat-activated nucleotide with 3 unmodified nucleotides increased extension rates by a mean of 14% compared to using all 4 heat-activated nucleotides. Reduced extension rates were likely caused by lower available dNTPs due to incomplete conversion of the heat-activated nucleotides.

The concentration of polymerase was reduced to 50 pmol/L to lengthen the reaction time and ensure initial rates were observed. This is at least 100-fold below typical PCR concentrations of 5–20 nmol/L *(7)*. To reduce protein loss with serial dilutions, polymerases were diluted from the commercial stock solution immediately before extension reactions in 50 mmol/L Tris (pH 8.3), 300 μg/mL BSA, and 0.03% Tween® 20. The reaction was initiated by activating the CleanAmp dGTP at 95 °C for 5 min, followed by fluorescence monitoring of nucleotide incorporation at 75 °C. This was accomplished by programming the LightCycler 480 for repeated holds at 75 °C for 1 s with a single acquisition. Reactions were allowed to continue to exhaustion (30–90 min). Four replicates of each reaction were performed and the SDs reported.

PCR DYES AND ADDITIVES

Monovalent cations, Tm depressors, DNA dyes, and $MgCl_2$ were titrated into extension reactions to determine their effects on extension rates. LiCl, NaCl, KCl, CeCl, and $(NH_4)_2SO_4$ were included at final monovalent cation concentrations up to 50 mmol/L. Final concentrations of betaine and 1,2-propanediol up to 2.5 mol/L, DMSO and glycerol up to 10%, and formamide up to 7.5% (v/v) were examined. LCGreen® Plus (BioFire Diagnostics), EvaGreen® (Biotium), and SYBR® Green I (Invitrogen) were studied from 0.1 to 5× (approximately 0.1–5 μmol/L) *(13)*, and Syto® 9 (Invitrogen) was examined from 0.4 to 10.0 μmol/L. $MgCl_2$ was studied at concentrations up to 6 mmol/L. In addition to Klentaq I, $MgCl_2$ titrations were also performed for Platinum, Amplitaq, *Taq* (NEB), GoTaq, Titanium, KAPA2G, MyTaq, Ex *Taq*, *Taq* (Roche), and SpeedSTAR.

HOT START ACTIVATION

The activation times of 2 chemical hot start polymerases (FastStart and Amplitaq Gold) and heat-activated nucleotide analogs (CleanAmp dNTPs) were assessed. Extension reactions were performed as described above, except that unmodified dNTPs were used with the hot start polymerases and all 4 heat-activated dNTPs were used with Klentaq I. Activation times between 5 s and 60 min at 95 °C were investigated. The concentration of polymerase was increased to 100 pmol/L with 60-min activation times to compensate for low extension rates.

ASSAY CALIBRATION

Linearity between fluorescence and dNTP incorporation was assumed. The first 15 s of data were excluded to eliminate artifacts of initial temperature equilibration. Polymerization was allowed to proceed to substrate exhaustion, apparent as a maximum plateau and taken as the fluorescence equivalent of 100% extension.

Calibration of fluorescence data allows measurement of polymerase activity. Additionally, specific activity in terms of extension rates can be calculated if polymerase quantification is performed.

POLYMERASE ACTIVITY

Extension curves were normalized between zero and the total number of nucleotides that can be extended, given by:

$$[\text{Template}] \times L \times V, \qquad \text{(Eq. 1)}$$

where [Template] is the concentration of template in nanomoles per liter, L is the extension length of the

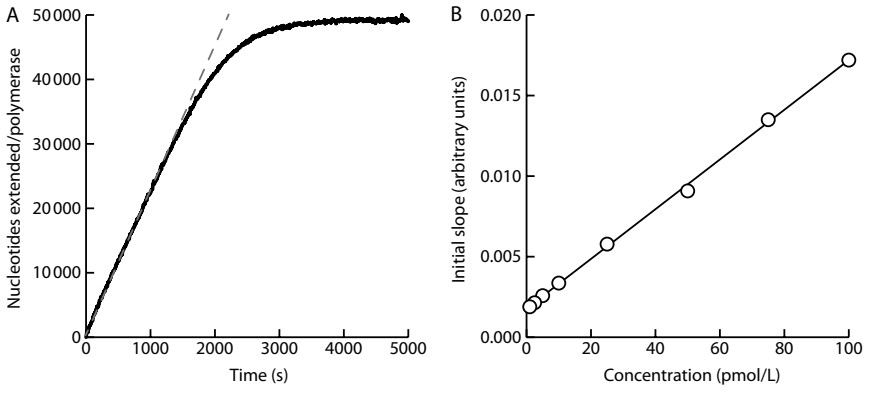

Fig. 1. Validation of a polymerase extension rate assay that mimics PCR with increased fluorescence from dye incorporation performed on a real-time PCR instrument.

Increase of fluorescence signal during nucleotide incorporation is linear with time for at least 40% of reaction completion (A). Initial slope of fluorescence data is linear with polymerase concentrations from 1 to at least 100 pmol/L with $R^2 = 0.999$ (B).

substrate in bases, and V is the volume of the reaction in liters. The initial slope of the normalized extension curves yields polymerase activity in nanomoles of nucleotides per second.

EXTENSION RATES

Extension curves were normalized between zero and the total number of nucleotides that each polymerase molecule can extend, given by:

$$[\text{Template}] \times \text{L}/[\text{Poly}], \qquad \text{(Eq. 2)}$$

where [Poly] is the concentration of the polymerase in nanomoles per liter. With time in seconds as the *x* axis, the initial slope is the extension rate in nucleotides per second per molecule of polymerase, or simply seconds^{-1}.

Results

Polymerase extension was linear with time for at least 40% of the reaction (Fig. 1A). The initial slope of extension was proportional to the polymerase concentrations from 1 pmol/L to at least 100 pmol/L (Fig. 1B). Polymerases were diluted in a buffer containing detergent and BSA. When diluted without these components, variable decreases in activity were observed. This was presumably due to loss of polymerase by adsorption onto surfaces during serial dilutions. Tween 20 was used here, but similar retention of activity was obtained with IGEPAL® CA-630, Triton™ X-100, and Brij® 58. The highest extension rates were observed with detergent at 0.03% and BSA at 0.3 g/L (data not shown).

All monovalent cations decreased extension rates (Fig. 2). Lithium, sodium, potassium, and cesium had a similar effect, with a mean decrease of 57% at 25 mmol/L. Ammonium most strongly reduced rates, with a decrease of 79% at 25 mmol/L. Extension assays were also performed with divalent cations replacing magnesium. Calcium, manganese, cobalt, and zinc

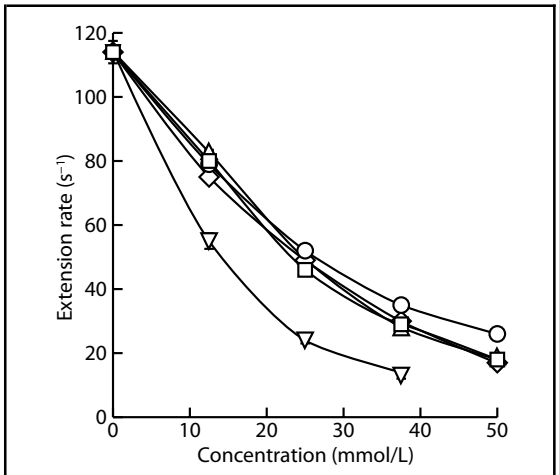

Fig. 2. Effect of monovalent cations on extension rates.

Cations of lithium (circles), sodium (squares), potassium (diamonds), and cesium (triangles) all produce similar decreases in rates. Cations of ammonium (inverted triangle) show the strongest inhibition.

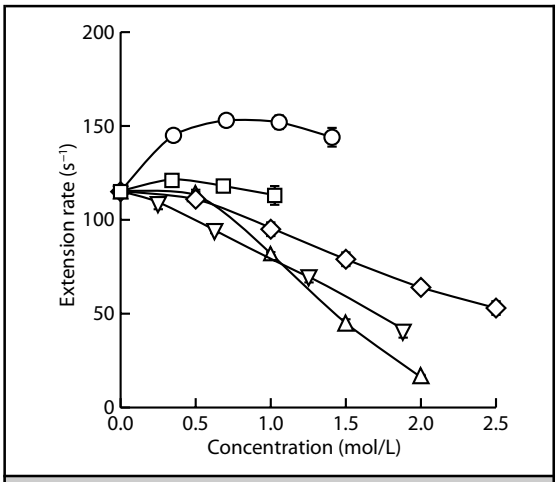

Fig. 3. Effect of Tm depressors on extension rates.
DMSO (circles), glycerol (squares), betaine (diamonds), propanediol (triangles), formamide (inverted triangles). DMSO increased extension rates at concentrations up to 10% (1.4 mol/L). Glycerol had little effect on rate. Betaine, propanediol, and formamide each decreased rates with increasing concentration. Propanediol at 2.5 mol/L was not measured because of low activity.

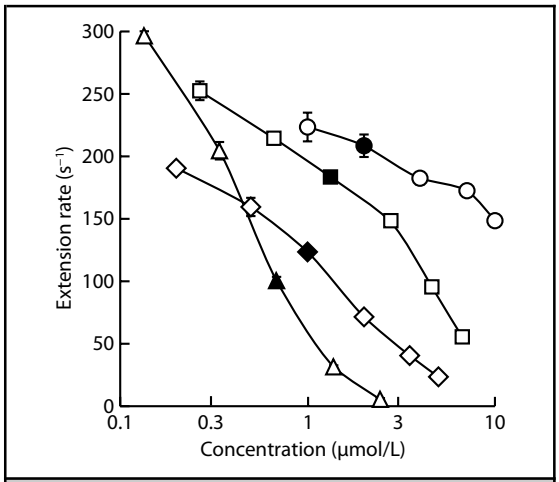

Fig. 4. Effect of DNA dyes on extension rates.
Syto 9 (circles), EvaGreen (squares), LCGreen Plus (diamonds), SYBR Green I (triangles). Typical 1× concentrations used in PCR are indicated by filled markers. Extension rates were not measured for SYBR Green I at 5× (3.4 μmol/L) because of low activity and for Syto 9 at 0.4 μmol/L because of low signal. Dye concentrations are plotted on a log scale.

were tested at concentrations ranging from 0.3 to 10 mmol/L. Each of these produced artifacts in fluorescence (i.e., quenching or enhancement) that precluded accurate analysis (data not shown).

The effect of Tm depressors on extension rates is shown in Fig. 3. DMSO enhanced rates at concentrations up to 10% (1.4 mol/L), with an optimum between 5 and 7.5% (0.7 and 1.1 mol/L). Glycerol had very little effect on extension, with a small increase of 5% at 2.5% (0.3 mol/L) and a decrease of 6% at 10% (1.4 mol/L). Betaine and propanediol did not influence rates at 0.5 mol/L but showed linear decreases above this concentration. Extension rates decreased with betaine at a rate of 16% with every increase of 0.5 mol/L beyond 0.5 mol/L. Propanediol showed twice the inhibition, with a decrease of 33% per 0.5 mol/L. A small decrease in rate of 6% was observed with formamide at a 1% concentration (0.3 mol/L). At higher concentrations, extension rates also declined linearly. The rates decreased 10% for every 1% increase of the formamide concentration.

Each of the DNA dyes studied decreased polymerase extension rates, but to varying degrees (Fig. 4). SYBR Green I showed the greatest inhibition, followed by LCGreen Plus, EvaGreen, and Styo 9. Extension rates for the dyes at typical 1× concentrations varied over a 2-fold range with SYBR Green I at 101 s^{-1}, LCGreen Plus at 124 s^{-1}, EvaGreen at 184 s^{-1}, and Syto 9 at 209 s^{-1}.

Extension rates increased with increasing concentrations of $MgCl_2$ up to 6 mmol/L for 9 of the 11 polymerases studied (see Fig. 1 in the Data Supplement that accompanies the online version of this report at http://www.clinchem.org/content/vol60/issue2). $MgCl_2$ between 4 and 5 mmol/L produced the fastest extension rates for Titanium and Klentaq I, 2 deletion variants of *Taq* polymerase, with decreasing rates at higher concentrations. Data from 4 additional polymerases (KOD, Paq5000, Herculase II, and Phusion) could not be analyzed because the template was degraded by 3′ to 5′ exonuclease activity before acquisition. Optimal conditions for fast polymerase extension found here and in our previous study *(7)* are summarized in Fig. 5.

Fig. 6 shows extension rates as a function of activation time at 95 °C for heat-activated nucleotide analogs (CleanAmp dNTPs) and 2 chemical hot start polymerases (FastStart and Amplitaq Gold). The heat-activated nucleotides were maximally active after 20 min with an extension rate of 110 s^{-1}, but activation was 92% complete after 5 min. Maximal activity of the hot start polymerases required 40 min, with extension rates of 45 s^{-1} for FastStart and 28 s^{-1} for Amplitaq Gold. After 20 min, activation was 90% complete for FastStart and 73% complete for AmpliTaq Gold. Consistent with prior findings *(7)*, the maximal extension

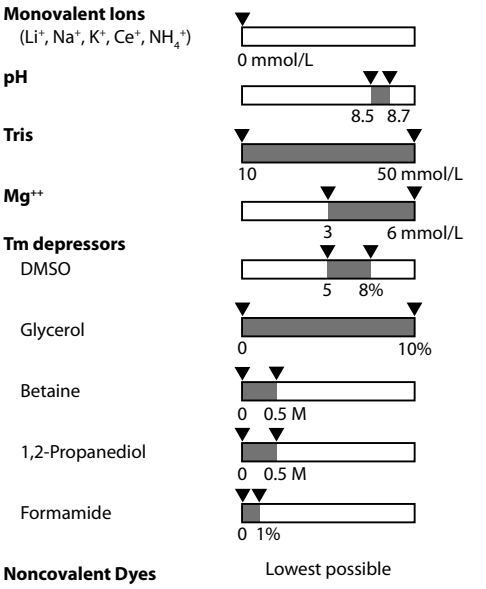

Fig. 5. Optimal conditions for fast polymerase extension. Fastest rates are obtained by eliminating monovalent ions, using high $MgCl_2$ between 3 and 6 mmol/L, and including DMSO between 5% and 8%. Optimal pH is narrow, between 8.5 and 8.7, and Tris has little effect *(7)*. Betaine and 1,2-propanediol are best kept below 0.5 mol/L and formamide below 1%. Noncovalent dyes are best used at the lowest concentration that produces the desired fluorescence intensity.

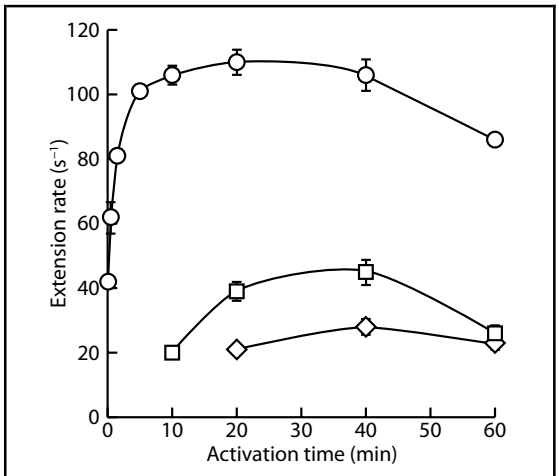

Fig. 6. Extension rates after activation with hot start polymerases and nucleotides. FastStart (squares), Amplitaq Gold (diamonds), hot-start nucleotide analogs (circles). FastStart showed nearly double the extension rates of Amplitaq Gold with the same activation time. The hot start nucleotides required half the activation time as the hot start polymerases for maximum activity.

rate of native Taqs was lower than with deletion variants.

Compared to the previously described stopped-flow assay *(7)*, convenience and throughput are greatly improved, with a 96/384 well plate format without compromise of accuracy or precision (data not shown). The instrument expense and setup requirements of a temperature-controlled stopped-flow apparatus also greatly exceed those of real-time PCR machines.

Discussion

Measurement of polymerase extension rates on common real-time PCR instruments enables systematic study of numerous PCR reagents and conditions. Prior work has been hindered by laborious radiolabeled assays or expensive instrumentation. Our previously reported stopped-flow assay conveniently used noncovalent DNA dyes to measure polymerase extension *(7)*. Conversion of the stopped-flow assay to real-time PCR instruments required (*a*) decreasing the concentration of polymerase to increase the reaction time to 30–90 min, (*b*) using a heat-activated nucleotide analog to prevent extension during sample preparation, and (*c*) activating the nucleotides at 95 °C for 5 min, followed by rapid cooling to the desired extension temperature (75 °C) to ensure that initial velocities are observed. It was also critical to dilute the polymerase in detergent and BSA, presumably to prevent polymerase adsorption on vessel walls during dilution. Although we used a LightCycler 480, any instrument capable of exporting fluorescence data as a function of time can be used. We have developed an online tool to simplify analysis of the kinetic data (https://www.dna.utah.edu/ext/ExtensionCalc.php).

Extension rates are normalized to a single polymerase molecule and are analogous to specific activity. However, unlike prior radiometric assays, initial velocities are measured, templates are standardized, and the buffers mimic those in PCR. As a result, extension rates better reflect the kinetics seen in PCR with processive extension of a defined template for more reproducible activity measurements.

Polymerase quantification is not necessary when only activity measurements are desired. The initial slope of calibrated curves yields polymerase activity in nanomoles of nucleotides per second. This is analogous to the unit definition of activity, except that initial velocities rather than end-point rates are measured.

All monovalent cations studied decreased extension rates in a concentration-dependent manner (Fig. 2). Oddly enough, potassium chloride and ammonium sulfate are frequently found in PCR buffers. With these components, amplification appeared more specific with higher yields in some reported studies *(14–16)*. Fig. 2 indicates that any benefit obtained from inclusion of monovalent cations in PCR does not result from enhanced extension rates.

Tm depressors are often added for PCR of GC-rich templates. We found that DMSO increases extension rates and glycerol has little effect at concentrations up to 10%. Other studies found that activity decreased 50% in the presence of 10% DMSO and 30% with 10% glycerol *(17, 18)*. These prior studies used radioactive assays and activated salmon sperm DNA as a template. We observed a linear decrease in extension rates with formamide concentrations above 1%. A previous study showed no effect up to 10% *(17)*. Another showed a 50% decrease in activity at 10%. Our study showed greater inhibition, with a 65% decrease in the presence of 7.5% formamide. The discrepancies in these studies suggest that greater uniformity in assay conditions and standardization of the template may improve the reproducibility of activity assays.

Betaine and propanediol both produced linear decreases in extension rates. When maximal polymerase extension rates are a concern, betaine, propanediol, and formamide should be used at the lowest concentrations possible for successful amplification.

The noncovalent DNA dyes studied here decrease polymerase extension rates (Fig. 4). Selection of the appropriate dye and concentration will depend on a number of factors, such as instrument optical requirements, desired extension rates, and post-PCR processing. For example, the fastest extension rate was observed for SYBR Green I at 0.2× (0.14 μmol/L). However, SYBR Green I does not detect heteroduplexes in high-resolution melting analysis *(19, 20)*. Faster extension rates can be obtained with each dye by lowering the concentration, but this is also accompanied by a lower signal and may be limiting, depending on the sensitivity of the instrument.

The choice of a hot start method determines the speed of activation before PCR. Chemical hot starts show low extension rates despite very long activation times, though FastStart appears to require about half the activation time of Amplitaq Gold for the same extension rate. Rates were faster for the heat-activated nucleotide analogs at all activation times, indicating a large difference in the specific activity of chemically modified hot start polymerases and Klentaq I. For faster PCR, heat-activated nucleotide analogs are more desirable than modified polymerases.

Routine measurements of activity and extension rates are enabled by this continuous fluorescence assay. High throughput is attained with microtiter plates, allowing simultaneous comparison of several polymerases and conditions. Components are easily optimized to identify suitable PCR reagents and storage buffers. Engineered polymerase variants can be screened for desired activity. Polymerase preparation lots can be assayed for consistent activity to ensure reproducible PCR efficiency. Polymerases screened for high extension rates are needed for rapid PCR applications. Because the extension rate is measured under PCR conditions, insight into the speed of extension obtainable during PCR can guide optimization of thermal cycling protocols for faster, more efficient amplification.

Is PCR constructed rationally, or are we following the initial choices of PCR pioneers and reluctant to change familiar reagents and ingrained protocols? Considering the data obtained from this and our prior stopped-flow study *(7)*, extension rates are improved by high Mg^{2+} (3–6 mmol/L) and DMSO (5%–10%) in a narrow pH range (8.5–8.7) and decreased by K^+, $(NH4)_2SO_4$, dyes, and most Tm suppressors. Of course, PCR is much more than just polymerase extension. Fidelity and specificity are also crucial. Nevertheless, polymerase extension is a central factor in understanding PCR and paramount to efforts to increase its speed.

Author Contributions: *All authors confirmed they have contributed to the intellectual content of this paper and have met the following 3 requirements: (a) significant contributions to the conception and design, acquisition of data, or analysis and interpretation of data; (b) drafting or revising the article for intellectual content; and (c) final approval of the published article.*

Authors' Disclosures or Potential Conflicts of Interest: *Upon manuscript submission, all authors completed the author disclosure form. Disclosures and/or potential conflicts of interest:*

Employment or Leadership: C.T. Wittwer, BioFire Diagnostics, and *Clinical Chemistry*, AACC.
Consultant or Advisory Role: None declared.
Stock Ownership: C.T. Wittwer, BioFire Diagnostics.
Honoraria: None declared.
Research Funding: C.T. Wittwer, BioFire Diagnostics.
Expert Testimony: None declared.
Patents: None declared.

Role of Sponsor: The funding organizations played no role in the design of study, choice of enrolled patients, review and interpretation of data, or preparation or approval of manuscript.

References

1. Kasas S, Thomson NH, Smith BL, Hansma HG, Zhu X, Guthold M, et al. Escherichia coli RNA polymerase activity observed using atomic force microscopy. Biochemistry 1997;36:461–8.
2. Schafer DA, Gelles J, Sheetz MP, Landick R. Transcription by single molecules of RNA polymerase observed by light microscopy. Nature 1991;352: 444–8.
3. Wuite GJ, Smith SB, Young M, Keller D, Bustamante C. Single-molecule studies of the effect of template tension on T7 DNA polymerase activity. Nature 2000;404:103–6.
4. Johnson RS, Strausbauch M, Cooper R, Register JK. Rapid kinetic analysis of transcription elongation by Escherichia coli RNA polymerase. J Mol Biol 2008;381:1106–13.
5. Gong P, Campagnola G, Peersen OB. A quantitative stopped-flow fluorescence assay for measuring polymerase elongation rates. Anal Biochem 2009;391:45–55.
6. Tang GQ, Anand VS, Patel SS. Fluorescence-based assay to measure the real-time kinetics of nucleotide incorporation during transcription elongation. J Mol Biol 2011;405:666–78.
7. Montgomery JL, Rejali N, Wittwer CT. Stopped-flow DNA polymerase assay by continuous monitoring of dNTP incorporation by fluorescence. Anal Biochem 2013;441:133–9.
8. Matsuno H, Niikura K, Okahata Y. Direct monitoring kinetic studies of DNA polymerase reactions on a DNA-immobilized quartz-crystal microbalance. Chemistry 2001;7:3305–12.
9. Griep MA. Fluorescence recovery assay: a continuous assay for processive DNA polymerases applied specifically to DNA polymerase III holoenzyme. Anal Biochem 1995;232:180–9.
10. Mestas SP, Sholders AJ, Peersen OB. A fluorescence polarization-based screening assay for nucleic acid polymerase elongation activity. Anal Biochem 2007;365:194–200.
11. Suarez AS, Stefan A, Lemma S, Conte E, Hochkoeppler A. Continuous enzyme-coupled assay of phosphate- or pyrophosphate-releasing enzymes. Biotechniques 2012;53:99–103.
12. Kallansrud G, Ward B. A comparison of measured and calculated single- and double-stranded oligodeoxynucleotide extinction coefficients. Anal Biochem 1996;236:134–8.
13. Mao F, Leung WY, Xin X. Characterization of EvaGreen and the implication of its physicochemical properties for qPCR applications. BMC Biotechnol 2007;7:76.
14. Olive DM, Simsek M, Al-Mufti S. Polymerase chain reaction assay for detection of human cytomegalovirus. J Clin Microbiol 1989;27: 1238–42.
15. Watanabe M, Abe K, Aoki M, Kameya T, Itoyama Y, Shoji M, et al. A reproducible assay of polymerase chain reaction to detect trinucleotide repeat expansion of Huntington's disease and senile chorea. Neurol Res 1996;18:16–8.
16. Higuchi R, Fockler C, Dollinger G, Watson R. Kinetic PCR analysis: real-time monitoring of DNA amplification reactions. Biotechnology 1993;11: 1026–30.
17. Gelfand DH. Taq DNA polymerase. In: Erlich HA, ed. PCR technology: principles and applications for DNA amplification. New York: Macmillan Publishers; 1989. p 17–22.
18. Landre PA, Gelfand DH, Watson RM. The use of cosolvents to enhance amplification by the polymerase chain reaction. In: Innis MA, Gelfand DH, Sninsky JJ, eds. PCR strategies. San Diego: Academic Press; 1995. p 3–16.
19. Wittwer CT, Kusukawa N. Real-time PCR and melting analysis. In: Persing DH, ed. Molecular microbiology: diagnostic principles and practice. 2nd ed. Washington, DC: ASM Press; 2011. p 63–83.
20. Wittwer CT, Reed GH, Gundry CN, Vandersteen JG, Pryor RJ. High-resolution genotyping by amplicon melting analysis using LCGreen. Clin Chem 2003;49:853–60.

CHAPTER 4

THE INFLUENCE OF NUCLEOTIDE SEQUENCE AND TEMPERATURE ON THE ACTIVITY OF THERMOSTABLE POLYMERASES

4.1 Abstract

Extension rates of a thermostable polymerase were measured from 50 to 90°C for templates with varying sequence using a fluorescent activity assay adapted for real-time PCR instruments. Templates consisted of identical hairpins with a melting temperature of 92°C and extension regions with either single-base repeats or guanosine-cytosine (GC) contents ranging from 0 to 100%. Optimum extension temperature was 70 to 75°C for all templates with a near linear decrease in extension rates outside this range. Extension rates increased with GC content up to 60% and decreased at higher GC. Rates varied greatly for each nucleotide with guanosine (214 s^{-1} at 75°C) >cytidine (150 s^{-1} at 75°C) >adenosine (81 s^{-1} at 75°C) >thymidine (46 s^{-1} at 75°C). Predictions were within 30% of measured rates for 59% of calculations with greatest agreement among lower GC content. Templates with higher GC contents exhibited slower rates and were increased to within 4 to 20% of prediction with the addition of 7.5% dimethyl sulfoxide (DMSO), indicating inhibition due to secondary structure. In the presence of oligonucleotide probes, polymerases with and without 5' to 3' exonuclease activity exhibited similar decreases in extension rates of 70 and 65%. Extension rates are influenced by template sequence, increasing with higher GC content and decreasing with secondary structure. Understanding these parameters across temperatures will enable improved temperature cycling for DNA amplification with higher yield and specificity.

4.2 Introduction

Understanding the parameters that influence DNA polymerase activity is essential for optimizing PCR conditions and preventing amplification failure. Sequence characteristics of templates such as GC content and secondary structure are known to reduce amplification efficiency. In addition, incorporation rates are base specific for a variety of polymerases [1]–[6]. However, the sequence dependence of activity has not been studied for thermostable DNA polymerases.

Kinetic analysis of nucleotide incorporation has been performed using stopped-flow [6], quench-flow [1], [4], [7], and quartz crystal microbalance [8]. These methods are capable of monitoring fast reaction times but have required fluorescent base analogs, radiolabeled nucleotides or immobilization of the template to a surface. Recently we introduced a fluorescent polymerase activity assay adapted for real-time PCR instruments [9]. Polymerase extension of defined oligonucleotide templates is monitored with fluorescent noncovalent dyes. This continuous assay allows sensitive measurement of polymerase extension rates with increased simplicity and throughput.

We apply this assay to determine the sequence dependence of thermostable polymerase activity. Various templates were used to measure the effect of GC content and incorporation rates of individual nucleotides. Extension rates were measured over a range of temperatures between 50 and 90°C. In addition the influences of secondary structure, oligonucleotide probes, and primer melting temperature (Tm) on polymerase extension were determined. Understanding the limitations of thermostable DNA polymerase imposed by temperature, template sequence and secondary structure will allow improved design of efficient and rapid amplification protocols.

4.3 Materials and Methods

4.3.1 DNA Polymerases

Klentaq I (purchased from Wayne Barnes at Washington University in St. Louis) and Amplitaq® (Life Technologies) were quantified as described previously [10] on sodium dodecyl sulfate (SDS) gels stained with Sypro® Orange (Life Technologies).

4.3.2 Oligonucleotides

Oligonucleotide template designs are shown in Figure 4.1 and sequences are listed in Appendix A. Both hairpin templates and linear templates (having separate primer and template oligonucleotides) were used. Hairpin templates (Figure 4.1A) included self-complementary regions with a six base loop, 14 base pair stem and an annealed 3'-end.

The melting temperature (Tm) of the hairpin was 92°C using 1X LCGreen® Plus dye and a 0.3°C/s ramp on an HR-1® melting instrument (BioFire Diagnostics). The extension region varied in length and sequence. Eleven templates were designed with 25 base extension regions with GC contents ranging from 0 to 100%. Four templates contained ten single-base repeats. Additional hairpin templates were designed with secondary structure in the extension region (Figure 4.1B) or included an 18 base oligonucleotide probe (Figure 4.1C).

Linear templates (Figure 4.1D) shared identical sequences in the extension region as well as seven identical bases at the 3'-end of the primer. The 5'-end of primer sequences were varied to achieve different Tms.

Oligonucleotides were purchased from Integrated DNA Technologies and purified by high-pressure liquid chromatography. Concentrations were determined by absorbance at 260 nm following digestion with purified phosphodiesterase [11]. Thermodynamic analysis of template secondary structures was performed with Quikfold (http://mfold.rna.albany.edu/?q=DINAMelt/Quickfold) using the default settings. Tms of oligonucleotides were measured before polymerase extension with a 0.3°C/s ramp and 1X LCGreen Plus on an HR-1 melting instrument (BioFire Diagnostics) at 100 nM concentrations for linear templates and at 1 μM for hairpin templates. Tms of fully extended hairpin templates were measured at 25 points/°C with a LightCycler® 480 (Roche) at a concentration of 500 nM. Tms are listed in Appendix A.

4.3.3 Polymerase Extension Assay

Polymerase extension reactions were performed with a LightCycler 480. Final reaction concentrations were 50 mM Tris, pH 8.3, 3 mM $MgCl_2$, 1X LCGreen Plus (BioFire Diagnostics), 200 μM each dNTP, and 100 pM polymerase. Oligonucleotide templates and primers were included at 100 nM. Where applicable, a probe was added in five-fold excess of the template at 500 nM. CleanAmp® dNTPs (TriLink BioTechnologies) were used to limit extension before equilibration. In some reactions, either CleanAmp 7-deaza-dGTP or CleanAmp dUTP was was substituted for dGTP or dTTP. Polymerases were diluted in 50 mM Tris, pH 8.3 and 0.03% Tween® 20 to reduce loss of enzyme by adsorption during serial dilutions. Except where otherwise noted, Klentaq I was used. Additional polymerase extension reactions were performed for templates with GC contents between 20 and 100% in the presence of 2.5, 5, 7.5 and 10% DMSO.

The reaction was initiated by activating the CleanAmp dNTPs at 95°C for 10 min, followed by fluorescence monitoring of nucleotide incorporation at the extension tempera-

ture. Fluorescence acquisition at a single temperature was achieved by programming the LightCycler 480 for repeated single acquisitions of 1 s at the desired temperature. Extension reactions were performed at temperatures ranging between 50 and 90°C in 5°C increments. Reactions were allowed to continue to exhaustion (60-120 min). Three replicates of each reaction were performed and the standard deviations reported. Extension reactions were immediately quenched on ice and stored at -20°C. Template extension was verified on 2 or 4% agarose gels (NuSieve® 3:1 agarose, Lonza) followed by staining with 1X SYBR® Green I (Life Technologies).

4.3.4 Assay Calibration

Polymerase extension reactions were allowed to proceed to exhaustion and the maximum fluorescence taken as complete extension of the template. Extension curves were normalized between zero and the total number of nucleotides that each polymerase molecule can extend, given by

$$\frac{[Template] \times L}{[Poly]} \tag{4.1}$$

where $[Template]$ is the concentration of template, L is the length of extension in base pairs and $[Poly]$ is the concentration of the polymerase. The initial slope of normalized extension curves yields extension rate in nucleotides per second per molecule of polymerase (s^{-1}). Template designs shown in Figures 4.1B and 4.1C contain double stranded structures in the extension region and are expected to reduce the net increase in fluorescence during extension. These reactions were calibrated by reducing L by the length of duplex in the extension region. For example, L was reduced from 25 bases to seven bases for reactions where a probe of 18 bases was used. Extension curves were not analyzed at temperatures above the Tm of the extended template. Above the Tm, the increase in fluorescence upon extension of the template was small relative to other templates with higher Tms. It is believed that this was caused by denaturation of the template, preventing accumulation of fluorescence by the noncovalent dye. We observed a continuous decrease in fluorescence during incorporation of 7-deaza-guanosine. This nucleotide has been reported to quench fluorescence of ethidium bromide [12]. Extension curves for these reactions were first inverted before calibration.

4.4 Results

Extension rates could not be measured for hairpin templates above the Tm of the fully extended template. However, extension of these templates still occurred. Figure 4.2A shows an agarose gel of templates between 0 to 100% GC after extension at 75°C as well

as unextended controls for the 0 and 12% GC templates. The extension temperature was above the Tm of full-length 0 and 12% GC templates. Bands of identical size were observed for all templates, indicating each was fully extended. In contrast, full extension of linear templates depended on the Tm of the primer. Figure 4.2B shows an agarose gel of linear templates after extension at 75°C. At this extension temperature, substrate exhaustion was only observed for templates with primers of 68, 70, and 78°C. Bands for these templates were of similar intensity while distinct bands were not observed for templates with lower primer Tms. Complete extension of templates was generally observed up to 5°C above the primer Tm.

Extension rates as a function of temperature for hairpin templates with varying GC contents are shown in Figure 4.3A. For all GC contents, the optimum temperature for extension was 70 to 75°C. Below 70°C, a near linear decrease of extension rates was observed. Rates declined 37 to 45% with every decrease of 10°C. At temperatures above 75°C, declines were more rapid with rates decreasing 50 to 67% every 10°C. Figure 4.3B shows extension rates for the 60% GC template that decreases linearly on both sides outside 70 to 75°C.

Rates were highest for templates between 60 and 80% GC. Figure 4.3C shows rates as a function of GC content at 75°C. Rates generally increased with increasing GC content up to 60% and declined towards higher GC. Two exceptions were the 20 and 50% GC templates that had consistently lower extension rates then surrounding templates (e.g., the 50% GC content template had lower rates than either the 40 or 60% GC templates) across all temperatures.

Hairpin templates were designed with ten, single-base repeats to measure incorporation rates of individual nucleotides. As shown in Figure 4.4, extension rates are strongly dependent on the nucleotide. The average extension rate for cytidine and guanosine was 2.8-fold higher than the average rate of adenosine and thymidine up to 75°C. A pairwise comparison of guanosine to cytidine and adenosine to thymidine show that incorporation of purines is faster than the complementary pyrimidine. Rates for guanosine were on average 50% higher than cytidine between 60 and 75°C and rates for adenosine were on average 75% higher than thymidine between 65 and 75°C. Incorporation of 7-deaza-guanosine was faster than guanosine and cytidine at low temperatures but exhibited only marginal increases with temperature, being surpassed in rate by both guanosine and cytidine above 65°C. Extension rates were lowest with uridine that were on average 50% lower than thymidine up to 65°C.

Polymerase extension rates were measured for templates with either stable secondary structure or an 18 base oligonucleotide probe in the extension region (Figures 4.1B and

4.1C). The sequence for both templates were identical except for the 5 bp duplex in the extension region of the secondary structure template. Extension rates for polymerases with (exo+) and without (exo–) 5' to 3' exonuclease activity were measured at 60°C, below the Tms of the duplexes. Results are shown in Table 4.1. The oligonucleotide probe decreased the exo– polymerase extension rates by 65% while the secondary structure caused a decrease of 38% . Exo+ polymerase extension rates were decreased by 70% with the probe. Extension rates could not be measured with the secondary structure template for this polymerase because the reaction did not plateau. However, it was apparent from visual observation that extension was slower than with the oligonucleotide probe.

To test whether extension rates of random templates are determined by their base sequence, measured nucleotide specific rates were used to predict the extension rates for the eleven templates with varying GC content from 50 to 75°C. For each template, the numbers of each base in the extension region were counted and a weighted average of the nucleotide incorporation rates obtained. Figure 4.5 displays predicted extension rates (Figure 4.5A) alongside measured rates (Figure 4.5B). Predictions were within 30% of measured rates for 59% of calculations with greatest agreement among lower GC content templates. Figure 4.5C shows particularly good agreement for the 40% GC template where predicted rates were within 5% of measured rates across the temperature range. Similar results were obtained for templates with 32 and 60% GC which were on average within 5 and 8% of measured values between 55 and 75°C. Large differences were observed for templates with high GC. As shown in Figure 4.5D, measured rates at 65°C are much lower than expected for templates above 70% GC. Deviations from predicted rates were also observed at 50°C for most templates.

DMSO was added to extension reactions at 75°C to see if measured rates for some templates would increase closer to predicted rates. Figure 4.6 compares extension rates with varying concentrations of DMSO to predicted rates. DMSO at 2.5% does little to change extension rates for the templates. With 5% DMSO, rates were increased for templates with GC contents of 50, 70, 80, 90, and 100%, bringing them to within 2 to 33% of predicted rates. Extension rates were further increased for the 90 and 100% GC templates with 7.5% DMSO to within 20 and 8% of predicted rates, respectively. Little change was observed for the other templates. At 10% DMSO, rates decreased for all except the 70% GC template. DMSO had little effect on the 40 and 60% GC templates that were already close to predicted rates. Rates decreased with increasing DMSO for the 32% GC template and extension rates for the 20% GC template could not be analyzed (Tms <75°C).

Linear templates were designed with primer Tms ranging between 41 and 78°C. Figure

4.7 shows the temperature dependence of extension rates for these templates. Maximum rates generally coincide with the Tm of the primer. At higher temperatures, a rapid decline is observed with very low rates 5°C above the Tm. At any given extension temperature, extension rates were faster for primers with increasing stability up to a Tm of 70°C. The primer with a Tm of 78°C resulted in slower extension rates than the 70°C primer up to an extension temperature of 70°C.

4.5 Discussion

A high throughput, continuous fluorescent assay for polymerase activity provides extension rates without specialized instrumentation. The influence of several different polymerases, buffer components and conditions on activity has been previously reported [9], [10]. Here we use this method to determine the effect of template sequence on polymerase activity across temperatures typically used in thermal cycling during PCR.

Extension rates vary for templates with single base repeats (Figure 4.4), indicating that extension rates depend on the inserted base. Similar variation has been reported for several polymerases including DNA polymerase β [1], DNA polymerase α [3], HIV reverse transcriptase [4], T7 RNA polymerase [6], mitochondrial DNA polymerase [2], and X family DNA polymerase of African swine fever virus [5]. However, differences in nucleotide incorporation ranged from 44% [6] to 6-fold [4]. Furthermore, the relative rates of incorporation for each base differ in each study. Bases reported most efficiently incorporated were adenosine [1], [2], cytidine [4], [6], or thymidine [5], whereas guanosine has the highest extension rate in our study. The efficiency with which specific nucleotides are incorporated may vary between polymerases.

The nucleotide analog 7-deaza-guanosine is often used to amplify GC rich templates. At typical extension temperatures between 70 and 75°C, the incorporation rate of 7-deaza-guanosine was as much as 2.3-fold lower than guanosine. Also, uridine was incorporated approximately half as fast as thymidine. Uridine and 7-deaza-guanosine are often used in place of their analogous nucleotide at two- to three-fold higher concentrations. While extension rates are lower for these nucleotides, this is only beneficial if the Km is also higher. Another study found the Km of dUTP to be the same as dTTP for Taq polymerase [13], suggesting increases in concentration would not result in faster incorporation.

Nucleotide specific incorporation rates help explain the low rates observed for low GC templates (Figures 4.3A, 4.3C). Low GC templates are rarely thought of as difficult to amplify. However, with the incorporation rates of adenosine and thymidine nearly one-third

of guanosine and cytidine, these templates are extended with lower efficiency and may become troublesome in very rapid PCR.

Despite higher incorporation rates for guanosine and cytidine, extension rates decline for templates with GC content above 60%. Very high GC content has a greater inhibitory effect on polymerase extension than does very low GC. Up to 70°C, the 90 and 100% GC templates were 1.5 to 4.3-fold lower than any of the 0, 12, or 20% GC templates. This inhibition may be caused by increased stability or likelihood of secondary structure in the extension region of the template.

Predicted extension rates of mixed sequences based on individual nucleotides were very close to experimental values for the 32, 40, and 60% GC templates (Figure 4.5). Measured rates for the other templates were lower than predicted. If secondary structure in the extension regions of these templates were inhibiting polymerase extension, then addition of DMSO might relieve this inhibition. DMSO is often used to improve amplification of high GC templates [14], [15] and is believed to reduce secondary structure. DMSO at 5 or 7.5% increased the extension rates of the 50, 70, 80 and 100% GC templates to within 7% of predicted rates (Figure 4.6). Extension rates of the 90% GC template increased to within 20% of prediction. It is unclear why extension rates for most templates decrease with 10% DMSO. It may be that increased concentrations of DMSO decrease the overall stability of the duplex and extension is slowed as is seen for the 32% GC template, or that overall activity of the polymerase is decreased by 10% DMSO. Interestingly, the extension rates for the templates, which were closely predicted by their sequence (40 and 60% GC templates), changed less than 4% with up to 7.5% DMSO. Extension rates of templates appear determined by their base sequence and are decreased by secondary structure.

Thermodynamic calculations of secondary structure in the extension region of templates produced mixed results. There were no secondary structures calculated for the 40% GC. This agrees well with our findings because the extension rates of this template were closely predicted from its sequence. The extension rates for the 60% GC template were also close to prediction. However, the calculated free energy of the secondary structure for this template (-1.35 kcal/mole) was similar to the 50% (-1.21 kcal/mole) and the 80% GC (-1.47 kcal/mole) templates for which measured rates were lower than predicted. The 90% and 100% GC templates had similar extension rates across all temperatures even though their free energies of secondary structure were quite different (-2.84 kcal/mole and -9.61 kcal/mole for the 90% GC template and 100% GC templates, respectively).

Tms of secondary structure were measured with high-resolution melting analysis of the

unextended GC content templates. No melting transitions were observed above 50°C for templates with 0 to 60% GC content, indicating these did not contain stable secondary structure. Secondary structures were observed for the other templates with Tms ranging from 55°C for the 70% GC template, to 73°C for the 100% GC template. If interference of thermodynamically stable secondary structure accounted for inhibited extension, sudden increases in rates would be expected at extension temperatures above the Tm of the secondary structure. However, this was not observed for any these higher GC templates. Templates with extension rates below their predicted rates remained low across temperature. For example, the 50 and 70% GC templates remained between 17 to 47% lower than the rates predicted by their sequence from 50 to 75°C. Only the addition of DMSO increased measured rates to near prediction. Two reasons may account for the discrepancies between the influence of DMSO and the thermodynamic calculation and melting analysis of secondary structures. 1) Thermodynamics algorithms cannot accurately account for secondary structure at high temperatures and melting analysis could not detect these (i.e., because of indistinguishable melting transitions). 2) Polymerase extension is inhibited by transient secondary structures that are not thermodynamically stable at higher temperatures. In other words, short-lived structures potentially block the polymerase progress.

Exo+ polymerases do not extend through double stranded regions faster than exo– polymerases (Table 4.1). This implies that the catalytic activity of the exonuclease domain is slower than nucleotide incorporation. The extension rate for the exo+ polymerase was slower for the template with secondary structure compared to the template with an oligonucleotide probe. On the other hand, the extension rate for the exo– polymerase increased with the secondary structure template compared to the probe, indicating that this polymerase is more capable of extending through secondary structure. It may be that the exonuclease activity of the exo+ polymerase decreases extension rates when the two catalytic domains act on the same DNA strand.

Polymerase activity is strongly influenced by temperature. We observed linear temperature decreases of extension rates outside the optimal temperature range. From 70 to 50°C, rates decreased between 72 and 92%. Another study measured the temperature dependent activity of Taq polymerase and a 5' to 3' exonuclease deficient enzyme similar to the exo– polymerase studied here [16]. The temperature optimum for the exo– polymerase was also between 70-75°C while an optimum for Taq polymerase was between 70 and 80°C. In agreement with our findings, rates declined for both polymerases by approximately 90% from 70 to 50°C, though the decrease was not as linear.

For linear templates, extension rates decline rapidly above the Tm of the primer (Figure 4.7). This is due to decreased availability of primed template rather than decreased activity of the polymerase. This has important implications in two-step PCR, where thermal cycling is performed between two temperatures rather than three as in traditional PCR. In two-step PCR, DNA is denatured at the high temperature while the lower temperature accommodates both primer annealing and polymerase extension. As shown in Figure 4.7, maximum extension rates are obtained when the lower temperature is set at the Tm of the primer. Given that the optimal temperature of extension is between 70 and 75°C, two-step PCR is more rapid when the primers have Tms in this range.

Polymerase activity is influenced by the sequence of the template. Between 70 and 75°C, extension rates vary by as much as threefold, depending on the GC content of the template. Secondary structure interferes with extension and is difficult to predict. However, this appears to be alleviated by the inclusion of DMSO and extension rates are closely approximated by the rates of individual nucleotide incorporation. Considering the sequence of a template and understanding modulation of extension rates with temperature will allow more rapid PCR protocols while maintaining high yield and specificity.

4.6 References

[1] J. Ahn, V. S. Kraynov, X. Zhong, B. G. Werneburg, and M. D. Tsai, "DNA polymerase beta: effects of gapped DNA substrates on dNTP specificity, fidelity, processivity and conformational changes," *Biochem. J.*, vol. 331 (Pt 1), pp. 79–87, 1998.

[2] A. A. Johnson and K. A. Johnson, "Fidelity of nucleotide incorporation by human mitochondrial DNA polymerase," *J. Biol. Chem.*, vol. 276, no. 41, pp. 38 090–6, 2001.

[3] L. V. Mendelman, J. Petruska, and M. F. Goodman, "Base mispair extension kinetics. Comparison of DNA polymerase alpha and reverse transcriptase," *J. Biol. Chem.*, vol. 265, no. 4, pp. 2338–46, 1990.

[4] J. E. Reardon, "Human immunodeficiency virus reverse transcriptase: steady-state and pre-steady-state kinetics of nucleotide incorporation," *Biochemistry*, vol. 31, no. 18, pp. 4473–9, 1992.

[5] A. K. Showalter and M. D. Tsai, "A DNA polymerase with specificity for five base pairs," *J. Am. Chem. Soc.*, vol. 123, no. 8, pp. 1776–7, 2001.

[6] G. Q. Tang, V. S. Anand, and S. S. Patel, "Fluorescence-based assay to measure the real-time kinetics of nucleotide incorporation during transcription elongation," *J. Mol. Biol.*, vol. 405, no. 3, pp. 666–78, 2011.

[7] J. J. Arnold and C. E. Cameron, "Poliovirus RNA-dependent RNA polymerase (3Dpol): pre-steady-state kinetic analysis of ribonucleotide incorporation in the presence of Mg2+," *Biochemistry*, vol. 43, no. 18, pp. 5126–37, 2004.

[8] H. Matsuno, K. Niikura, and Y. Okahata, "Direct monitoring kinetic studies of DNA polymerase reactions on a DNA-immobilized quartz-crystal microbalance," *Chemistry*, vol. 7, no. 15, pp. 3305–12, 2001.

[9] J. L. Montgomery and C. T. Wittwer, "The influence of PCR reagents on DNA polymerase extension rates measured on real-time PCR instruments," *Clin. Chem.*, 10.1373/clinchem.2013.212829, 2013.

[10] J. L. Montgomery, N. Rejali, and C. T. Wittwer, "Stopped-flow DNA polymerase assay by continuous monitoring of dNTP incorporation by fluorescence," *Anal. Biochem.*, vol. 441, no. 2, pp. 133–9, 2013.

[11] G. Kallansrud and B. Ward, "A comparison of measured and calculated single- and double-stranded oligodeoxynucleotide extinction coefficients," *Anal. Biochem.*, vol. 236, no. 1, pp. 134–8, 1996.

[12] L. J. Latimer and J. S. Lee, "Ethidium bromide does not fluoresce when intercalated adjacent to 7-deazaguanine in duplex DNA," *J. Biol. Chem.*, vol. 266, no. 21, pp. 13 849–51, 1991.

[13] P. H. Patel and L. A. Loeb, "Multiple amino acid substitutions allow DNA polymerases to synthesize RNA," *J. Biol. Chem.*, vol. 275, no. 51, pp. 40 266–72, 2000.

[14] M. Ralser, R. Querfurth, H. J. Warnatz, H. Lehrach, M. L. Yaspo, and S. Krobitsch, "An efficient and economic enhancer mix for PCR," *Biochem. Biophys. Res. Commun.*, vol. 347, no. 3, pp. 747–51, 2006.

[15] M. Musso, R. Bocciardi, S. Parodi, R. Ravazzolo, and I. Ceccherini, "Betaine, dimethyl sulfoxide, and 7-deaza-dGTP, a powerful mixture for amplification of GC-rich DNA sequences," *J. Mol. Diagn.*, vol. 8, no. 5, pp. 544–50, 2006.

[16] F. C. Lawyer, S. Stoffel, R. K. Saiki, S. Y. Chang, P. A. Landre, R. D. Abramson, and D. H. Gelfand, "High-level expression, purification, and enzymatic characterization of full-length Thermus aquaticus DNA polymerase and a truncated form deficient in 5' to 3' exonuclease activity," *PCR Methods Appl.*, vol. 2, no. 4, pp. 275–87, 1993.

Table 4.1. Extension inhibition by secondary structure and oligonucleotide probes

	Exo– polymerase		**Exo+ polymerase**	
	Extension Rate (s^{-1})	Inhibition (%)	Extension Rate (s^{-1})	Inhibition (%)
Without probe	66 ± 1	–	10 ± 1	–
With probe	23 ± 1	65 ± 2	3 ± 1	70 ± 2
Secondary structure	41 ± 1	38 ± 2	<3	>70

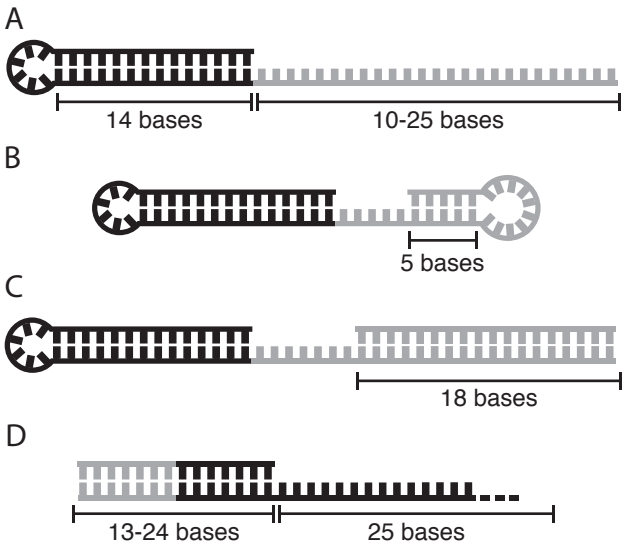

Figure 4.1. Polymerase template designs for sequence dependence studies. (A) Hairpin oligonucleotides contained a 14 base pair stem and a six base loop. The extension regions were either 25 bases with GC contents ranging between 0 and 100% or ten bases with ten single-base repeats of A, T, C, or G. (B) A hairpin template was designed with a five base pair secondary structure in the extension region. (C) An 18 base oligonucleotide probe was included with a hairpin template. The sequence of this template was identical to that of (B) except for the ten complementary bases of the secondary structure. (D) Linear templates having separate primer and template oligonucleotides had experimental primer Tms ranging between 41 and 78°C.

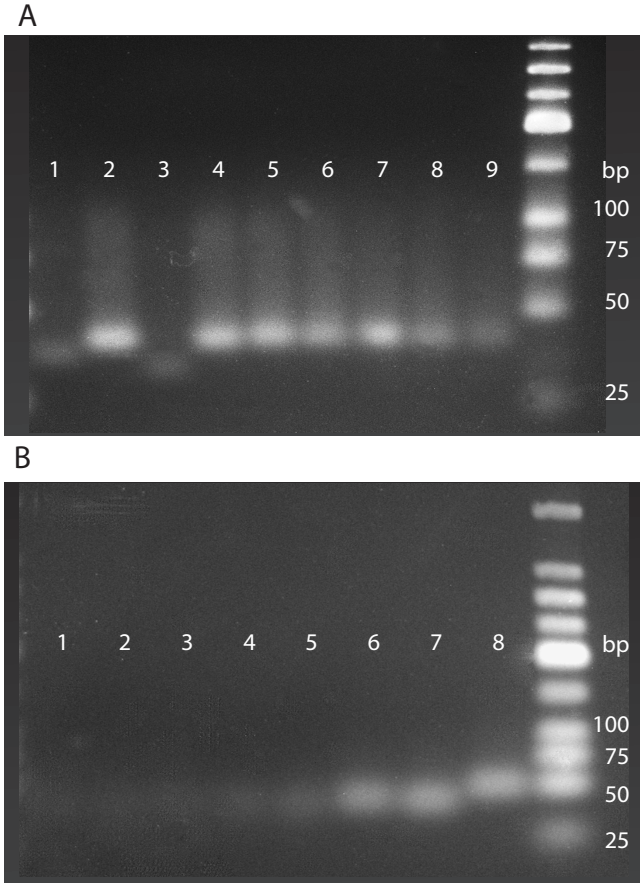

Figure 4.2. Agarose gels of templates with varying sequences after extension at 75°C. (A) Extension of templates with varying GC contents. Lane 1: Unextended 0% GC template; Lane 2: Extended 0% GC template; Lane 3: Unextended 12% GC template; Lane 4: Extended 12% GC template; Lane 5: Extended 20% GC template; Lane 6: Extended 40% GC template; Lane 7: Extended 60% GC template; Lane 8: Extended 80% GC template; Lane 9: Extended 100% GC template; Lane 10: Molecular weight DNA ladder. The extension temperature was above the Tms of the extended 0 and 12% templates (Lanes 2 and 4). However, bands were the same size as the other templates with higher Tms. Bands were more intense and migrated differently than their unextended templates (Lanes 1 and 3), indicating these templates were fully extended. (B) Extension of linear templates with varying primer Tms. Lane 1: Primer Tm = 41°C; Lane 2: Primer Tm = 49°C; Lane 3: Primer Tm = 54°C; Lane 4: Primer Tm = 60°C; Lane 5: Primer Tm = 63°C; Lane 6: Primer Tm = 68°C; Lane 7: Primer Tm = 70°C; Lane 8: Primer Tm = 78°C; Lane 9: Molecular weight DNA ladder. Substrate exhaustion was only observed for templates with primer Tms of 68, 70, and 78°C and these three templates show bands of similar intensity, indicating each of these were completely extended. Only indistinct bands were observed for the other templates.

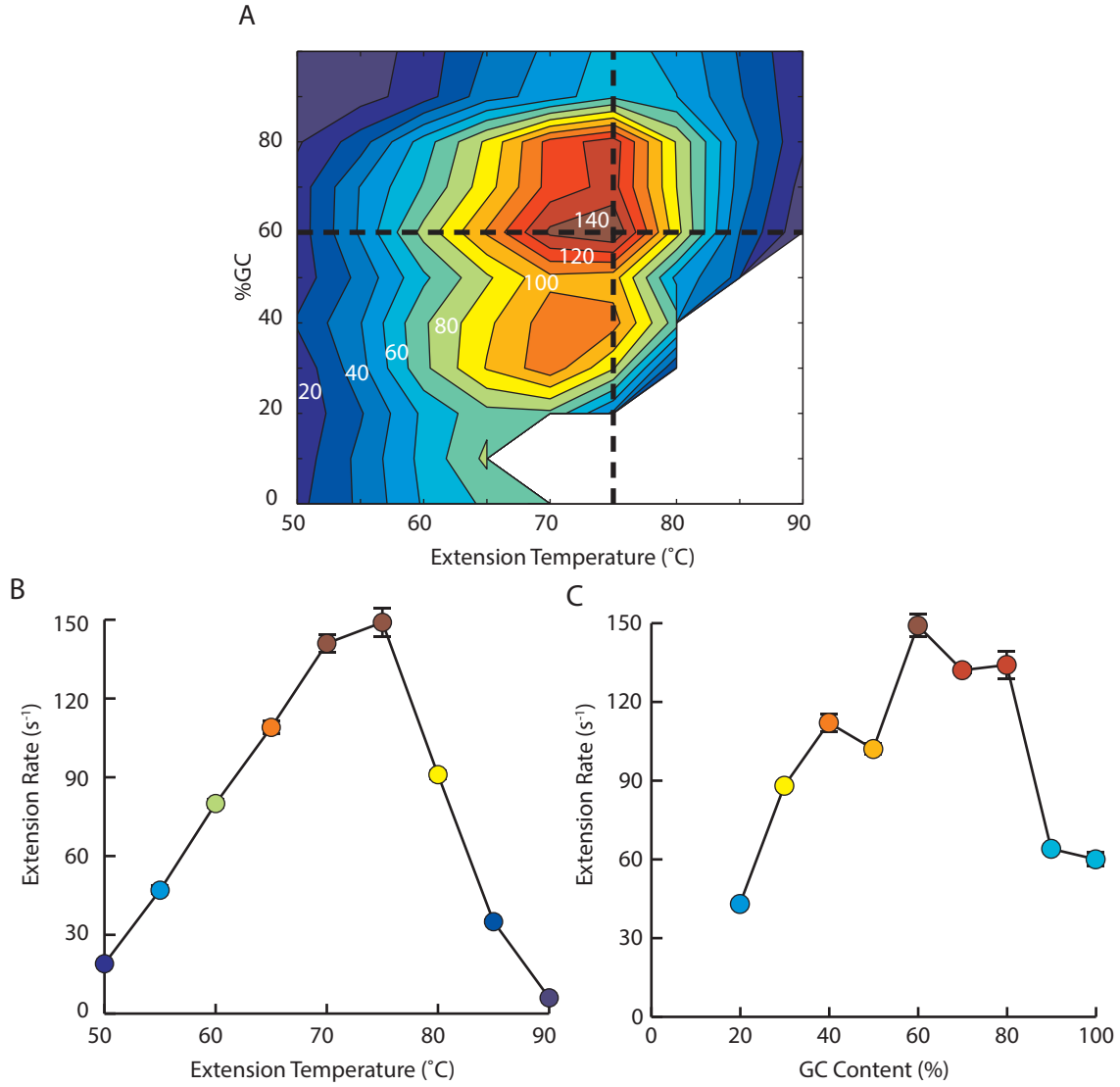

Figure 4.3. Extension rates as a function of temperature for hairpin templates with varying GC contents. (A) Contour graph of extension rates for each of the GC content templates from 50 to 90°C. Extension rates are indicated on the contour graph. The white area in the lower right corner of the plot indicates where no data could be collected because temperatures were above the Tm of the extended template. Black dashed lines show cross sections of data that are plotted in the lower graphs. (B) Extension rates as a function of temperature for the 60% GC template. Optimal extension temperatures were between 70 and 75°C. Linear decreases in rates are observed outside the optimal temperature. (C) Extension rates as a function of template GC content at 75°C. Extension rates increase with GC content up to 60% and decrease with higher GC content.

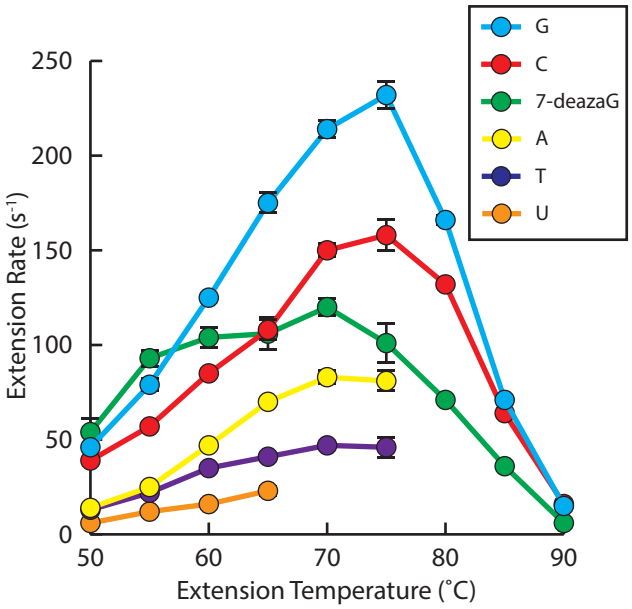

Figure 4.4. Incorporation rates of individual nucleotides as a function of temperature. Hairpin templates with single-base repeats were used to measure the incorporation rates of guanosine, cytidine, 7-deaza-guanosine, adenosine, thymidine, and uridine. Incorporation of guanosine and cytidine is faster than incorporation of adenine and thymidine up to 75°C. Purines are incorporated more quickly than the corresponding pyrimidine (e.g. guanosine is faster than cytidine). Incorporation rates of 7-deaza-guanosine changes only moderately between 55 and 75°C. Uridine on average is incorporated about half as quickly as thymidine.

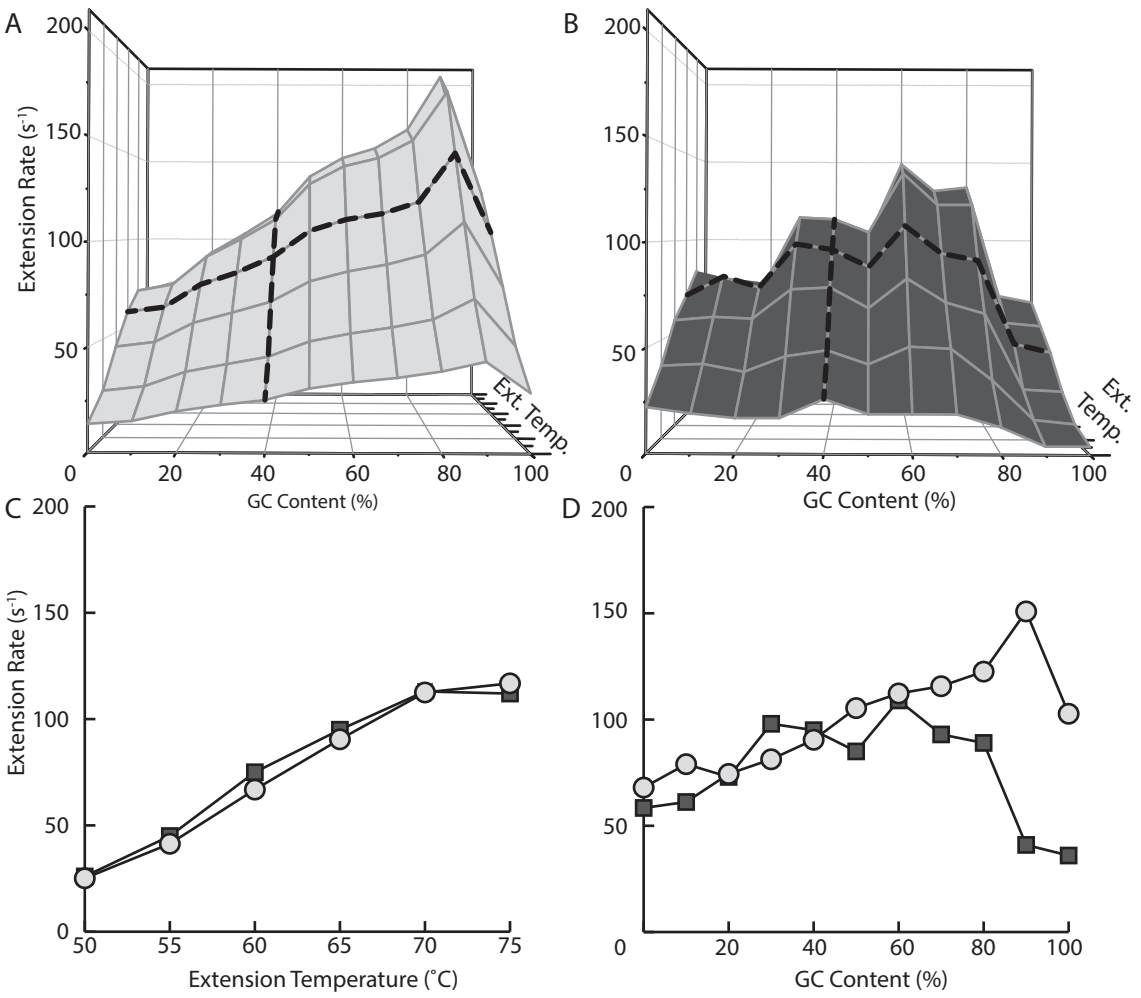

Figure 4.5. Comparison of measured extension rates and rates predicted from base sequence. (A) Predicted rates of GC content templates. Extension temperature is indicated by the depth axis. Because guanosine and cytidine have the fastest incorporation rates, an increase in extension rates was expected with increasing GC content. (B) Measured extension rates. Extension rates generally increase with GC content up to 60%, but decline with higher GC content. Dashed black lines in (A) and (B) indicate cross sections shown in lower graphs. (C) Comparison of predicted (light gray circles) and measured (dark gray squares) extension rates for the 40% GC template. Measured rates were on average within 10% of prediction for the 32, 40, and 60% GC templates. (D) Comparison of predicted (light gray circles) and measured (dark gray squares) extension rates for each GC content template at 65°C. Measured extension rates are generally more concordant with prediction for templates with GC contents below 60%.

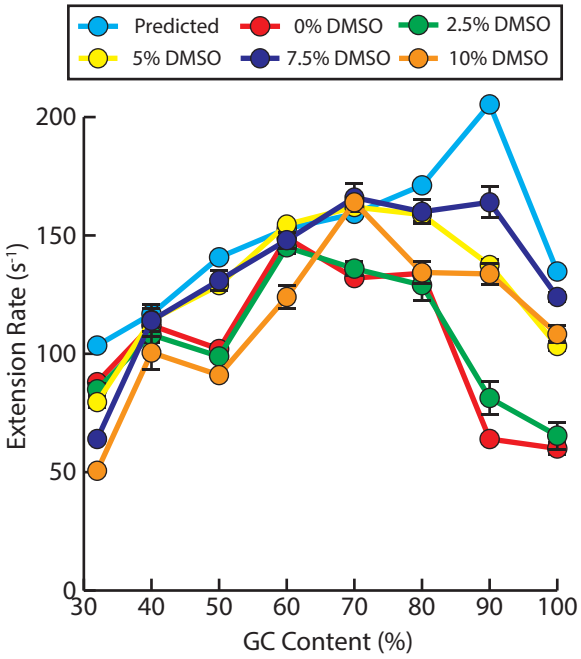

Figure 4.6. Comparison of predicted extension rates with measured rates in the presence of increasing DMSO. Measured extension rates become closer to predicted rates in the presence of DMSO. DMSO at 2.5% has little effect on rates while DMSO at 5 to 7.5% increases extension rates closer prediction. DMSO produced only small changes to extension rates for templates that were close to predicted rates (40 and 60% GC templates). Increasing DMSO to 10% decreased extension rates below prediction. Extension rates for the 32% GC template decreased with increasing DMSO, possibly due to destabilization of template.

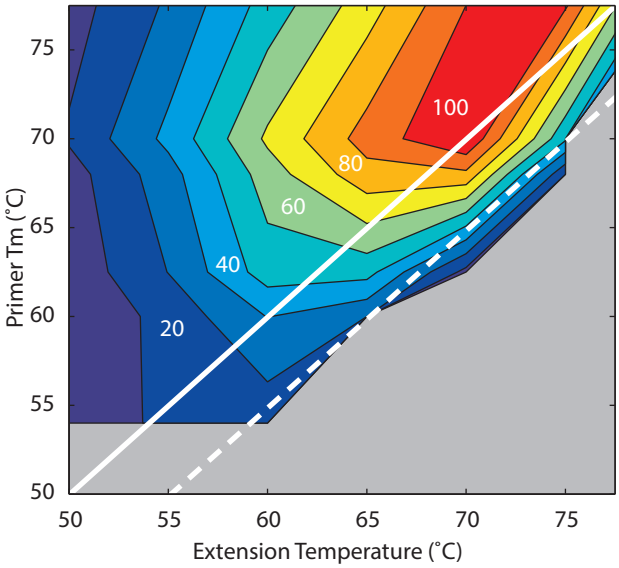

Figure 4.7. Extension rates as a function of temperature for linear templates with varying primer melting temperatures. Extension rates are indicated on the contour graph. The temperatures at which maximum extension rates were observed are correlated to the Tm of the template primer (solid diagonal line). Extension rates decline rapidly within 5°C above the primer Tm (dashed diagonal line). Substrate exhaustion does not occur when extension rates are very slow and could not be calculated. This is indicated by the gray region dominating the lower right corner of the graph.

CHAPTER 5

COMPARISON OF KINETIC AND EQUILIBRIUM MODELS FOR POLYMERASE EXTENSION

5.1 Introduction

Several mathematical models of PCR have been attempted [1]–[5]. These employ the equilibrium model (Figure 1.1) and consider the three main reactions of PCR as independent processes, occurring at defined temperatures with static rates. While this assumption may be sufficient for thermal cycling with long hold times, rapid cycle PCR is never in a state of equilibrium. Transitions between temperatures dominate and reactions are likely to occur over a range of temperatures with varying rates.

A more accurate model of rapid PCR is the kinetic model. This model accounts for continuous temperature changes with temperature-dependent reaction rates. The impact of the kinetic model on polymerase extension is considered here. Measured extension rates as a function of temperature taken from Chapter 4 are applied to various temperature traces from a real-time PCR instrument. Saturation rates as a function of temperature are also considered. Extension rates or saturation rates as a function of time are obtained and the number of nucleotides extended in a single cycle are calculated. These results are compared to the equilibrium model of polymerase extension.

5.2 Methods

Sample chamber temperature traces were obtained from a LightCycler® 1.5 (Roche). Thermal cycling was programmed for 50°C for 0 s, 75°C for 0, 1, 2, 5, 10, 15, 20, 30, 45, or 60 s, and 95°C for 0 s with a ramp rate of 20°C/s. The portion of the temperature traces from 50°C increasing up to 90°C were used to model polymerase extension. Decreasing temperature ramps were omitted. Total number of nucleotides extended during the temperature increase of thermal cycling was calculated using extension rates and saturation rates for both kinetic and equilibrium models.

5.2.1 Number of Nucleotides Extended with a Kinetic Model

A kinetic model for extension was implemented using extension rates as well as saturation rates. Extension rates were obtained from initial slopes of calibrated data as described in Chapters 2 through 4. Saturation rate refers to the reciprocal of the time required for extension reactions to reach completion. Reaction completion time was defined as the time corresponding to 98% of maximum fluorescence. These are normalized to the amount of polymerase and template using

$$\frac{[Template] \times L}{[Poly] \times t_{sat}} \tag{5.1}$$

where $[Template]$ is the concentration of template, L is the length of extension in base pairs, $[Poly]$ is the concentration of the polymerase, and t_{sat} is the reaction completion time.

A kinetic model requires extension rates or saturation rates as a function of temperature. These were obtained for the 60% GC content template in Chapter 4. Figure 5.1 illustrates the method to calculate polymerase extension with a kinetic model using extension rates. Extension rates as a function of temperature (Figure 5.1A) are combined with thermal cycling temperature traces (Figure 5.1B) by linear interpolation to obtain extension rates as a function of time (Figure 5.1C). The area under the curve represents the number of nucleotides extended by a single polymerase molecule within that period of time. This was calculated by numerical integration using the trapezoidal method. A kinetic model using saturation rates is similar except that saturation rates as a function of temperature are used in place of extension rates.

5.2.2 Number of Nucleotides Extended with an Equilibrium Model

For both extension rates and saturation rates, the number of nucleotides extended by a molecule of polymerase was also calculated using the equilibrium model (Figures 5.1C and 5.2C). The extension hold time programmed on the real-time PCR instrument was multiplied by the extension rate or the saturation rate of the 60% GC template at 75°C (149 s^{-1} and 74 s^{-1}, respectively). This model fails for extension hold times of 0 s allowed by some thermal cycling instruments. To allow comparison of the equilibrium and kinetic models in the case of 0 s extension at 75°C, the length of time at which the temperature was 75 ± 1°C was used in the equilibrium model. This was estimated at 0.3 s using rapid cycling with no extension hold time. The results from the two models were compared by taking the ratio of the number of nucleotides extended calculated by the kinetic model to

the number of nucleotides extended calculated by the equilibrium model. Both models were compared using extension rates and saturation rates.

5.3 Results

The kinetic model calculated more nucleotides extended per polymerase than the equilibrium model for all extension temperature hold times. This was true whether the models used extension rates or saturation rates. The fold differences of the kinetic model over the equilibrium model (i.e., the kinetic model calculations divided by the equilibrium model) for each extension hold time are shown in Figure 5.3. Increasing discrepancies were observed with decreasing hold times. For a 60 s hold time, the models agreed within 3% using extension rates and saturation rates. At 5 s, the difference increased to 57% using extension rates and 63% using saturation rates. With a hold time of 0 s, the kinetic model calculated 11.4-fold and 11.9-fold more nucleotides extended than the equilibrium model using extension rates and saturation rates, respectively (508 vs. 45 bases with extension rates and 265 vs. 22 bases with saturation rates). For all extension hold times, the nucleotides extended using extension rates were approximately double (between 1.9 and 2.0-fold) those calculated using saturation rates for both the kinetic and equilibrium models.

5.4 Discussion

The assumption of negligible temperature transitions in the equilibrium model poorly describes fast PCR. Because the kinetic model accounts for extension during temperature ramps, it more accurately describes polymerase extension with rapid thermal cycling. Extension is modeled here as the total number of nucleotides extended by a polymerase molecule as temperature increases during thermal cycling. This is calculated using both extension rates and saturation rates.

Extension rates are derived from the initial slope of extension reactions. This represents the maximum nucleotide incorporation rates of polymerases under conditions with large excess of substrate. As the reaction continues, substrate (i.e., extension template, dNTPs) diminishes and incorporation rates decline. In addition to substrate exhaustion, rates may also decrease due to build up inhibitors such as pyrophosphate. An alternative approach is to use saturation rate, which takes into account decreasing nucleotide incorporation rates by considering the length of the entire extension reaction. The precise time for reaction completion from real-time data can be ambiguous. This was defined as the time required for fluorescence to reach 98% of the maximum value. This means the maximum efficiency of each cycle would be 98%, assuming both denaturation and annealing were 100%. Because

saturation rate varies depending on the amount of reagents used in a particular reaction, these must be normalized to the concentration of the template and polymerase.

The kinetic model of extension presented here is susceptible to inaccuracies whether extension rates or saturation rates are used. This model considers extension during the temperature increase of thermal cycling between 50 and 90°C and does not account for annealing and denaturation. It is assumed that annealing of primers is complete at 50°C and denaturation does not occur until 90°C. The model also does not account for product annealing. Extension is assumed not to occur during temperature decreases from denaturation down to annealing even though substrate is being formed as primers anneal to the template. An accurate description of extension can only be obtained by considering all reactions in a kinetic model.

An example of a kinetic model of PCR is described in Appendix B. This model is based on differential equations derived from mass action equations for each reaction. The kinetic model describes the temporal change in concentration of each reactant during PCR considering the rate constants of each reaction and the initial concentrations of reactants. Because rates of reaction fluctuate with temperature during thermal cycling, this model requires rate constants as a function of time. An example of how these are obtained for extension is provided here. The rate constants are the maximum rates of reaction under conditions with a large excess of substrate. For the extension reaction, this is represented by extension rates. Reactions dominate if rate constants are sufficiently high and reactant concentrations are substantial. For example, primer annealing to template continues virtually unimpeded in early cycles of PCR. However, as PCR progresses, product accumulates while primers diminish and product annealing dominates. This complex interplay of reactions is not described by the model presented in this chapter. Modeling of product amplification beyond a single cycle is not possible without the rates of the other reactions in PCR.

The results obtained here provide an initial estimate of the length of DNA that can be successfully amplified under given thermal cycling conditions. In the earliest stages of PCR, polymerase and primers are in large excess of template. Typical PCR in a 10 μL volume begins with 1.6×10^4 copies of template (50 ng genomic DNA). Primers are usually included at 3×10^{11} (0.5 μM) and polymerase between 1×10^{10} and 1×10^{12} molecules (Table 2.1). Primers and polymerase at such high relative concentrations push the extension reaction to completion and initial rates dominate. With high efficiency reactions, the amount of template is doubled each temperature cycle and by definition, the efficiency of amplification is 100%. However, this is only the case when the polymerase has sufficient time to extend to

the end of the template. If full extension fails to occur before denaturation of DNA strands, then a primer cannot anneal to the newly synthesized strand within the next temperature cycle. With primers in large excess of template, the probability of the partially extended template annealing during subsequent cycles is very small and amplification failure is likely. For example, assume a template with a 500 base extension region. If thermal cycling conditions permit polymerase molecules to extend 500 bases, then efficiency will be 100%. However, if the polymerase is only able to extend 100 bases, amplification is not likely to continue.

A kinetic model predicts that amplification can occur for products with much faster thermal cycling. Consider the previous example of a template with a 500 base extension region. Using extension rates, the kinetic model predicts successful amplification with a 0 s extension hold time because each polymerase molecule can potentially extend up to 508 bases under these thermal cycling conditions. However, the equilibrium model indicates that an extension hold time of 5 s is required. Using saturation rates, the models predict successful amplification of products approximately half the length compared to using extension times. A kinetic model provides a better description of extension with fast thermal cycling. Further expansion of this model to include all contributing reactions will help define the limits of PCR.

5.5 References

[1] M. Garlick, J. Powell, D. Eyre, and T. Robbins, "Mathematically modeling PCR: an asymptotic approximation with potential for optimization," *Math. Biosci. Eng.*, vol. 7, no. 2, pp. 363–84, 2010.

[2] J. L. Gevertz, S. M. Dunn, and C. M. Roth, "Mathematical model of real-time PCR kinetics," *Biotechnol. Bioeng.*, vol. 92, no. 3, pp. 346–55, 2005.

[3] S. Mehra and W. S. Hu, "A kinetic model of quantitative real-time polymerase chain reaction," *Biotechnol. Bioeng.*, vol. 91, no. 7, pp. 848–60, 2005.

[4] G. Stolovitzky and G. Cecchi, "Efficiency of DNA replication in the polymerase chain reaction," *Proc. Natl. Acad. Sci. U.S.A.*, vol. 93, no. 23, pp. 12 947–52, 1996.

[5] S. E. Whitney, A. Sudhir, R. M. Nelson, and H. J. Viljoen, "Principles of rapid polymerase chain reactions: mathematical modeling and experimental verification," *Comput. Biol. Chem.*, vol. 28, no. 3, pp. 195–209, 2004.

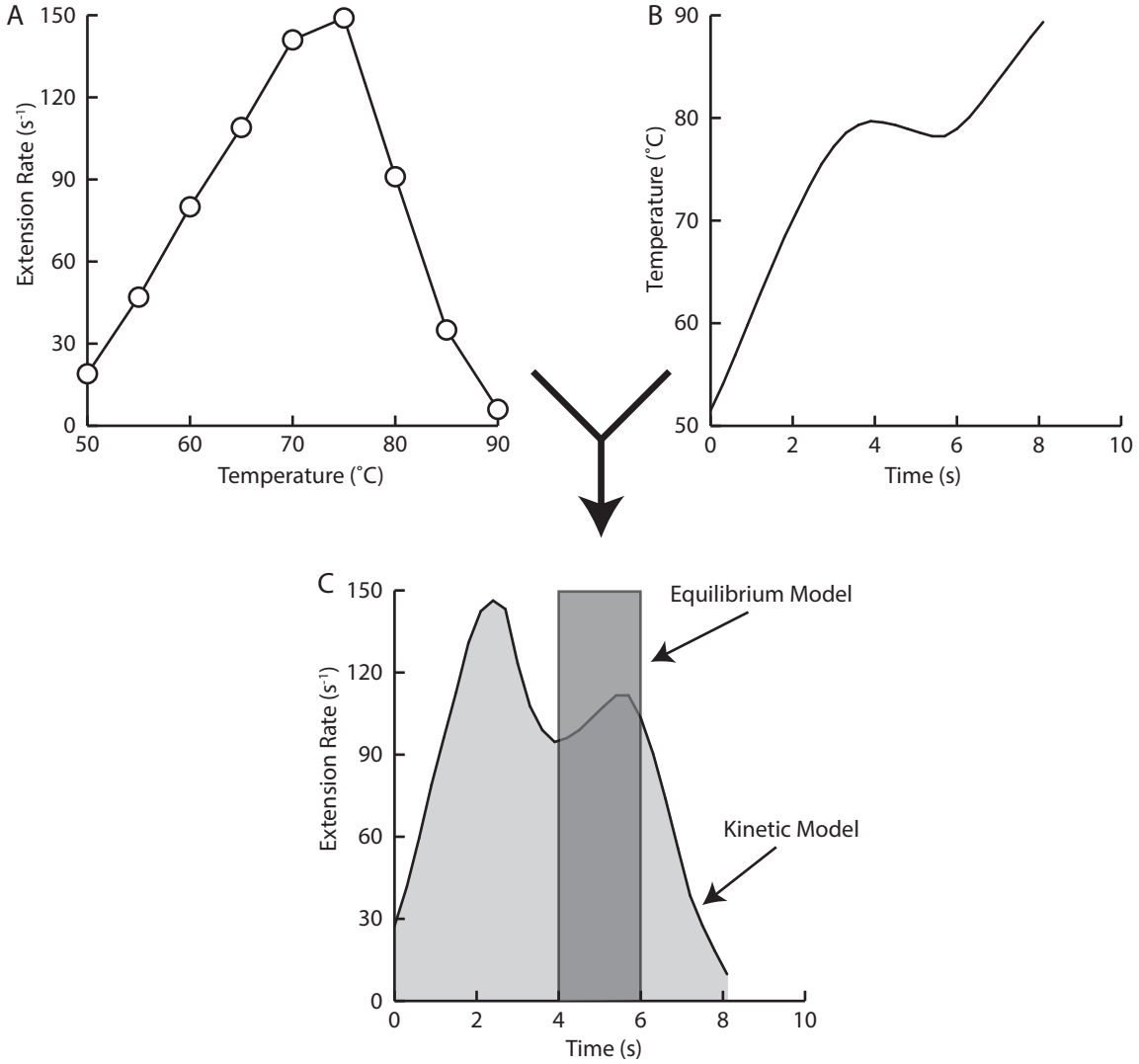

Figure 5.1. Implementing a kinetic model for polymerase extension using extension rates. (A) Extension rates are measured over the range of temperatures encountered in PCR. (B) These rates are applied to typical rapid thermal cycling conditions of PCR. (C) Combining these two plots by linear interpolation provides extension rates as a function of time. The area under the curve represents the total number of nucleotides extended by a polymerase molecule. The equilibrium model only considers extension for the duration and the temperature programmed. Extension rates as a function of time are shown for the 60% GC template from Chapter 4. The temperature trace represents the increase in temperature for a programmed hold time of 2 s.

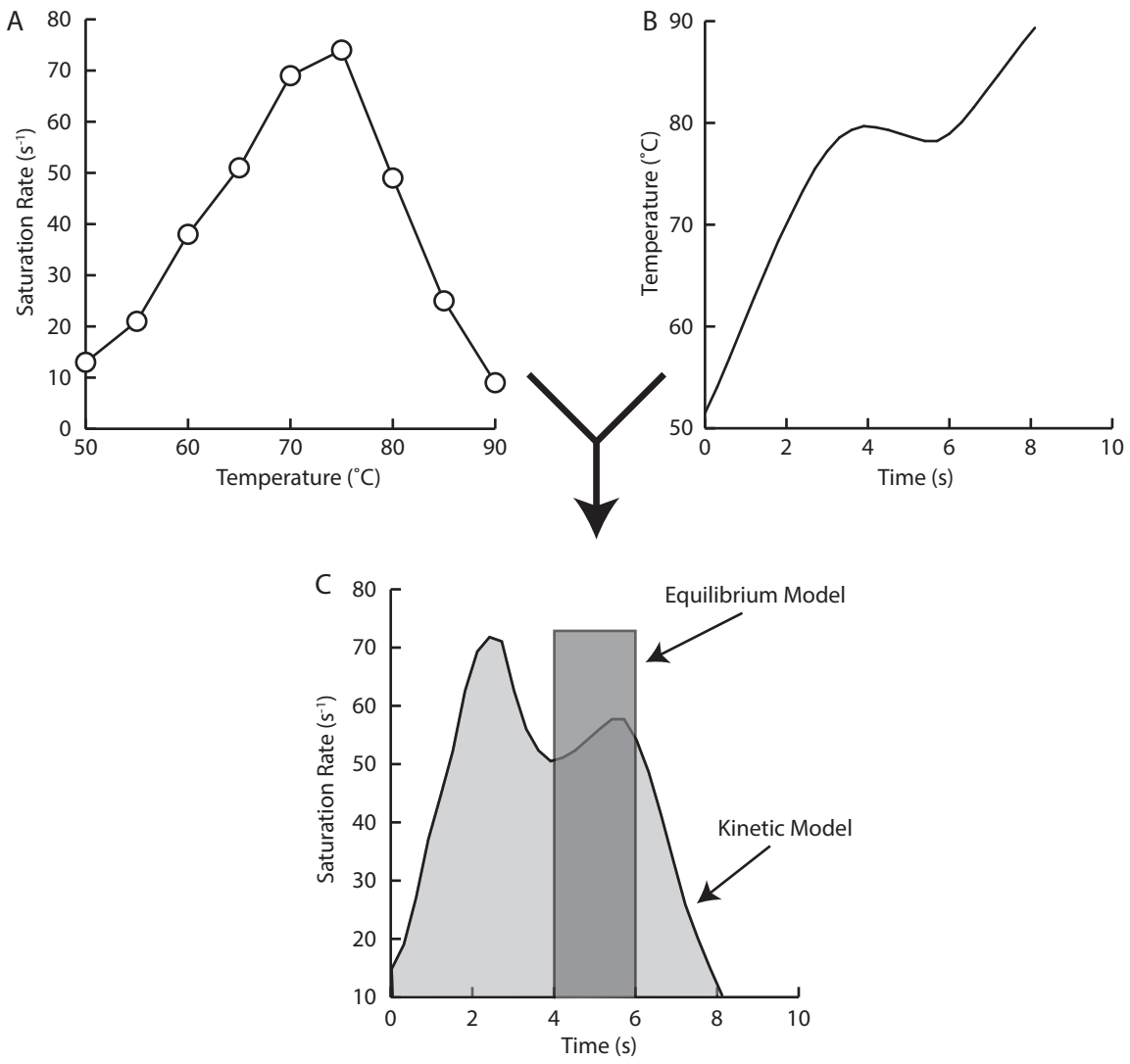

Figure 5.2. Implementing a kinetic model for polymerase extension using saturation rates. (A) Saturation rates were calculated from 50 to 90°C. (B) A temperature trace was collected on a real-time PCR instrument. (C) Saturation rates as a function of time were obtained by linear interpolation of (A) and (B). The area under the curve represents the total number of nucleotides extended by a polymerase molecule. The equilibrium model is represented by a rectangle with a width of the extension hold time and a height equal to the maximum saturation rate. Saturation rates as a function of time are shown for the 60% GC template from Chapter 4. The temperature trace represents the increase in temperature for a programmed hold time of 2 s. The saturation rates are approximately half as great as the extension rates shown in Figure 5.1.

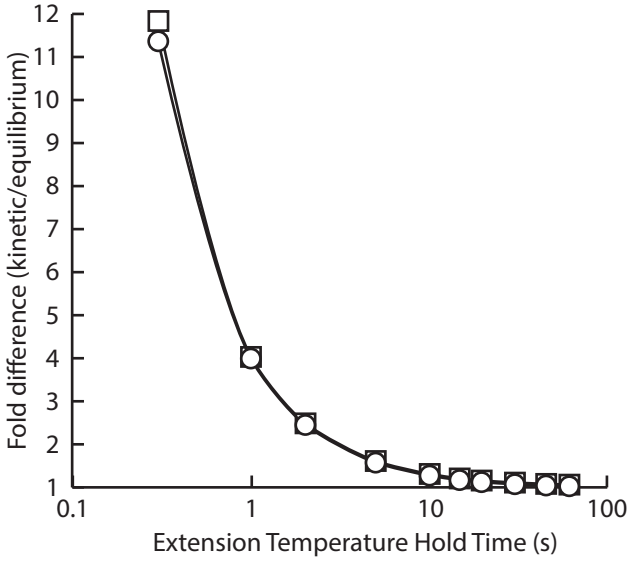

Figure 5.3. Fold difference of nucleotides incorporated calculated by the kinetic model over the equilibrium as a function of programmed extension hold times. The models were compared using extension rates (circles) and saturation rates (squares). With both comparisons, the kinetic model calculates more nucleotides extended than the equilibrium model. The difference between the two models becomes more significant with shorter hold times and faster thermal cycling.

CHAPTER 6

CONCLUSION

PCR is a dynamic process with interdependent and competing reactions. Polymerase extension is dependent on primer annealing; primer annealing competes with annealing of extended template; and denaturation of DNA competes with each of these. Rates are in constant flux and accounting for each reaction during rapid thermal cycling is a significant challenge. The simplest way to understand the dynamics of PCR is to study each reaction in isolation. The influences of parameters such as temperature and solutes on reaction rates can be determined independently. Descriptions of each reaction can be combined into a kinetic model that will aid in identification of optimal thermal cycling conditions and reagent concentrations for fast PCR. An example of a kinetic model based on differential equations derived from mass action equations is provided in Appendix B.

The work presented here is an important step in expanding our understanding of the kinetics of PCR. Optimal conditions for fast extension were determined for a number of parameters, several of which are counter to prevalent conventions. For example, ammonium sulfate and KCl are frequently included in reaction buffers to increase specificity. Magnesium is often kept low for the same purpose. However, these conditions greatly diminish polymerase extension. Increased specificity is also achieved with faster thermal cycling [1], suggesting we have been headed in the wrong direction in our optimization efforts. In our attempts to improve PCR, we have been slowing it down.

The polymerase assay developed here has the potential to be a useful tool in biotechnology. The current method for characterizing polymerases is inadequate and provides little insight into their performance in PCR. In contrast, the fluorescent assay used in these studies enables quantitative comparisons of polymerases. Results are intuitive and directly applicable to PCR. Adapting the assay for common instrumentation is essential to wide adoption. Routine measurements of activity can be performed in any laboratory setting. Buffer chemistries are easily optimized. Quality control of polymerase production is simplified. New polymerase variants are more clearly screened. This assay promises to

improve the quality of PCR now as well as identify the polymerases and conditions that will take us into the next generation of fast PCR.

6.1 Future Work

6.1.1 Rates for a Kinetic Model of PCR

A complete kinetic model of PCR requires rates of reaction for denaturation, annealing, and extension. The work presented here collected rates of extension across relevant PCR temperatures for templates with a variety of GC contents. Rates of the other reactions must also be obtained.

6.1.1.1 Template Denaturation

Denaturation could also be followed with noncovalent dyes with rapid heating of double stranded DNA. Reaction containers with high surface to volume ratios and materials with high thermal conductivity will maximize the speed of heating. For example, copper capillaries quickly plunged into heated gallium would allow monitoring of fast denaturation events. The stopped-flow instrument in Chapter 2 is also capable of mixing lines of differing temperatures to achieve rapid temperature jumps. Double-stranded DNA would be held in a mixing line at a low temperature and mixed with buffer at a higher temperature to measure denaturation at an intermediate temperature. Mixing ratios and mixing line temperatures can be adjusted to achieve the desired temperature jump.

6.1.1.2 Primer and Template Annealing

Rates of primer annealing to template as well as annealing of complementary extended template strands should be measured. These are competing reactions and can be measured under conditions relevant to PCR. Noncovalent DNA dyes could be used to monitor annealing of DNA strands. Determining the influence of nucleotide sequence, solutes, and temperature on rates is essential. These paramaters were shown to greatly influence polymerase extension and are likely to influence annealing as well. The stopped-flow instrument discussed in Chapter 2 is especially suited for these studies. Complementary oligonucleotides can be separated in mixing lines. Fast reactions can be monitored and temperature control allows rate measurements over a range of temperatures relevant to PCR. These experiments can be performed under pseudo-first order conditions, holding one oligonucleotide strand in excess of the other and varying the concentration of the limiting strand. This assumes a second order mechanism for annealing. Alternatively, annealing

may be fit to mechanisms of any order by nonlinear least squares fitting (e.g., using the Levenberg-Marquardt algorithm) of real-time data to a system of differential equations.

6.1.2 Expanded Buffer Component Studies

The effect of the most common buffer components were studied here, but many additional reagents may also influence polymerase extension.

6.1.2.1 PCR Enhancers

Several components are frequently included in PCR with the intention of improving amplification. However, their influences on polymerase extension have not been studied. These include gelatin, BSA, polyethylene glycol, tetramethyl ammonium chloride, trehalose, dithiothreitol, and several proprietary formulations. The effects of these components on extension can be studied with increasing concentrations as described in Chapters 2 and 3. Components that increase extension rates are especially desirable for fast PCR.

6.1.2.2 Detergents

Detergents were necessary for dilution of polymerase in Chapters 3 and 4. However, the effects of these on the rates of polymerase extension were not studied. A variety of ionic and nonionic detergents may be studied over a range of concentrations such as sodium dodecyl sulfate, Tween 20, IGEPAL CA-630, Triton X-100, Laureth 12, Brij 35, or Brij 58. These are best studied with polymerase at typical PCR concentrations where several dilutions are not required. A stopped-flow instrument is suitable for these studies.

6.1.2.3 PCR Dyes

The dyes most frequently used in real-time PCR were studied here but other dyes may also be useful to monitor extension. Possible advantages may be less inhibition of extension or greater quantum yield allowing studies with lower concentrations of template. Other dyes known to bind specifically to double-stranded DNA are ethidium bromide, SYBR Gold, Pico Green, SYTOX Blue, SYTOX Green, SYTOX Orange, TOTO-1, TOTO-3, YOYO-1, YOYO-3, SYTO 9, SYTO 11, SYTO 12, SYTO 13, SYTO 14, SYTO 15, SYTO 20, SYTO 21, SYTO 23, SYTO 24, SYTO 25, SYTO 43, SYTO 44, SYTO 45, SYTO 82, PO-PRO-1, JO-PRO-1, BO-PRO-1, GelStar, YO-PRO-1, POPO-3, thiazole orange, BOBO-3, LO-PRO-1, TO-PRO-1, BOBO-1, and POPO-1.

6.1.2.4 Combinatorial Influences of Reagents

The influences of buffer components were each examined individually and most studies were performed at one temperature with a single polymerase. Combinatorial effects were not considered and may influence optimum conditions. For example, does optimal pH change with 5 mM $MgCl_2$ versus 2 mM? This represents a large matrix of variables and the number of experiments required can be reduced with a multifactorial design of experiments (DOE) [2].

6.1.3 Expanded Polymerase Studies

The influences of buffer components, temperature, and template sequence were studied for Klentaq I. The influences of these parameters on the extension rates of other polymerases are also desirable. Particularly, full length *Taq* polymerase and polymerases from other organisms such as *Pyrococcus furiosis*, *Thermococcus litoralis*, *Thermus flavus*, and *Thermus thermophilus* are of interest.

6.1.4 Reverse Transcriptase Polymerases

Reverse transcription polymerase chain reaction (RT-PCR) is a powerful technique to assess RNA expression levels. This uses a combination of DNA polymerase and reverse transcriptase enzymes. Several RT-PCR diagnostic assays have been developed [3]–[5] and time requirements for these can be reduced by determining the optimal conditions for reverse transcriptase activity. Extension rates of reverse transcriptase can be studied with an RNA template and DNA primers. Figure 4.7 indicates that extension rates are influenced by the melting temperature of the primer. Therefore, primers with melting temperatures above the extension temperature are recommended.

6.1.5 Structure-Function Relationships for Nucleotide Incorporation

Figure 4.4 shows incorporation rates are strongly dependent on the nucleotide. Several studies have attempted to elucidate the mechanism of nucleotide incorporation and the relative contributions of hydrogen bonding [6], partial charge [7], nearest neighbor [8], base stacking and steric interactions [9] have been debated. Measuring the incorporation rates of nucleotide analogs could provide insight into polymerization. For example, the contribution of hydrogen bonding could be studied by comparing the incorporation rates of an adenosine nucleotide to an analog that replaces the C6 amino group with a methyl group. In addition to mechanism information, nucleotide analogs that incorporate more quickly than natural

nucleotides could be used to further increase the speed of PCR, provided the analogs have sufficient base-pairing specificity to maintain fidelity of nucleotide sequence.

6.2 References

[1] C. T. Wittwer and D. J. Garling, "Rapid cycle DNA amplification: time and temperature optimization," *Biotechniques*, vol. 10, no. 1, pp. 76–83, 1991.

[2] R. L. Plackett and J. P. Burman, "The design of optimum multifactorial experiments," *Biometrika*, vol. 33, no. 4, pp. 305–325, 1946.

[3] G. Risatti, L. Holinka, Z. Lu, G. Kutish, J. D. Callahan, W. M. Nelson, E. Brea Tió, and M. V. Borca, "Diagnostic evaluation of a real-time reverse transcriptase PCR assay for detection of classical swine fever virus," *J. Clin. Microbiol.*, vol. 43, no. 1, pp. 468–71, 2005.

[4] R. K. H. Hui, F. Zeng, C. M. N. Chan, K. Y. Yuen, J. S. M. Peiris, and F. C. C. Leung, "Reverse transcriptase PCR diagnostic assay for the coronavirus associated with severe acute respiratory syndrome," *J. Clin. Microbiol.*, vol. 42, no. 5, pp. 1994–9, 2004.

[5] S. B. Kleiboeker, "Applications of competitor RNA in diagnostic reverse transcription-PCR," *J. Clin. Microbiol.*, vol. 41, no. 5, pp. 2055–61, 2003.

[6] M. F. Goodman, "Hydrogen bonding revisited: geometric selection as a principal determinant of DNA replication fidelity," *Proc. Natl. Acad. Sci. U.S.A.*, vol. 94, no. 20, pp. 10 493–5, 1997.

[7] S. Xia, A. Vashishtha, D. Bulkley, S. H. Eom, J. Wang, and W. H. Konigsberg, "Contribution of partial charge interactions and base stacking to the efficiency of primer extension at and beyond abasic sites in DNA," *Biochemistry*, vol. 51, no. 24, pp. 4922–31, 2012.

[8] L. V. Mendelman, M. S. Boosalis, J. Petruska, and M. F. Goodman, "Nearest neighbor influences on DNA polymerase insertion fidelity," *J. Biol. Chem.*, vol. 264, no. 24, pp. 14 415–23, 1989.

[9] E. T. Kool, "Hydrogen bonding, base stacking, and steric effects in DNA replication," *Annu. Rev. Biophys. Biomol. Struct.*, vol. 30, pp. 1–22, 2001.

APPENDIX A

OLIGONUCLEOTIDE TEMPLATE SEQUENCES

Table A.1 Hairpin templates with varying GC contents

Sequence[1]	GC Content (%)	ΔG Secondary Structure (kcal/mol)	Tm (°C)	
			Secondary Structure	Extended Template
attataatataaataatattaaataTGCTCCCGCGGCC GatctgcCGGCCGCGGGAGCA	0	-1.79	ND[2]	70
attattataatattaataatggaTCTGCTCCCGCGGCC GatctgCCGGCCGCGGGAGCA	12	-1.77	ND	69
gttgtaagtatatgtttattataacTGCTCCCGCGGCC GatctgcCGGCCGCGGGAGCA	20	ND	ND	76
gtcaaatgacgttatcgttatattcTGCTCCCGCGGCC GatctgcCGGCCGCGGGAGCA	32	-2.06	ND	82
gtccaatttaagtcgaagtatcagcTGCTCCCGCGGC CGatctgcCGGCCGCGGGAGCA	40	ND	ND	84
tagcgaaggatgtgaacctaatcccTGCTCCCGCGGC CGatctgcCGGCCGCGGGAGCA	48	-1.21	ND	87
gagacaaccagttgggcccacactcTGCTCCCGCGG CCGatctgcCGGCCGCGGGAGCA	60	-1.35	ND	93
ccaggccatgcagcagccgccacacTGCTCCCGCGG CCGatctgcCGGCCGCGGGAGCA	70	-2.62	55	95
ccaccccggcgcgttggcatgccccTGCTCCCGCGG CCGatctgcCGGCCGCGGGAGCA	80	-1.47	57	96
ggccgccgccactcccgcgcgccccTGCTCCCGCGG CCGatctgcCGGCCGCGGGAGCA	90	-2.84	68	>100
ggcggcggcggcggcggcggcggccTGCTCCCGCG GCCGatctgcCGGCCGCGGGAGCA	100	-9.61	73	>100

[1] Capital letters denote self-complementary sequences.
[2] ND = Not determined. No secondary structure was calculated or no melting transition was observed.

Table A.2 Hairpin template with secondary structure

Sequence[1]	Tm Secondary Structure (°C)
GTACCaaggatgtgaGGTACatcccTGCTCCCGCGGCCGatctgcCGGCC GCGGGAGCA	62

[1] Capital letters denote self-complementary sequences.

Table A.3 Hairpin template with oligonucleotide probe

Sequences[1]		Tm Probe (°C)
Template	Probe	
gagacaaccagttgggcccacactcTGCTCCCGCG GCCGatctgcCGGCCGCGGGAGCA	GGTTCACATCCTTCG CTA	68

[1] Capital letters denote self-complementary sequences.

Table A.4 Hairpin templates with single-base repeats

Sequences[1]	Tm Extended Template (°C)
aaaaaaaaaaTGCTCCCGCGGCCGatctgcCGGCCGCGGGAGCA	77
ttttttttttGCTCCCGCGGCCGatctgcCGGCCGCGGGAGCA	75
ccccccccccTGCTCCCGCGGCCGatctgcCGGCCGCGGGAGCA	96
ggggggggggTGCTCCCGCGGCCGatctgcCGGCCGCGGGAGCA	96

[1] Capital letters denote self-complementary sequences.

Table A.5 Linear templates with primers having varying melting temperatures

Sequences		Primer Tm (°C)
Template	Primer	
TAGCGAAGGATGTGAACCTAATCCCTGC TCCCTTAATT	AATTAAGGGAGCA	41
TAGCGAAGGATGTGAACCTAATCCCTGC TCCCTTGATAA	TTATCAAGGGAGCA	49
TAGCGAAGGATGTGAACCTAATCCCTGC TCCCGTGATTTA	TAAATCACGGGAGCA	54
TAGCGAAGGATGTGAACCTAATCCCTGC TCCCGTAGCGTA	TACGCTACGGGAGCA	60
TAGCGAAGGATGTGAACCTAATCCCTGC TCCCGTAGCGCA	TGCGCTACGGGAGCA	63
TAGCGAAGGATGTGAACCTAATCCCTGC TCCCGCGGCACGTA	TACGTGCCGCGGGAGC A	68
TAGCGAAGGATGTGAACCTAATCCCTGC TCCCGCGGCCGCG	CGCGGCCGCGGGAGCA	70
TAGCGAAGGATGTGAACCTAATCCCTGC TCCCGCGGCCGCCATGACGTC	GACGTCATGGCGGCCGC GGGAGCA	78

APPENDIX B

A PROPOSED KINETIC MODEL OF PCR

The kinetic model of PCR described here is a deterministic model based on the reactions comprising PCR. The mass action equations below describe the key processes in PCR.

Primer annealing and denaturation:

$$\mathrm{P}_1 + \mathrm{T}_1 \underset{k_{d,H1}(\Theta)}{\overset{k_{a,H1}(\Theta)}{\rightleftharpoons}} \mathrm{H}_1 \tag{B.1}$$

$$\mathrm{P}_2 + \mathrm{T}_2 \underset{k_{d,H2}(\Theta)}{\overset{k_{a,H2}(\Theta)}{\rightleftharpoons}} \mathrm{H}_2 \tag{B.2}$$

Product annealing and denaturation:

$$\mathrm{T}_1 + \mathrm{T}_2 \underset{k_{d,D}(\Theta)}{\overset{k_{a,D}(\Theta)}{\rightleftharpoons}} \mathrm{D} \tag{B.3}$$

Polymerase binding:

$$\mathrm{E} + \mathrm{H}_1 \underset{k_{d,EH1}(\Theta)}{\overset{k_{a,EH1}(\Theta)}{\rightleftharpoons}} \mathrm{E} \cdot \mathrm{H}_1 \tag{B.4}$$

$$\mathrm{E} + \mathrm{H}_2 \underset{k_{d,EH2}(\Theta)}{\overset{k_{a,EH2}(\Theta)}{\rightleftharpoons}} \mathrm{E} \cdot \mathrm{H}_2 \tag{B.5}$$

Polymerase extension:

$$\mathrm{E} \cdot \mathrm{H}_{1,\mathrm{n}} + \mathrm{dNTP} \underset{k_{d,pol1}(\Theta)}{\overset{k_{a,pol1}(\Theta)}{\rightleftharpoons}} \mathrm{E} \cdot \mathrm{H}_{1,\mathrm{n}} \cdot \mathrm{dNTP} \xrightarrow{k_{pol1}(\Theta)} \mathrm{E} \cdot \mathrm{H}_{1,\mathrm{n+1}} \tag{B.6}$$

$$\mathrm{E} \cdot \mathrm{H}_{1,\mathrm{n+1}} + \mathrm{dNTP} \underset{k_{d,pol1}(\Theta)}{\overset{k_{a,pol1}(\Theta)}{\rightleftharpoons}} \mathrm{E} \cdot \mathrm{H}_{1,\mathrm{n+1}} \cdot \mathrm{dNTP} \xrightarrow{k_{pol1}(\Theta)} \mathrm{E} \cdot \mathrm{H}_{1,\mathrm{n+2}} \tag{B.7}$$

.

.

.

$$\mathrm{E} \cdot \mathrm{H}_{1,\mathrm{n+m}} + \mathrm{dNTP} \underset{k_{d,pol1}(\Theta)}{\overset{k_{a,pol1}(\Theta)}{\rightleftharpoons}} \mathrm{E} \cdot \mathrm{H}_{1,\mathrm{n+m}} \cdot \mathrm{dNTP} \xrightarrow{k_{pol1}(\Theta)} \mathrm{D} \tag{B.8}$$

$$\mathrm{E} \cdot \mathrm{H}_{2,\mathrm{n}} + \mathrm{dNTP} \underset{k_{d,pol2}(\Theta)}{\overset{k_{a,pol2}(\Theta)}{\rightleftharpoons}} \mathrm{E} \cdot \mathrm{H}_{2,\mathrm{n}} \cdot \mathrm{dNTP} \xrightarrow{k_{pol2}(\Theta)} \mathrm{E} \cdot \mathrm{H}_{2,\mathrm{n+1}} \tag{B.9}$$

$$\mathrm{E} \cdot \mathrm{H}_{2,\mathrm{n+1}} + \mathrm{dNTP} \underset{k_{d,pol2}(\Theta)}{\overset{k_{a,pol2}(\Theta)}{\rightleftharpoons}} \mathrm{E} \cdot \mathrm{H}_{2,\mathrm{n+1}} \cdot \mathrm{dNTP} \xrightarrow{k_{pol2}(\Theta)} \mathrm{E} \cdot \mathrm{H}_{2,\mathrm{n+2}} \tag{B.10}$$

.

.

.

$$\mathrm{E \cdot H_{2,n+m} + dNTP} \underset{k_{d,pol2}(\Theta)}{\overset{k_{a,pol2}(\Theta)}{\rightleftharpoons}} \mathrm{E \cdot H_{2,n+m} \cdot dNTP} \xrightarrow{k_{pol2}(\Theta)} \mathrm{D} \tag{B.11}$$

Equations B.1 and B.2 describe association of both sets of primers (P) to their complementary templates (T) to form primer-template hybrids (H). Equation B.3 is the association of template molecules to form full length duplex (D). Equations B.4 and B.5 are the binding of polymerase (E) to primer-template hybrids. Equations B.6 through B.11 describe processive nucleotide incorporation during polymerization where $\mathrm{E \cdot H_{1,n+1}}$ is $\mathrm{E \cdot H_{1,n}}$ extended by one base pair, $\mathrm{E \cdot H_{1,n+2}}$ is extended one base further, and so forth. Equations B.8 and B.11 represent complete polymerization to form a full length duplex. Rate constants are represented as a function of temperature, Θ. These are obtained by measuring rates of reaction over the range of temperatures being modeled. Forward rate constants for primer and duplex association can be obtained from annealing studies using a stopped-flow instrument as suggested in the Conclusion. Dissociation rate constants can be obtained from denaturation studies by fast melting of oligonucleotide duplexes.

The release of inorganic phosphate as well as release of duplex upon completion of polymerization are both ignored in this model. The model can be further simplified to reduce the number of experiments required to obtain rate constants. A previous study found that binding of polymerase to template-primer hybrids is a negligible step in extension [1]. The primer-template hybrids $\mathrm{H_1}$ and $\mathrm{H_2}$ are immediately converted to $\mathrm{E \cdot H_1}$ and $\mathrm{E \cdot H_2}$, and Equations B.4 and B.5 are simplified to forward reactions with rate constants $k_{a,EH1}(\Theta)$ and $k_{a,EH2}(\Theta)$, reflecting a fast reaction on the order of diffusion. Also, dNTP is used in PCR at concentrations >>Km and in large excess of primers. The concentration of dNTP will not change substantially throughout PCR and it is expected that the rate of dNTP binding will remain constant. Therefore, Equations B.8 and B.11 can be simplified to

$$\mathrm{E \cdot H_{1,n+m} \cdot dNTP} \xrightarrow{k_{ext,H1}(\Theta)} \mathrm{D} \tag{B.12}$$

$$\mathrm{E \cdot H_{2,n+m} \cdot dNTP} \xrightarrow{k_{ext,H2}(\Theta)} \mathrm{D} \tag{B.13}$$

where $k_{ext,H_1}(\Theta)$ and $k_{ext,H_2}(\Theta)$ are the temperature dependent extension rates and are measured using the polymerase extension assay developed in this work.

Equations B.1 through B.13 can be described by a series of ordinary differential equations as shown below. For simplicity, $\mathrm{E \cdot H_1 \cdot dNTP}$ and $\mathrm{E \cdot H_2 \cdot dNTP}$ will be written as $\mathrm{E \cdot H_1}$ and $\mathrm{E \cdot H_2}$.

$$\frac{d[\mathrm{P_1}]}{dt} = -k_{a,H1}(t)[\mathrm{P_1}][\mathrm{T_1}] + k_{d,H1}(t)[\mathrm{H_1}] \tag{B.14}$$

$$\frac{d[\mathrm{T_1}]}{dt} = -k_{a,H1}(t)[\mathrm{P_1}][\mathrm{T_1}] + k_{d,H1}(t)[\mathrm{H_1}] - k_{a,D}(t)[\mathrm{T_1}][\mathrm{T_2}] + k_{d,D}(t)[\mathrm{D}] \tag{B.15}$$

$$\frac{d[\mathrm{H_1}]}{dt} = k_{a,H1}(t)[\mathrm{P_1}][\mathrm{T_1}] - k_{d,H1}(t)[\mathrm{H_1}] - k_{a,EH1}(t)[\mathrm{E}\cdot\mathrm{H_1}] \tag{B.16}$$

$$\frac{d[\mathrm{P_2}]}{dt} = -k_{a,H2}(t)[\mathrm{P_2}][\mathrm{T_2}] + k_{d,H2}(t)[\mathrm{H_2}] \tag{B.17}$$

$$\frac{d[\mathrm{T_2}]}{dt} = -k_{a,H2}(t)[\mathrm{P_2}][\mathrm{T_2}] + k_{d,H2}(t)[\mathrm{H_2}] - k_{a,D}(t)[\mathrm{T_1}][\mathrm{T_2}] + k_{d,D}(t)[\mathrm{D}] \tag{B.18}$$

$$\frac{d[\mathrm{H_2}]}{dt} = k_{a,H2}(t)[\mathrm{P_2}][\mathrm{T_2}] - k_{d,H2}(t)[\mathrm{H_2}] - k_{a,EH2}(t)[\mathrm{E}\cdot\mathrm{H_2}] \tag{B.19}$$

$$\frac{d[\mathrm{E}]}{dt} = -k_{a,EH1}(t)[\mathrm{E}][\mathrm{H_1}] - k_{a,EH2}(t)[\mathrm{E}][\mathrm{H_2}] \tag{B.20}$$

$$\frac{d[\mathrm{E}\cdot\mathrm{H_1}]}{dt} = k_{a,H1}(t)[\mathrm{P_1}][\mathrm{T_1}] - k_{ext,H1}(t)[\mathrm{H_1}] \tag{B.21}$$

$$\frac{d[\mathrm{E}\cdot\mathrm{H_2}]}{dt} = k_{a,H2}(t)[\mathrm{P_2}][\mathrm{T_2}] - k_{ext,H2}(t)[\mathrm{H_2}] \tag{B.22}$$

The differential equations below describe the temporal concentrations of template in different stages of polymerization. Extension ceases when the template has been fully extended.

$$\frac{d[\mathrm{E}\cdot\mathrm{H_{1,n+1}}]}{dt} = k_{ext,H1}(t)[\mathrm{E}\cdot\mathrm{H_1}] \tag{B.23}$$

$$\frac{d[\mathrm{E}\cdot\mathrm{H_{1,n+2}}]}{dt} = k_{ext,H1}(t)[\mathrm{E}\cdot\mathrm{H_{1,n+1}}] \tag{B.24}$$

.

.

.

$$\frac{d[\mathrm{D}]}{dt} = k_{ext,H1}(t)[\mathrm{E}\cdot\mathrm{H_{1,n+m}}] \tag{B.25}$$

Similarly, for extension of $\mathrm{E}\cdot\mathrm{H_2}$

$$\frac{d[\mathrm{E}\cdot\mathrm{H_{2,n+1}}]}{dt} = k_{ext,H2}(t)[\mathrm{E}\cdot\mathrm{H_2}] \tag{B.26}$$

$$\frac{d[\mathrm{E}\cdot\mathrm{H_{2,n+2}}]}{dt} = k_{ext,H2}(t)[\mathrm{E}\cdot\mathrm{H_{2,n+1}}] \tag{B.27}$$

.

.

.

$$\frac{d[\mathrm{D}]}{dt} = k_{ext,H2}(t)[\mathrm{E} \cdot \mathrm{H}_{2,\mathrm{n+m}}] \tag{B.28}$$

Equations B.14 through B.28 can be solved numerically to calculate the concentration of each species during PCR. A number of numerical analysis methods may be used, but the simplicity and stabilities of the trapezoidal and Fourth-Order Runge-Kutta methods [2] make them appropriate choices for this model.

The rate constants in equations B.14 through B.28 are a function of time, rather than a function of temperature as is the case for rate constants in Equations B.1 through B.13. Temperatures fluctuate with time during PCR, therefore the numerical algorithm must be presented with a new rate constant at each time step. Rate constants as a function of temperature are obtained with kinetic studies over a range of temperatures. These are combined with simulated or measured thermal cycling data to obtain rate constants as a function of time as described in Chapter 5.

The efficiency of PCR can be calculated as the difference of the concentration of product duplex at some time t and some previous time t_0

$$\mathrm{E(t)} = \frac{[\mathrm{D}]_t - [\mathrm{D}]_{t0}}{[\mathrm{D}]_{t0}} \tag{B.29}$$

The times t and t_0 would correspond to the same temperature of thermal cycling, separated by one cycle.

B.1 References

[1] R. D. Kuchta, V. Mizrahi, P. A. Benkovic, K. A. Johnson, and S. J. Benkovic, "Kinetic mechanism of DNA polymerase I (Klenow)," *Biochemistry*, vol. 26, no. 25, pp. 8410–7, 1987.

[2] R. S. Palais and R. A. Palais, "Numerical methods," in *Differential Equations, Mechanics, and Computation*. American Mathematical Society, 2009, ch. 5, pp. 133–224.

APPENDIX C

LINEARITY OF FLUORESCENCE WITH LENGTH OF DOUBLE-STRANDED DNA

In response to a question concerning the linearity of fluorescence with polymerase extension of a template, the following experiment was performed.

C.1 Methods

The fluorescence of hairpin oligonucleotides with varying lengths of double-stranded DNA were measured using real-time PCR instrument (LightCycler 480, Roche). Final reaction concentrations were 50 mM Tris, pH 8.3, 3 mM $MgCl_2$, 1X LCGreen Plus (BioFire Diagnostics), 200 μM each dNTP, and 100 nM oligonucleotide. Fluorescence was collected at 37°C and each oligonucleotide was measured in triplicate. Oligonucleotides consisted of a template used for the studies in Chapters 2 and 3 (Figure C.1 A) and blunt-end hairpins corresponding to template extended by five base increments (Figure C.1 B-F).

C.2 Results

Fluorescence was linear with the length of the double-stranded region of the hairpin (Figure C.2). Large well-to-well fluorescence variations are inherent with the real-time PCR instrument and are reflected in the error bars.

C.3 Discussion

Linearity of fluorescence with the length of double-stranded DNA justifies using initial slopes to quantify extension rates.

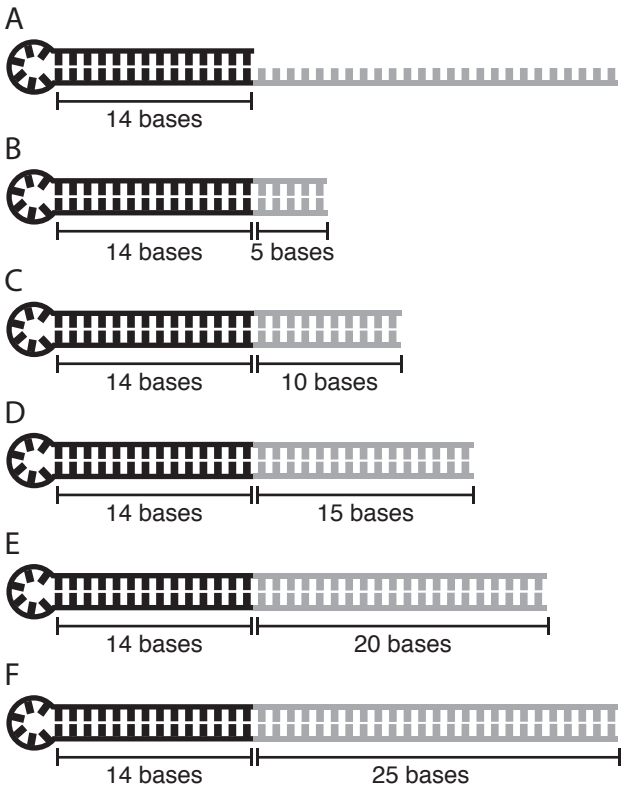

Figure C.1. Oligonucleotides used to assess linearity of fluorescence with length of double-stranded DNA. (A) Hairpin oligonucleotide template. (B) A hairpin representing the template extended five bases. (C) A hairpin representing the template extended ten bases. (D) A hairpin representing the template extended 15 bases. (E) A hairpin representing the template extended 20 bases. (F) A hairpin representing the template fully extended.

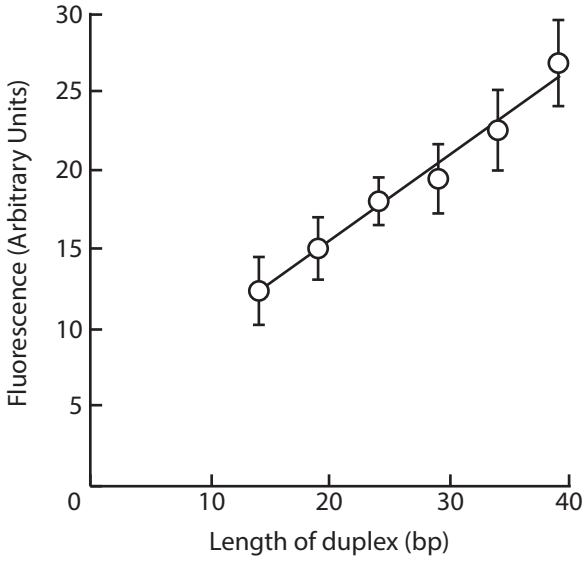

Figure C.2. Fluorescence of hairpin oligonucleotides increase linearly with the length of double-stranded DNA. R^2=0.983.